UNIVERSITY OF THE AEGEAN

SCHOOL OF ENGINEERING

DEPARTMENT OF INFORMATION AND COMMUNICATION SYSTEMS ENGINEERING

"REAL TIME CONTROL FOR WIRELESS NETWORKED MULTI-CHANNEL SYSTEMS WITH SAFE SWITCHING TECHNIQUES"

PHD DISSERTATION

Giannaris Georgios

Supervisor:

Demosthenes Vouyioukas
Professor of Mobile and Satellite Communication Systems
University of the Aegean

Members of committee:

Fotis N. Koumboulis
Professor of Robotics and Industrial Automation
National and Kapodistrian University of Athens

Nikolaos D. Kouvakas
Associate Professor of Automatic Control in Motion and Navigation Systems
National and Kapodistrian University of Athens

Submitted in fulfilment of the requirements for the degree of

Doctor of Philosophy

[May 2021]

Keywords

Networked Control System, Disturbance Output Diagonalization, Disturbance Attenuation, Dynamic multi-delay Controller, Input Output Decoupling, Remote Control, Redundant Manipulator, Synchronization/Signal Reconstruction Algorithm, Stepwise Safe Switching, Time Delay, Wireless Network.

Abstract

The aim of this thesis is to deploy and develop appropriate algorithms to overcome the problem of wireless remote control that is the presence of varying time delays imposed from wireless network communication between sensors and controller and between controller and actuators. From the technological point of view the goal is to develop new communication infrastructure decreasing the delays. Although the communication delays will be provisionally smaller, they will remain time varying, unknown, and uncertain. The current approaches in the literature study this issue in this direction. In the present work, we move towards the opposite direction of the standard technological trends, using larger but constant delays. This thesis replay to two fundamental questions; will a multi delay controller, designed using the linear approximants of the original plant, perform satisfactory to a nonlinear plant with large but constant and known delays? Are there any significant applications justifying the proposed "opposite direction" approach? The design requirements of I/O decoupling and/or asymptotic disturbance rejection are successfully applied through a wireless network to some of the most representative applications in networked control systems a) electric motors, b) tower cranes, c) robotics and d) quadrotors. The significance of this study is that the above design requirements for networked control systems are met successfully for the first time.

List of Figures

Table of Contents

Statement of Original Authorship

The work contained in this thesis has not been previously submitted to meet requirements for an award at this or any other higher education institution. To the best of my knowledge and belief, the thesis contains no material previously published or written by another person except where due reference is made.

Signature: _____

Date: _____

Acknowledgements

I would like to thank the members of the committee Professor Koumboulis Fotis and Associate Professor Kouvakas Nikolaos for their valuable advices, explanations, key points, and suggestions that contributed to the improvement and completion of this work. Their constructive criticism, patience as well as their availability throughout the implementation of this work is highly appreciated.

I would especially like to thank my supervisor Professor Demosthenes Vouyioukas for his valuable scientific guidance and his creative criticism and patience. Without his help it would be extremely difficult to achieve the refinement of this dissertation.

I am grateful for their sincere and selfless help but also the trust they showed me.

To the women of my life,

Elina and Natasha

Chapter 1: Introduction

1.1 NETWORKED CONTROL SYSTEMS

Thanks to the extended technological evolution in the modern world, communication over networks is predicted to be the main way of point to point information transmission. With the gradual increase of bandwidth and data transfer rate, this way of communication has become safer and more resilient [1]. One of the most promising applications of networked communication is on the domain of control engineering. In a control system, complex connections between the various components of a closed loop scheme are replaced with wired or wireless network communication, making the connectivity more flexible and the system itself lighter and easier to maintain.

Networked Control Systems (NCS) and Wireless Networked Control Systems (WNCS) are systems distributed in space where the interconnection between main components like sensors, controllers, and actuators is implemented via a communication (wired or wireless) protocol. The inherent complexity of large distributed modern control systems, where a large number of sensor and controller data has to be processed, makes this kind of interconnection of the system inevitable. Some examples of NCS and WNCS are complex autopilot control systems and large industrial systems while their application is extended to teleoperations, efficient guidance and navigation of mobile robots and tele-medicine.

In any control system to be controlled the stability of the closed loop system is the main issue. In NCS the loop is closed over a network, which by nature, automatically introduces variable delays from the sensors to the controller after sampling and quantizing measured data, from the controller to the actuators after synchronising and reconstructing the controller's output data and computational delays. In addition, packet losses occur in wireless communication mainly due to long transmission delays. As it is well known, the overall delays and packet dropouts affects the controller's effectiveness and in worst case may lead the closed-loop system in instability.

In Wired Control Systems, wired interconnection of the components provide the needed reliability but because of the inherent huge complexity it displays disadvantages related to the

cost and flexibility within these systems. For instance, in an intra-vehicle wired network, 40 Kg of almost 4 km wires augment the construction cost, the maintenance and fuel consumption [2]. The wiring harness represents 2-5% of an aircraft weight which for an Airbus A350-900 represents 23000 kg [3]. The industrial control systems also suffer from this disadvantage. As a result, Wireless Sensors Network is an emerging trend in industrial monitoring and control according to [4].

The NCS plan needs to include appropriate protocols and routing algorithms to overcome the delays and message loss introduced by the communication network, outcome system performance degradation that affect the controller's feasibility reducing the human safety [5].

The NCS, that are a continuation of the Integrated Communication Control systems [6], represent the third generation of control systems, with the first generation being the analogue control and the second one the digital control, and can be classified as hybrid control systems since they possess both analogue and discrete properties [7]. These systems, when the information is transmitted via wired or wireless connections, operate in an asynchronous manner. Thus, the network must be considered explicitly as it affects directly the behaviour of the control system [8]. The variable delays that are introduced by the wireless communication between several components of the closed-loop system must be considered in the analysis and the design of the control system. There are essentially three kinds of delays in such a system: delay between the sensors and the controller, computational delay in the controller, and communication delay between the controller and the actuator [9]. These delays can degrade the performance of control systems and even destabilize them [10], [11]. In fact, data packets transferred through networks suffer not only transmission delays, but also, transmission loss or packet dropout that also affects the closed-loop control system dynamics [12]. Packet dropout is considered as a kind of varying delays as the drop of a packet cause an increase in the delay [13].

As many applications make use of computing and communication networks, the possible issues of scheduling, network delay, and data loss need to be dealt systematically as communication constraints [14],[15].

A recent survey [16] summarizes the main two techniques and key research directions for WNCS. The first one is the 'Control of networks' that investigates the quality and performance of the communication network in order to improve the control performance and

the second one ‘Control over networks’ that investigates the robustness of the control loop relative to impeded network constraints. Concerning the latter, five issues have to be carefully researched: sampled-data control, dealing with the ways the choice of sampling period has an impact on system stability, quantization control, where packets of data quantized after the sampling procedure can be regarded as a lossy procedure affecting the stability of the closed-loop system, networked control, that focuses on finding the appropriate control law which handles efficiently the induced delays, event triggered control, an event decision maker that releases the sampling data to the network and avoids the Zeno behaviour (a phenomenon of infinite number of control updates over a finite time period), and security control, that ensures the safety against malicious attacks [11].

The main concern of WNCS is the design of an appropriate controller that ensures the closed-loop stability and handles the network constraints. In the last two decades many researchers have contributed on several control methodologies that have introduced new ways to control networked systems. In what follows, several control methods are presented in review.

The method introduced by Luck and Ray [17], proposed an algorithm for sensor-to-controller and controller-to-actuator variable delays compensation the sum of which is considered bounded and constant. For this purpose, they used a state observer to overcome the sensor’s measurement noise and a state predictor that uses the state transition matrix of the system model stored in buffers. This method highly depends on the model reliability. A familiar control method is to construct an augmented discrete time model whose state vector contains the original states of the system and the previous inputs based on a state feedback controller that incorporates the delays [18]. The stability of the control system is examined using the transition matrix of the augmented system. The gain of the state feedback controller must be optimal relative to time-dependent delays [9] and is designed by solving a Linear Quadratic Gaussian dynamic programming problem. Walsh et al. [20], for the control synthesis, consider the networked induced error as a perturbation on the system and investigate the error boundaries that ensure stability using the Lyapunov method on the error dynamics. Many researchers start with designing a control law without considering the network induced constraints and then examining its extension in order to overcome the network imperfection to guarantee stability on the closed-loop system [16].

Networked control systems are described by multi delay models including of course the communication channels used for the implementation of the control loop. Obviously, the nature of the communication channel imposes that delays are time varying, uncertain, and unknown. Existing studies in the field focus on stabilizability, Linear Quadratic Gaussian and parameter perturbation analysis, indicatively see [18]-[20] and the references therein. From the technological point of view the goal is to develop new communication infrastructure decreasing the delays. Although the communication delays will be provisionally smaller, they will remain time varying, unknown, and uncertain.

From the control point, most of the techniques require the precise knowledge of the delays or many of them require that the delays of the controlled plant be known and non-uncertain. In these techniques, if the delays of the plant are different than the delays considered for the controller design, then in a short period the performance of the closed loop system is not satisfactory. Such techniques are those expressing the design goal as a desired closed loop transfer matrix, i.e. I/O decoupling, disturbance rejection and model matching.

In the present work, the main idea is to move towards the opposite direction of the standard technological trends, using larger delays. In particular, the controller is designed by considering upper bounds of the original delays. For the controller to be successful the communication delays are increased till these upper bounds. Following this line of thinking, the first important question is: will a multi delay controller, designed using the linear approximants of the original plant, perform satisfactory to a nonlinear plant with large but constant and known delays? The second important question is are there any significant applications justifying the proposed “opposite direction” approach? Towards answering these questions, the design requirements of I/O decoupling and/or asymptotic disturbance rejection are successfully applied through a wireless network to some of the most representative applications in networked control systems a) electric motors, b) tower cranes, c) robotics and d) quadrotors. It is important to mention that the above design requirements for networked control systems are studied here for the first time. The detailed contribution of the present material is presented in the thesis outline that follows.

1.2 THESIS OUTLINE

The structure of the thesis is as follows:

In Chapter 2 the problem of speed control of a permanent magnet synchronous motor is investigated in the presence of constant time delays due to wireless signal transmission among the controller, the sensors, and the actuators. A novel control algorithm is proposed in order to compensate the presence of the delays and to achieve satisfactory performance despite their presence. The controller design focuses mainly on the stability of the time delay closed loop system.

In Chapter 3 the problem of independent control of the performance variables of a tower crane through a wireless sensor and actuator network is investigated. The complete nonlinear mathematical model of the tower crane is developed. Based on appropriate data norms an accurate linear approximant of the system, including an upper bound of the communication delays, is derived. Using this linear approximant, a dynamic measurable output multi delay controller for independent control of the performance outputs of the system is fully analysed.

In Chapter 4 the problem of remote position control of a planar redundant manipulator is studied for the case of a 3dof Cartesian robot including disturbance forces at the end effector. The robotic manipulator controlled through a wireless network using the ZigBee protocol, imposing communication delays between the sensors and the controller, as well as between the controller and the actuators. A static feedback with dynamic precompensator controller involving time delays is proposed. Based on these two aspects the following four design goals are imposed: a) non-square input/output decoupling, b) Disturbance/output diagonalization, c) attenuation of the influence of the disturbances to the performance outputs, and d) balanced allotment of the steady state behaviour of the redundant degrees of freedom.

In Chapter 5 the problem of remotely controlling a quadrotor in longitudinal motion and under atmospheric disturbances is studied. The controller – communication system is enriched with a synchronization / signal reconstruction algorithm imposing constant delays. The design goal is to independently control the horizontal and vertical velocity of the quadrotor while simultaneously attenuating the influence of the disturbances to these velocities. To this end, a linear dynamic time delay controller is designed. The satisfactory performance of the proposed

control scheme is illustrated through computational experiments for the case of a climbing manoeuvre.

In Chapter 6 the problem of a stepwise safe switching procedure is analysed in order to increase the range of the external commands for a remotely controlled quadrotor in longitudinal motion under atmospheric disturbances. The stepwise safe switching algorithm is based on the approximate minimization of a composite criterion including the infinity norm and the H_2 norm of the variations around trim points under hard constraints for the steady state performance and the overshoot of the performance variables. The satisfactory performance of the proposed control scheme is illustrated through simulations for a climbing manoeuvre passing through different target operating areas.

In chapter 7 conclusions and future work are presented.

REFERENCES

[1] Eloy Garcia, Panos J. Antsaklis, Luis A, Montestruque, Model-Based Control of Networked Systems, *Systems and Control: Foundations and Applications*, pp. 1, ISBN 978-3-319-07802-1, © Springer International Publishing Switzerland 2014.

[2] Y. Sadi, S. Coleri Ergen, Optimal Power Control, Rate Adaptation, and Scheduling for UWB-Based Intravehicular Wireless Sensor Networks, *IEEE Transactions on Vehicular Technology*, vol. 62 ,pp. 219-234, January 2013.

[3] Technical Characteristics and Operational Objectives for Wireless *Avionics Intra-communication (WAIC), Report ITU M.2197*, November 2010.

[4] M. Chithik Raja, Wireless Sensor Networks Application and Control in Industrial System: A Study Report, *International Journal of Computer Science Engineering and Technology*, vol. 2, pp. 1181-1185, May 2012,

[5] P. Park, S. Ergen, C. Fischione, C. Lu, K. Johansson, Wireless Network Design for Control Systems: A Survey, *IEEE Communications Surveys & Tutorials*, vol. 20 pp. 978-1013 , January 2018.

[6] Y. Halevi, A. Ray, Integrated Communication and Control Systems: Part I-Analysis, *Journal of Dynamic Systems Measurement and Control-transactions*, vol. 110, pp. 367-373, December 1988.

[7] P. Kumar, Towards a Third Generation of Control Systems, book, pp.2, January 2006.

[8] P. Antsaklis, J. Baillieul, Special Issue on Technology of Networked Control Systems, *Proceedings of the IEEE*, vol. 95, pp. 5-8, February 2007.

[9] J. Nilsson, B. Bernhardsson, B. Wittenmark, Stochastic Analysis and Control of Real-Time Systems with Random Time Delays, IFAC Procedings Volumes, vol. 29, pp.7106-7111,

[10] M. Branicky, S. Philips, W. Zhang, Stability of networked control systems: Explicit analysis of delay, *Proc. IEEE. Conf. Amer. Contr. Conf*, vol. 4 , pp. 2352-2357, February 2000.

[11] X. Zhang et al, Networked control systems: a survey of trends and techniques, *IEEE/CAA Journal of Automatica Sinica* , vol. 7, pp. 1-17, January 2020.

[12] J. Wu, T. Chen, Design of Networked Control Systems With Packet Dropouts, *IEEE Transactions on Automatic Control*, vol. 52, pp. 1314-1319, August 2007.

[13] Mikael Bjorkbom, Wireless Control Sytem Simulation and Network Adaptive Control, *PHD Dissertation AALTO UNIVERSITY*, Report 167, October 2010.

[14] L. Schenato, B. Sinopoli, M. Franceschetti et al., Foundations of Control and Estimation Over Lossy Networks, *Proceedings of the IEEE*, vol. 95, pp. 163-187, February 2007.

[15] W. Heemels, A. Teel, N. Wouw, et al., Networked control systems with communication constraints: Tradeoffs between transmission intervals and delays, *IEEE Transactions in Automatic Control*, *European Control Conference, ECC 2009*, vol. 55 , pp. 1781-1796 , August 2010.

[16] J. Hespanha, P. Naghshtabrizi, Y. Xu, A Survey of Recent Results in Networked Control Systems, *in Proceedings of the IEEE*, vol. 95, pp. 138-162, 2007.

[17] R. Luck, A. Ray, An Observer-based Compensator for Distributed Delays, Automatica, vol. 26, pp. 903-908, September 1990.

[18] Y. Halevi, A. Ray, Integrated Communication and Control Systems: Part I-Analysis, *Journal of Dynamic Systems Measurement and Control-transactions of The Asme*, vol. 110, pp. 367-373, December 1998.

[19] A. Ray, Y. Halevi, Integrated Communication and Control Systems: Part II—Design Considerations, *Journal of Dynamic Systems Measurement and Control-transactions of The Asme*, vol. 110, pp. 374-381, December 1988.

[20] G. C. Walsh, O. Beldiman and L. G. Bushnell, Asymptotic behavior of nonlinear networked control systems, *IEEE Transactions on Automatic Control*, vol. 46, pp. 1093-1097, July 2001

Chapter 2: Wireless Control for a PMS Motor

2.1 INTRODUCTION

Permanent magnet synchronous motors (PMSM) are widely used in industry providing significant advantages as compared to other types of electric motors. Several control techniques have been developed in the field of PMSM control, ([1]-[12] and the references therein). Specifically, remote control applications of electric motors appear to be of special industrial interest (see [13]). In the present work, the problem of speed control of a PMSM is investigated in the presence of time delays due to wireless signal transmission between the controller and the sensors and the actuators of the motor. The two stage decoupling controller approach proposed in [1], is appropriately extended to achieve satisfactory performance despite the presence of the communication delays. An inner and an outer controller are designed. The inner controller is designed to derive a stable time delay closed loop system and achieve asymptotic command following of the direct and quadrature stator currents. This way, the linear approximant of the plant is stabilized independently of the delays. The outer controller is a PI controller to achieve speed command following and regional stability. The performance of the proposed scheme is illustrated through simulation.

2.2 MATHEMATICAL MODEL

A PMSM, in d-q frame, for the case of wireless driven actuators is described as follows [1]-[2]

$$\frac{di_d(t)}{dt} = -\frac{R_l}{L} i_d(t) + \omega(t) i_q(t) + \frac{1}{L} u_d(t-\tau) \tag{2.1a}$$

$$\frac{di_q(t)}{dt} = -\frac{R_l}{L} i_q(t) - \omega(t) i_d(t) - \frac{\psi_r}{L}\omega(t) + \frac{1}{L} u_q(t-\tau) \tag{2.1b}$$

$$\frac{d\omega(t)}{dt} = \frac{n_p \psi_r}{J} i_q(t) - \frac{\beta}{J}\omega(t) - \frac{1}{J} T_L(t) \tag{2.1c}$$

where i_d and i_q are the stator currents in $d-q$ frame respectively, ω is the angular velocity of the rotor, T_L is the external load torque, J is the polar moment of inertia, β is the viscous damping coefficient, R_l is the stator winding resistance, L is the motor inductor, ψ_r is the permanent magnet flux and n_p is the number of pole pairs. Finally, u_d and u_q are the direct and quadrature axis stator voltage components, respectively. As already mentioned, the voltages are delayed since they are driven through a wireless network. The wireless network is used to transmit measurable variable signals from the motor sensors to the remote controller as well as from the remote controller to the motor's actuators. After appropriate modifications of the transmission-receive protocol, the communication delay (including signal reconstruction), let τ, can be assumed to be approximately constant in both ways of transmission [14].

2.3 CONTROLLER DESIGN

For the delayless mathematical model of the PMSM, a two stage control scheme towards stability and robustness has been proposed in [1] where the internal controller was a robust controller satisfying I/O decoupling and pole assignment for the direct and the quadrature phase stator currents. The external controller was a PI controller regulating the angular velocity of the rotor. Although that controller was successful in the absence of delays, in the presence of delays it performs satisfactorily only for dissuasively small delays. For example, the maximum delay for which the closed loop system remains stable is $\tau_{\max} = 0.0036\left[\sec\right]$. To improve the stability margin, an inner loop controller will first be designed (see Fig. 2.1).

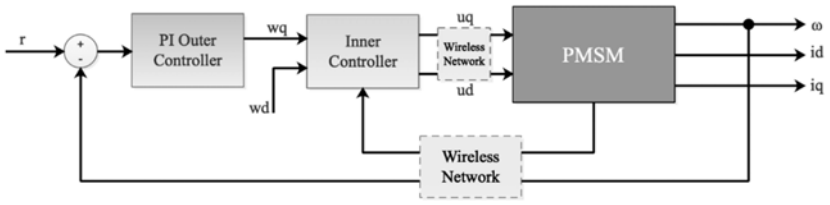

Fig. 2.1 Block diagram of the closed loop system

2.3.1 Inner loop bilinear controller

To extend the results in [1] incorporating time delays, the following nonlinear static inner loop controller is proposed

$$u_d(t) = (R_l - L\lambda_1) i_d(t-\tau) + L\left[\lambda_1 w_d(t) - i_q(t-\tau)\omega(t-\tau)\right] \tag{2.2a}$$

$$u_q(t) = (R_l - L\lambda_2) i_q(t-\tau) + \left[\psi_r + L i_d(t-\tau)\right]\omega(t-\tau) + L\lambda_2 w_q(t) \tag{2.2b}$$

where λ_1, $\lambda_2 \in \mathbb{R}$ are free parameters and w_d, w_q are the inner loop external commands. Substituting (2.2) to (2.1), the resulting inner closed loop system is derived to be

$$\begin{aligned} \frac{di_d(t)}{dt} &= -\frac{R_l}{L} i_d(t) + \left(\frac{R_l}{L} - \lambda_1\right) i_d(t-2\tau) + i_q(t)\omega(t) - \\ &- i_q(t-2\tau)\omega(t-2\tau) + \lambda_1 w_d(t-\tau) \end{aligned} \tag{2.3a}$$

$$\begin{aligned} \frac{di_q(t)}{dt} &= -\frac{R_l}{L} i_q(t) + \left(\frac{R_l}{L} - \lambda_2\right) i_q(t-2\tau) - \left[\frac{\psi_r}{L} + i_d(t)\right]\omega(t) + \\ &+ \left[\frac{\psi_r}{L} + i_d(t-2\tau)\right]\omega(t-2\tau) + \lambda_2 w_q(t-\tau) \end{aligned} \tag{2.3b}$$

$$\frac{d\omega(t)}{dt} = \frac{n_p \psi_r}{J} i_q(t) - \frac{\beta}{J}\omega(t) - \frac{1}{J} T_L(t) \tag{2.3c}$$

From (2.3) observe that I/O decoupling is not satisfied in the exact sense. Also observe that the inner closed loop system is in nonlinear retarded time delay form. To address the problem of inner closed loop stability, the linear approximant of the nonlinear model in (2.3) will be used. This linear approximant is computed to be

$$\delta\dot{x}(t) = A_1 \delta x(t) + A_3 \delta x(t-2\tau) + B_2 \delta w(t-\tau) + D_1 \delta\xi(t) \tag{2.4}$$

$$\delta x(t) = \left[i_d(t) - \bar{i}_d \quad i_q(t) - \bar{i}_q \quad \omega(t) - \bar{\omega}\right]^T = \left[\delta i_d(t) \quad \delta i_q(t) \quad \delta\omega(t)\right]^T$$

$$\delta\xi(t) = \xi(t) - \bar{\xi}$$

$$\delta w(t) = \begin{bmatrix} w_d(t) - \overline{w}_d & w_q(t) - \overline{w}_q \end{bmatrix}^T = \begin{bmatrix} \delta w_d(t) & \delta w_q(t) \end{bmatrix}^T$$

$$A_1 = \begin{bmatrix} -\dfrac{R_l}{L} & \dfrac{n_p \overline{w}_q \psi_r - \overline{T}_l}{\beta} & \overline{w}_q \\ \dfrac{\overline{T}_l - n_p \overline{w}_q \psi_r}{\beta} & -\dfrac{R_l}{L} & -\dfrac{L\overline{w}_d + \psi_r}{L} \\ 0 & \dfrac{n_p \psi_r}{J} & -\dfrac{\beta}{J} \end{bmatrix}$$

$$A_3 = \begin{bmatrix} \dfrac{R_l}{L} - \lambda_1 & \dfrac{\overline{T} - n_p \overline{w}_q \psi_r}{\beta} & -\overline{w}_q \\ \dfrac{n_p \overline{w}_q \psi_r - \overline{T}_l}{\beta} & \dfrac{R_l}{L} - \lambda_2 & \overline{w}_d + \dfrac{\psi_r}{L} \\ 0 & 0 & 0 \end{bmatrix}$$

$$B_2 = \begin{bmatrix} \lambda_1 & 0 & 0 \\ 0 & \lambda_2 & 0 \end{bmatrix}^T, \; D_1 = \begin{bmatrix} 0 & 0 & J^{-1} \end{bmatrix}^T$$

where $\overline{\bullet}$ is the nominal value of the argument quantity $\bullet$. According to [15], system (2.4) is stable, independently of the delay τ if and only if

a) A_1 is stable,

b) $\rho\left(A_1^{-1}A_3\right) < 1$ or $\rho\left(A_1^{-1}A_3\right) = 1$ but $\det\left(A_1 + A_3\right) \neq 0$ and

c) $\rho\left(\left(j\omega I_3 - A_1\right)^{-1} A_3\right) < 1,$

where $\rho(\bullet)$ is the spectral radius of the argument matrix $\bullet$. Condition (a) is satisfied. Also, using appropriate λ_1 and λ_2 the conditions (b) and (c) are satisfied. Thus, asymptotic command following is achieved for the direct and quadrature stator currents.

2.3.2 Speed control via an outer loop PI controller

With respect to the speed of the rotor, it holds that

$$\delta\Omega(s) = zC\left[sI_3 - \left(A_1 + z^2 A_3\right)\right]^{-1} B_2 \delta W(s) + C\left[sI_3 - \left(A_1 + z^2 A_3\right)\right]^{-1} D_1 \delta\Xi(s) \quad (2.5)$$

where $C = \begin{bmatrix} 0 & 0 & 1 \end{bmatrix}$, $\delta\Omega(s)$, $\delta W(s)$ and $\delta\Xi(s)$ are the Laplace transforms of $\delta\omega(t)$, $\delta w(t)$ and $\delta\xi(t)$ respectively and $z = e^{-s\tau}$. In the frequency domain the PI controller is

$$\delta W_q(s) = \left(f_p + \frac{1}{s} f_i\right)\left[\delta R(s) - z\delta\Omega(s)\right] \quad (2.6)$$

where $\delta R(s)$ is the speed external command. The characteristic polynomial of the overall closed loop system is

$$p(s,z) = s^4 + \alpha_3(z)s^3 + \alpha_2(z)s^2 + \alpha_1(z)s + \alpha_0(z) \quad (2.7)$$

where

$$\alpha_3(z) = \left\{L\beta + J\left[Lz^2\left(\lambda_1 + \lambda_2\right) - 2\left(z^2 - 1\right)R_l\right]\right\}(JL)^{-1}$$

$$\alpha_2(z) = \left(z^2 - 1\right)^2 \bar{\omega}^2 + \frac{1}{L^2}\left[\left(z^2 - 1\right)R_l - Lz^2\lambda_1\right]\times$$
$$\left[\left(z^2 - 1\right)R_l - Lz^2\lambda_2\right] + \frac{1}{JL}\left\{\left(1 - z^2\right)\psi_r^2 n_p + 2\left(1 - z^2\right)\beta R_l +\right.$$
$$\left. + Lz^2\beta\left(\lambda_1 + \lambda_2\right) + L\psi_r n_p\left[\bar{i}_d\left(1 - z^2\right) + f_p z^2\lambda_2\right]\right\}$$

$$\alpha_1(z) = \left(z^2 - 1\right)^2 \frac{\beta R_l^2}{JL^2} + \left(z^2 - 1\right)\frac{R_l}{JL^2}\left\{\left(z^2 - 1\right)\psi_r^2 n_p -\right.$$
$$\left. Lz^2\beta\left(\lambda_1 + \lambda_2\right) + L\psi_r n_p\left[\bar{i}_d\left(z^2 - 1\right) - f_p z^2\lambda_2\right]\right\} +$$
$$+\frac{1}{JL}\left[L\bar{T}_l\left(z^2 - 1\right)^2\bar{\omega} + 2L\left(z^2 - 1\right)^2\beta\bar{\omega}^2 + z^2\left(\left(1 - z^2\right)\psi_r^2 n_p\lambda_1\right.\right.$$
$$\left.\left. + Lz^2\beta\lambda_1\lambda_2 + L\psi_r n_p\left\{f_i\lambda_2 + \lambda_1\left[\bar{i}_d\left(1 - z^2\right) + f_p z^2\lambda_2\right]\right\}\right)\right]$$

$$\alpha_0\left(z\right)=f_i z^2\psi_r n_p\left[\left(1-z^2\right)R_l+Lz^2\lambda_1\right]\lambda_2\left(JL\right)^{-1}$$

The outer loop design goal is to find f_p and f_i such that the closed loop system has desirable stability properties. Due to stability, the steady state gains from $\delta R\left(s\right)$, $\delta W_d\left(s\right)$ and $\delta\Xi\left(s\right)$ to the speed are equal to 1, 0 and 0, respectively. Hence asymptotic command following is achieved. Using, the criteria in [15], it is observed that independent of the delay, stability of the closed loop system cannot be achieved. Thus, following [16], a clustering treatment, for the characteristic roots of the system, will be used to estimate the maximum delay for which the characteristic polynomial is regionally stable, i.e. the poles of the closed loop system to be leftmost a desired point on the real axis, let λ.

2.4 SIMULATIONS RESULTS

The performance of the control scheme, proposed in the previous sections, will be tested through simulations. To this end, consider the model parameters presented in [1], [2], i.e.

$L=14.25[\mathrm{mH}]$, $R_l=0.9\left[\Omega\right]$, $\psi_r=0.9\left[\mathrm{Nm/A}\right]$, $n_p=1$, $J=4.7\times10^{-5}[\mathrm{Kgm^2}]$, $\beta=0.0162\left[\mathrm{N/rad/sec}\right]$. Assume that the nominal values for the state variables are $\bar{i}_d=\bar{w}_d$, $\bar{i}_q=\bar{w}_q$, $\bar{\omega}=n_p\bar{w}_q\psi_r/\beta$. Let $\bar{w}_d=0.5\left[\mathrm{A}\right]$ and $\bar{w}_q=10\left[\mathrm{A}\right]$. Testing the conditions (b) and (c) in 2.3.1, the range of λ_1 and λ_2 for which the inner closed loop system is stable independently of the delay is presented in Figure 2.2(a).

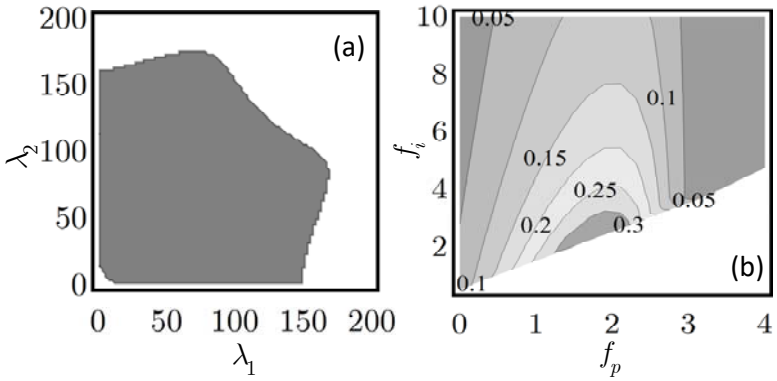

Fig. 2.2 Stability regions for the inner and outer closed loop system.

Let the time delay, imposed by the network, be $\tau = 30\left[\text{msec}\right]$. This is an acceptable value for to several commercial/industrial applications (see [17]). According to Figure 2.2(a), we may choose $\lambda_1 = 20$ and $\lambda_2 = 20$. A settling time of $1.5\left[\text{sec}\right]$ is achieved for both $i_d\left(t\right)$ and $i_q\left(t\right)$. According to Figure 2.2(b), the maximum delay preserving stability for several values of the PI parameters is presented. Let $\lambda = -1$. Thus, we may choose $f_p = 2$ and $f_i = 6$ which provide stability delay margin being greater than $0.15\left[\text{sec}\right]$ and far greater than the $30\left[\text{msec}\right]$ referred above.

To demonstrate the proposed scheme, the controllers developed in 2.3 evaluated as in the previous paragraph, will be applied to the delayed nonlinear model (1). Initially, the motor is assumed to rest. The external commands for the direct phase stator current and the motor speed become

$$w_d\left(t\right) = \frac{0.5}{1+\exp\left\{-\dfrac{t-1.1}{0.12}\right\}},\ r\left(t\right) = \frac{40}{1+\exp\left\{-\dfrac{t-1.1}{0.12}\right\}}$$

With respect to the external load torque, we will firstly examine the case of a zero load torque. Secondly, we will examine the case of a random and fast varying load torque, see Figure 2.3. In Figures 2.4 to 2.6 the respective closed loop responses for the state variables and actuatable inputs are presented. With respect to the angular velocity in Figure 4, it is observed that in both torque cases it follows accurately the external command with small deviations in the case of random load torque. Comparing the present results to those in the non-networking case, namely the case where the delay is equal to zero, it can be observed that the influence of the delay does not significantly affect the performance of the closed loop system with respect to the speed, thus suggesting that the proposed controller herein is robust with respect to the delay. With respect to the direct phase stator current, although the reference curve is not accurately followed during the transition, asymptotic command following is achieved (see Figure 2.5). On the contrary, in the delayless case, the direct phase stator current does follow accurately the external command. The divergence among these two cases is due to the presence of the delay producing a non-decoupled closed loop

system. The quadrature phase stator current and the actuatable inputs (see Figures 5, 6) remain well within acceptable limits.

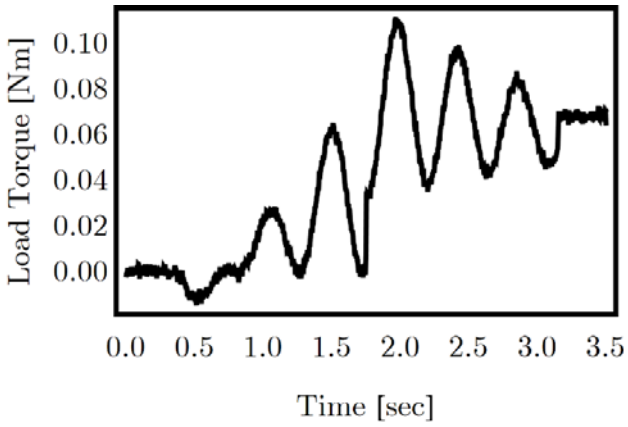

Fig. 2.3 Random external load torque.

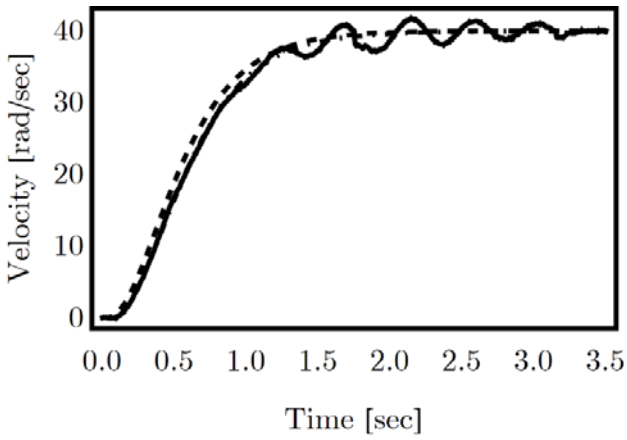

Fig. 2.4 Closed loop angular velocity (*Cont*. – random torque, *DotDashed* – no torque, *Dashed* – reference)

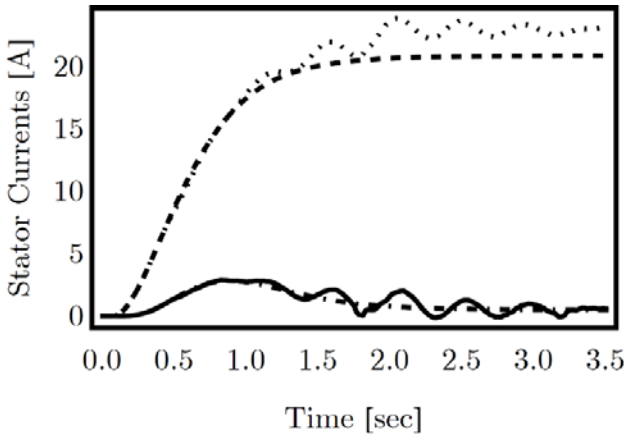

Fig. 2.5 Closed loop stator currents (*Cont*. – random torque direct, *DotDashed* – no torque direct, *Dashed* – random torque quadrature, *Dotted* – no torque quadrature)

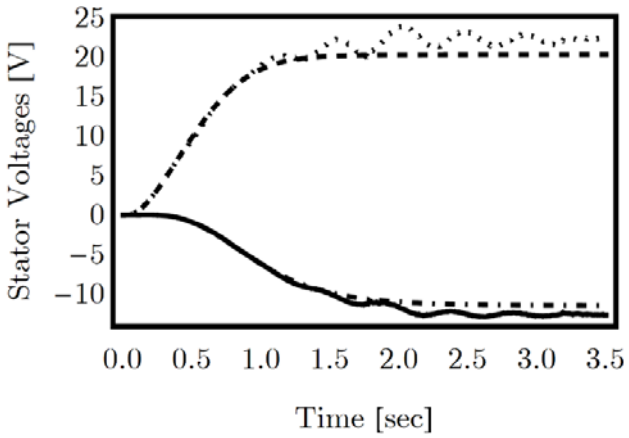

Fig. 2.6 Closed loop stator voltages (*Cont*. – random torque direct, *DotDashed* – no torque direct, *Dashed* – random torque quadrature, *Dotted* – no torque quadrature)

2.5 SUMMARY

The problem of speed control of a PMSM has been investigated in the presence of time delays due to wireless signal transmission between the controller and the motor. In particular, the two stage decoupling controller presented in [1] has been used and the controller parameters selection algorithm has been appropriately extended to cope with the influence of the delays and to derive a closed loop system that remained stable even in the presence of them. With respect to the inner loop controller, asymptotic command following for the direct and quadrature stator currents is achieved while simultaneously producing a closed loop system whose linear approximation is stable independently of the delays. With respect to the outer PI controller delay dependent regional stability, with drastic improvement of the delay stability margin has been proposed. The performance of the controller has been tested through computational experiments.

Future research will focus on a) the production of a unified inner and outer loop scheme, b) investigation of different or even time varying transmission delays, c) examination of jitter and packet losses, d) examination of the influence of sampling and quantization as well as model parameter uncertainties.

REFERENCES

[1] N. D. Kouvakas and F. N. Koumboulis, A Two Stage Control Scheme towards Stability and Robustness for PMSM with Unknown Load Torque, *Proceedings of the 19th Mediterranean Conference on Control & Automation (MED 2011)*, pp. 533-539, 20-23 June 2011, Corfu, Greece.

[2] Z. Li, B. Zhang, L. Tian and Z. Mao, Strange Attractors in Permanent-magnet Synchronous Motors, *Proceedings of the IEEE 1999 International Conference on Power Electronics and Drive Systems (PEDS 99)*, pp. 150-155, vol. 1, 26-29 July 1999, Hong Kong.

[3] F. N. Koumboulis, N. D. Kouvakas, G. E. Panagiotakis and A. G. Pantelios, Adaptive Speed Control of PMSMs with Unknown Load Torque, *Proceedings of the 16th IFAC World Congress (IFAC 2005)*, pp. 1764-1771, 4-8 July 2005, Prague, Czech Republic.

[4] I. C. Baik, K.H. Kim and M.J. Youn, "Robust nonlinear speed control of PM synchronous motor using adaptive and sliding mode control techniques", *IEE Proceedings – Electric Power Applications*, vol. 145, pp. 369-376, 1998.

[5] E. A. Cerruto, A. Consoli, A. Raciti and A. Testa, "A Robust Adaptive Controller for PM Motor Drives in Robotic Applications", *IEEE Transactions on Power Electronics*, vol. 10, pp.62-71, 1995.

[6] K. T. Chang, T.S. Low and T.H. Lee, "An Optimal Speed Controller for Permanent-Magnet Synchronous Motor Drives", *IEEE Transactions on Industrial Electronics*, vol. 41, pp. 503-510, 1994.

[7] F. J. Lin and Y.S. Lin, " A Robust PM Synchronous Motor Drive with Adaptive Uncertainty Observer", *IEEE Transactions on Energy Conversion*, vol. 14, pp. 989-995, 1999.

[8] G. Zhu, G., O. Dessaint, O. Akhrif and A. Kaddouri, "Speed Tracking Control of a Permanent-Magnet Synchronous Motor with State and Load Torque Observer", *IEEE Transactions on Industrial Electronics*, vol. 47, pp. 346-355, 2000.

[9] H. Z. Jin and J. M. Lee, A novel adaptive current regulator for Permanent Magnet Synchronous Motor based on modified current dynamics, *Proceedings of the 6th IEEE International Conference on Industrial Informatics (INDIN 2008)*, pp. 927-932, 2008.

[10] L. Huixian, D. Shihong, L. Shihua and C. Xisong, A PMSM position servo system based on finite-time control, *Proceedings of the 27th Chinese Control Conference*, pp. 234-238, 2008.

[11] A.E. Leon, J. M. Mauricio, A. Gomez-Exposito, and J. A. Solsona, An Improved Control Strategy for Hybrid Wind Farms, *IEEE Transactions on Sustainable Energy*, vol. 1, no. 3, pp. 131-141, 2010.

[12] C. De Angelo, G. Bossio, G. O. Garcia, J. Solsona and M. I. Valla, *Speed control of PMSMs with Interconnection and Damping Assignment or Feedback Linearization*, in Proceedings of the 2006 IEEE International Symposium on Industrial Electronics, 9-13 July, Montreal, Canada, 2006.

[13] Y. Rosenfeld, Automation of existing cranes: from concept to prototype, *Automation in Construction*, vol. 4, pp. 125-138, 1995.

[14] Z. Sun, B. Li, S. Dyke and C. Lu, A novel data utilization and control strategy for wireless structural control systems with TDMA network, *2013 ASCE International Workshop on Computing in Civil Engineering (ASCE IWCCE 2013)*, June 23-25, Los Angeles, USA, 2013.

[15] K. Gu, V. L. Kharitonov and J. Chen, *Stability of Time-Delay Systems*, Birkhäuser Engineering, 2003.

[16] N. Olgac and R. Sipahi, An Exact Method for the Stability Analysis of Time-Delayed Linear Time Invariant (LTI) Systems, *IEEE Transactions on Automatic Control*, vol. 47, no. 5, pp.793-797, 2002.

[17] E.D. Pinedo-Frausto and J.A. Garcia-Macias, An experimental analysis of Zigbee networks, *Proceedings of the 33rd IEEE Conference on Local Computer Networks (LCN 2008)*, pp. 723-729, 14-17 October 2008, Montreal, Canada.

Chapter 3: Independent Motion Control of a Tower Crane through Wireless Sensor and Actuator Networks

3.1 INTRODUCTION

Cranes in various forms are used in several applications having significant economic impact. Classical uses are in construction (bridges, dams, buildings), in transportation (loading and unloading cargo), in industry (oil platforms, refineries), in nuclear power plants and in bio/ecological applications (see [1] and [2] and the references therein).

For efficient crane maneuverability, appropriate control schemes are required. To develop such schemes, accurate mathematical model of the crane is recommended. Several results have been published towards this aim (see [3]-[6] and the references therein). In [3], crane models are classified and related to applications and limitations. In [5], a tower crane is modeled as a robot. In [6], the dynamics of a tower crane (i.e. a point mass suspended by a light cable from a horizontally moving support) are considered. The general equations of motion are derived, and two cases are examined in detail, the linearly accelerating support and the support describing a circle at constant speed. In [7] a simplified with respect to the coupling terms model of a test crane is presented. In [8] a kinematic but not dynamic, model of the test crane is presented.

To increase crane productivity and accuracy, wireless technology was adopted (see [7], [9]-[12] and the references therein). Indicatively, in [10], the possibility to use Bluetooth for wireless short-range communication in an industrial environment is examined. In this line, a distributed control system based on Bluetooth has been proposed for a bridge crane system. Its configuration is mainly based on the use of distributed nodes connected by means of Bluetooth. In [11], the design and real-time implementation of an event-triggered controller for a nonlinear 3D tower crane model is performed, where the communication between the controller and the actuators, is

implemented over a low-power wireless network. In [12], a networked control scheme of multiple tower cranes under event-triggered control policy is designed and simulated. In [7] event triggered control is proposed.

To improve crane maneuverability, several control approaches have been proposed ranging from classical to optimal, intelligent, heuristic and adaptive approaches (see [8] and [13]-[26] and the references therein).

In what follows the problem of independent control - Input Output (I/O) Decoupling of the performance variables of a system is considered for a tower crane through a wireless sensor and actuator network. In particular, the nonlinear mathematical model of a tower crane equipped with preinstalled approximate PID controllers is presented. The nonlinear model is used to produce a linear approximant of the system whose accuracy is investigated via series of computational experiments. Considering that the system is remotely operated, the mathematical model is extended to include transmission and signal reconstruction delays. The extended linear approximant of the system is used to develop a dynamic measurable output controller including delays for the independent control of the performance outputs of the system. With regard to the signal transmission from the sensors to the remote controller and from the controller to the actuators, the ZigBee protocol is used since it presents significant advantages with respect to resistance to noise and other user's interference as compared to other well established approaches. Furthermore, an appropriate synchronization technique is proposed in order to guarantee constant transmission delay. Additionally, a signal reconstruction approach of the continuous time signals from the transmitted signals is used that presents significant advantages with respect to the accuracy of the reconstructed signal, as well as the performance of the closed loop system.

The contribution of the present work can be analyzed into five points. The first point is the derivation of a more general dynamic model of the crane as compared to [7] and [8], in the sense that it includes variable cable length, as well as all coupling terms in the system dynamics. The second point is the derivation of an accurate linear approximant of the nonlinear plant. It is important to mention that since wireless control is required, a nonlinear controller compensating the dynamics of the nonlinear plant (e.g. inverse dynamics controller) is not applicable to the present case. Towards

this aim, the linear approximant has been derived as well as the third point of the contribution, namely the derivation of an appropriate realizable multi-delay dynamic controller providing I/O Decoupling. The controller depends upon the constant communication delays. To achieve such delays, as well as accurate signal transmission through digital wireless communication, a synchronization algorithm and a signal reconstruction algorithm are proposed, as the fourth point of the contribution of this presentation. Last but not least, the accuracy of the linear approximant of both the open loop and the closed loop system is preserved.

3.2 DYNAMICS OF A TOWER CRANE

Cranes are worksite mechanisms used to lift and lower loads as well as to place them in the site. A tower crane (see Fig. 3.1) is a modern form of balance crane consisting, from an abstractive point of view, of three mechanical parts: an arm rotating around a vertical mast, a trolley moving along the arm and finally a cable drum with a load at the end of the cable. The arm rotates around the mast by an arm motor (actuator 1), the trolley moves along the arm by a second motor (actuator 2) and the payload is lifted or lowered by a third motor (actuator 3) rotating the cable drum to gather or release the cable. The tower crane is a highly oscillatory system described by linear and nonlinear dynamics. The nonlinear dynamics come mainly from the rotational motion inducing centripetal and Coriolis accelerations producing instability.

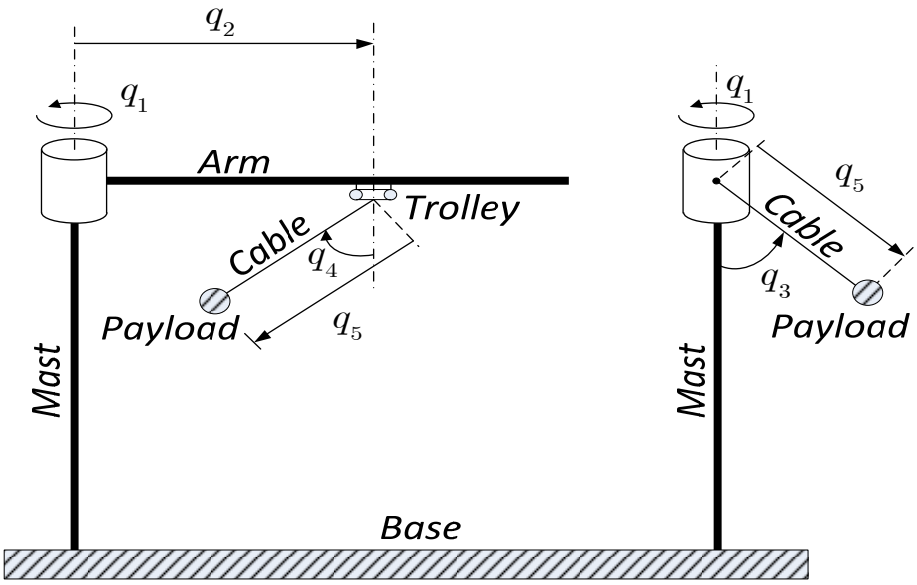

Fig. 3.1 Tower crane configuration.

In what follows, the mathematical description of the tower crane will be developed using the Euler-Lagrange approach. The tower crane is inherently unstable with respect to all motion variables. In such mechanical systems it is a common practice (see [27]) to use pre-installed three term controllers to regulate local performance variables. Such pre-installed local PID controllers are necessary for the safe ground operation. Here, three pre-installed approximate PID controllers are considered. The 1st PID stabilizes the velocity of the arm, the 2nd stabilizes the position of the trolley along the arm and the 3rd the cable length.

3.2.1 State Space Model of the Crane

Define

$$x = \begin{bmatrix} x_1 & \cdots & x_{16} \end{bmatrix}^T = \begin{bmatrix} q_1 & q_2 & q_3 & q_4 & q_5 & \dot{q}_1 & \dot{q}_2 \\ \dot{q}_3 & \dot{q}_4 & \dot{q}_5 & \chi_{1,1} & \chi_{1,2} & \chi_{2,1} & \chi_{2,2} & \chi_{3,1} & \chi_{3,2} \end{bmatrix}^T$$

$$w = \begin{bmatrix} w_1 & w_2 & w_3 \end{bmatrix}^T,\ y = \begin{bmatrix} y_1 & y_2 & y_3 \end{bmatrix}^T,\ \psi = \begin{bmatrix} \psi_1 & \cdots & \psi_5 \end{bmatrix}^T$$

where x is the state vector, y is the performance output vector, ψ is the measurable output vector, w is the vector of external commands of the pre-installed PID controllers, q_1 is the arm rotation angle with respect to an inertial frame, q_2 is the distance of the trolley from the crane's revolution axis, q_3 and q_4 are the cable's angles and q_5 is the cable length, $\chi_{i,j}$ ($i = 1,2,3$ and $j = 1,2$) are internal variables of the approximate PID controllers while w_1, w_2 and w_3 are the external commands of the PID controllers for the rotational velocity of the crane, the position of the trolley and the cable length, respectively. The mathematical model of the tower crane is developed to be

$$\frac{dx}{dt} = \left[E\left(x\right)\right]^{-1} f\left(x,w\right),\ \ y = r\left(x\right),\ \ \psi = Lx \tag{3.1}$$

where $E\left(x\right) \in \mathbb{R}^{16\times16}$, $f\left(x,w\right) \in \mathbb{R}^{16\times1}$, $r\left(x\right) \in \mathbb{R}^{3\times1}$ and $L \in \mathbb{R}^{5\times16}$. The nonzero elements of $E\left(x\right)$ and $f\left(x,w\right)$ are:

$$e_{1,1}\left(x\right)=1,\ e_{2,2}\left(x\right)=1,\ e_{3,3}\left(x\right)=1,\ e_{4,4}\left(x\right)=1,\ e_{5,5}\left(x\right)=1$$
$$e_{6,6}\left(x\right)=J_1+J_2+J_5+l_c^2m_1+\left(m_2+m_5\right)x_2^2-2s_{x_4}m_5x_2x_5-$$
$$+0.25\left(c_{2x_3}+2c_{x_3}^2c_{2x_4}-3\right)m_5x_5^2,\ e_{6,7}\left(x\right)=-c_{x_4}s_{x_3}m_5x_5,$$
$$e_{6,8}\left(x\right)=c_{x_3}c_{x_4}m_5x_5\left(x_2-s_{x_4}x_5\right),\ e_{6,9}\left(x\right)=s_{x_3}J_5+m_5s_{x_3}x_5\left(x_5-s_{x_4}x_2\right),$$
$$e_{6,10}\left(x\right)=c_{x_4}s_{x_3}m_5x_2,\ e_{7,6}\left(x\right)=-c_{x_4}s_{x_3}m_5x_5,\ e_{7,7}\left(x\right)=m_2+m_5\ e_{7,9}\left(x\right)=-c_{x_4}m_5x_5,$$
$$e_{7,10}\left(x\right)=-s_{x_4}m_5,\ e_{8,6}\left(x\right)=c_{x_3}c_{x_4}m_5x_5\left(x_2-s_{x_4}x_5\right),\ e_{8,8}\left(x\right)=c_{x_4}^2m_5x_5^2+J_5,$$
$$e_{9,6}\left(x\right)=s_{x_3}J_5+m_5s_{x_3}x_5\left(x_5-s_{x_4}x_2\right),\ e_{9,7}\left(x\right)=-c_{x_4}m_5x_5,\ e_{9,9}\left(x\right)=m_5x_5^2+J_5,$$
$$e_{10,6}\left(x\right)=c_{x_4}s_{x_3}m_5x_2,\ e_{10,7}\left(x\right)=-s_{x_4}m_5,\ e_{10,10}\left(x\right)=m_5,\ e_{11,11}\left(x\right)=1,\ e_{12,12}\left(x\right)=1,$$
$$e_{13,13}\left(x\right)=1,\ e_{14,14}\left(x\right)=1,\ e_{15,15}\left(x\right)=1,\ e_{16,16}\left(x\right)=1$$

$$f_1\left(x,w\right)=x_6,\ f_2\left(x,w\right)=x_7,\ f_3\left(x,w\right)=x_8,\ f_4\left(x,w\right)=x_9,\ \ f_5\left(x,w\right)=x_{10},$$
$$f_6\left(x,w\right)=-2m_2x_2x_6x_7+0.5m_5x_5\left\{x_6\left[4s_{x_4}x_7+\right.\right.$$
$$\left.-2x_5\left(c_{x_4}^2s_{2x_3}x_8+c_{x_3}^2s_{2x_4}x_9\right)\right]-x_5x_8\left(s_{x_3}s_{2x_4}x_8+4c_{x_3}s_{x_4}^2x_9\right)+$$
$$\left.\left[\left(c_{2x_3}+2c_{x_3}^2c_{2x_4}-3\right)x_6+2c_{x_3}s_{2x_4}x_8-4s_{x_3}x_9\right]x_{10}\right\}+$$
$$m_5x_2\left(-2x_6x_7+c_{x_4}\left\{x_5\left[2x_6x_9+s_{x_3}\left(x_8^2+x_9^2\right)\right]-2c_{x_3}x_8x_{10}\right\}+\right.$$
$$\left.+2s_{x_4}\left[c_{x_3}x_5x_8x_9+\left(x_6+s_{x_3}x_9\right)x_{10}\right]\right)+w_1\left(\gamma_1f_{D,1}+f_{P,1}\right)$$
$$-J_5c_{x_3}x_8x_9-\gamma_1^2x_{12}f_{D,1}+\left(\gamma_1x_{11}+x_{12}\right)f_{I,1}-x_6\left(\gamma_1f_{D,1}+f_{P,1}\right),$$
$$f_7\left(x,w\right)=m_2x_2x_6^2+m_5x_2x_6^2+2m_5x_5c_{x_3}c_{x_4}x_6x_8-$$
$$m_5x_5s_{x_4}\left(x_6^2+2s_{x_3}x_6x_9+x_9^2\right)+2m_5c_{x_4}\left(s_{x_3}x_6+x_9\right)x_{10}+$$
$$\gamma_2f_{D,2}\left(w_2-x_2\right)-\gamma_2^2x_{14}f_{D,2}+\left(\gamma_2x_{13}+x_{14}\right)f_{I,2}+\left(w_2-x_2\right)f_{P,2}$$
$$f_8\left(x,w\right)=J_5c_{x_3}x_6x_9-gm_5c_{x_4}x_5s_{x_3}-2m_5c_{x_4}^2x_5x_8x_{10}+m_5c_{x_4}x_5^2\times$$
$$\left[2s_{x_4}x_8x_9+c_{x_3}c_{x_4}x_6\left(s_{x_3}x_6+2x_9\right)\right]-2m_5c_{x_3}c_{x_4}x_5x_6\left(x_7-s_{x_4}x_{10}\right)$$
$$f_9\left(x,w\right)=m_5s_{x_4}x_5\left(2s_{x_3}x_6x_7-gc_{x_3}\right)-J_5c_{x_3}x_6x_8-m_5c_{x_4}x_5x_2x_6^2$$
$$+m_5c_{x_4}x_5^2\left(c_{x_3}^2s_{x_4}x_6^2-2c_{x_3}c_{x_4}x_6x_8-s_{x_4}x_8^2\right)-2m_5x_5\left(s_{x_3}x_6+x_9\right)x_{10}$$
$$f_{10}\left(x,w\right)=-m_5s_{x_4}x_2x_6^2+m_5c_{x_4}\left(gc_{x_3}-2s_{x_3}x_6x_7\right)+$$
$$+m_5x_5x_6\left(2s_{x_3}x_9-c_{x_3}s_{2x_4}x_8\right)+m_5x_5\left(c_{x_4}^2x_8^2+x_9^2\right)-$$
$$0.25m_5x_5\left(2c_{2x_3}c_{x_4}^2+c_{2x_4}-3\right)x_6^2-\gamma_3^2x_{16}f_{D,3}+$$
$$+\left(\gamma_3x_{15}+x_{16}\right)f_{I,3}+\left(w_3-x_5\right)\left(\gamma_3f_{D,3}+f_{P,3}\right),\ f_{11}\left(x,w\right)=x_{12},$$

$$f_{12}\left(x,w\right)=w_1-x_6-\gamma_1 x_{12},\ f_{13}\left(x,w\right)=x_{14},\ f_{14}\left(x,w\right)=w_2-x_2-\gamma_2 x_{14},$$
$$f_{15}\left(x,w\right)=x_{16},\ f_{16}\left(x,w\right)=w_3-x_5-\gamma_3 x_{16}$$

The 1st performance output is the angular velocity of the payload (around the mast), i.e. $y_1=r_1\left(x\right)=x_6+s_{x_3}x_9$. The 2nd is the radial position of the payload, i.e. $y_2=r_2\left(x\right)=\left[x_2^2-2s_{x_4}x_2x_5+\left(c_{x_4}^2s_{x_3}^2+s_{x_4}^2\right)x_5^2\right]^{0.5}$ and the 3rd is the vertical distance of the payload from the ground, i.e. $y_3=r_3\left(x\right)=h_0-c_{x_3}c_{x_4}x_5$. Clearly it holds that $r\left(x\right)=\left[r_1\left(x\right)\quad r_2\left(x\right)\quad r_3\left(x\right)\right]^T$. The 1st measurable variable is the position of the trolley, i.e. x_2, the 2nd is the cable length, i.e. x_5, the 3rd is the angular velocity of the arm, i.e. x_6, the 4th is the velocity of the trolley, i.e. x_7 and the 5th is the rate of change of the cable's length, i.e. x_{10}. Hence, the nonzero elements of L are $l_{1,2}=1$, $l_{2,5}=1$, $l_{3,6}=1$, $l_{4,7}=1$ and $l_{5,10}=1$. m_1, m_2 and m_5 are the arm, trolley and payload masses respectively, J_1, J_2 and J_5 are the arm, trolley and payload moments of inertia respectively, g is the gravitational acceleration, l_c is the distance of the center of mass of the arm from the revolution axis of the crane, h_0 is the length of the mast. Note that Christoffel symbols have been used, i.e. $c_\alpha=\cos\left(\alpha\right)$ and $s_\alpha=\sin\left(\alpha\right)$. As already mentioned, each PID controller regulates one part of the crane. In particular, $f_{P,1}$, $f_{I,1}$ and $f_{D,1}$ are the proportional, integral and derivative gains respectively of the approximate PID controller that regulates the angular velocity of the crane, $f_{P,2}$, $f_{I,2}$ and $f_{D,2}$ are the gains of the approximate PID controller that regulates the position of the trolley, $f_{P,3}$, $f_{I,3}$ and $f_{D,3}$ are the gains of the approximate PID controller that regulates the cable length and γ_1, γ_2 and γ_3 are the three filter coefficients for the proper approximate implementation of the derivative terms of the three PID controllers, respectively. The parameters of the PID controllers are dedicated to achieve pole placement and asymptotic command following for the respective outputs. Additionally, the parameters of the 1st PID controller increase the properness of the respective closed loop transfer function. To satisfy the above requirements, the PID

controller parameters are derived to be

$$f_{P,1}=\frac{\left(J_1+l_c^2m_1\right)\left(\lambda_{1,1}\lambda_{2,1}-\lambda_{0,1}\right)}{\lambda_{2,1}^2},\ f_{P,2}=\frac{m_2\left(\lambda_{1,2}\lambda_{3,2}-\lambda_{0,2}\right)}{\lambda_{3,2}^2},$$

$$f_{P,3}=\frac{m_5\left(\lambda_{1,3}\lambda_{3,3}-\lambda_{0,3}\right)}{\lambda_{3,3}^2},$$

$$f_{I,1}=\frac{\left(J_1+l_c^2m_1\right)\lambda_{0,1}}{\lambda_{2,1}},\ f_{I,2}=\frac{m_2\lambda_{0,2}}{\lambda_{3,2}},\ f_{I,3}=\frac{m_5\lambda_{0,3}}{\lambda_{3,3}},$$

$$f_{D,1}=\frac{\left(J_1+l_c^2m_1\right)\left(\lambda_{0,1}-\lambda_{1,1}\lambda_{2,1}\right)}{\lambda_{2,1}^3},\ \gamma_1=\lambda_{2,1},\ f_{D,2}=\frac{m_2\left[\lambda_{0,2}+\lambda_{3,2}\left(\lambda_{2,2}\lambda_{3,2}-\lambda_{1,2}\right)\right]}{\lambda_{3,2}^3},$$

$$\gamma_2=\lambda_{3,2},\ f_{D,3}=\frac{m_5\left[\lambda_{0,3}+\lambda_{3,3}\left(\lambda_{2,3}\lambda_{3,3}-\lambda_{1,3}\right)\right]}{\lambda_{3,3}^3},\ \gamma_3=\lambda_{3,3}$$

where the parameters $\lambda_{i,j}$ $(i=0,1,2,3,\ j=1,2,3)$ are free to be chosen by the designer. They are the coefficients of the characteristic polynomials of each subsystem of the crane, i.e. it holds that

$$p_1\left(s\right)=s^3+\sum_{j=0}^{2}\lambda_{j,1}s^j,\ p_i\left(s\right)=s^4+\sum_{j=0}^{3}\lambda_{j,i}s^j\ \ (i=2,3)$$

Clearly, the parameters $\lambda_{j,i}$ should be chosen such that $p_i\left(s\right)$ $(i=1,2,3)$ are stable.

It is important to mention that, except the PID dynamics, the developed here dynamic model of the crane is more general than those presented in [7] and [8], in the sense that it includes variable cable length, as well as all coupling terms in the system dynamics.

3.2.2 Linear Approximant of the Model for Constant Velocity of the Arm

Here, a linear approximant of the nonlinear model (1) will be produced assuming that the arm of the crane rotates at constant angular velocity ω. Let $\overline{x}_i$ be the nominal points of x_i for $i=2,...,16$, where $\overline{x}_6=\omega$. So, the nominal trajectory of the angle of the arm is $\overline{x}_1\left(t\right)=\omega t+q_{1,0}$, where $q_{1,0}$ is the initial angle of the mast. Let $\overline{x}\left(t\right)$, $\overline{y}\left(t\right)$

and $\overline{w}(t)$ be the nominal trajectories of the state, performance output and input vectors of the model (1). It holds that $\overline{\dot{x}}(t) = \begin{bmatrix} \omega & 0_{1\times 15} \end{bmatrix}^T$. Let $\overline{w}(t) = \begin{bmatrix} \omega & x_2^* & x_5^* \end{bmatrix}^T$, where x_2^* and x_5^* are the nominal values of the position of the trolley along the arm and the cable length respectively. Using the above assumptions $\overline{x}(t)$ and $\overline{y}(t)$ are evaluated to be

$$\overline{x}_1(t) = \omega t + q_{1,0},\ \overline{x}_2 = x_2^*,\ \overline{x}_3 = 0,\ \overline{x}_5 = x_5^*,\ \overline{x}_6 = \omega,\ \overline{x}_7 = 0,\ \overline{x}_8 = 0,\ \overline{x}_9 = 0,$$
$$\overline{x}_{10} = 0,\ \overline{x}_{11} = 0,\ \overline{x}_{12} = 0,\ \overline{x}_{13} = -(m_2 + m_5)x_2^*\omega^2 / f_{I,2}\gamma_2,\ \overline{x}_{14} = 0,$$
$$\overline{x}_{15} = -m_5 g / f_{I,3}\gamma_3, \overline{x}_{16} = 0,\ \overline{y}_1 = \omega,\ \overline{y}_2 = x_2^* - x_5^* s_{\overline{x}_4},\ \overline{y}_3 = h_0 - x_5^* c_{\overline{x}_4}$$

where the nominal value $\overline{x}_4$ is evaluated by the equation

$$g s_{\overline{x}_4} + \omega^2 c_{\overline{x}_4}\left(x_2^* - x_5^* s_{\overline{x}_4}\right) = 0 \tag{3.2}$$

The deviations around the nominal values of the external commands and the performance, state and measurable variables are, $\Delta w = w - \overline{w}$, $\Delta y = y - \overline{y}$, $\Delta x = x - \overline{x}$ and $\Delta\psi = \psi - \overline{\psi}$ respectively. The linear approximant of the nonlinear model (1) is derived to be

$$\frac{d}{dt}\delta x = A\delta x + B\delta w,\ \delta y = C\delta x,\ \delta\psi = L\delta x \tag{3.3}$$

where $\delta w = \Delta w$ and, δx, δy and $\delta\psi$ are the responses of the linear approximant, approximating the deviations, Δx, Δy and $\Delta\psi$ respectively. The linear approximation takes place around an operating point $o(t) = \overline{o}(t)$ where $o(t) = \{w, x, y\}$ and $\overline{o}(t) = \{\overline{w}, \overline{x}, \overline{y}\}$. The linear approximant system matrices are of the form

$$\begin{bmatrix} A & B \end{bmatrix} = \begin{bmatrix} \dfrac{\partial}{\partial x} & \dfrac{\partial}{\partial w} \end{bmatrix}\left[E(x)\right]^{-1} f(x,w)\Big|_{o=\overline{o}},\ C = \left.\frac{\partial r(x)}{\partial x}\right|_{o=\overline{o}} \tag{3.4}$$

From (4) it can be concluded that A and B can be expressed in the form $A = \tilde{E}^{-1}\tilde{A}$ and $B = \tilde{E}^{-1}\tilde{B}$, where the nonzero elements of $\tilde{A}$, $\tilde{B}$ and $\tilde{E}$ are

$$\tilde{e}_{1,1} = 1,\ \tilde{e}_{2,2} = 1,\ \tilde{e}_{3,3} = 1,\ \tilde{e}_{4,4} = 1,\ \tilde{e}_{5,5} = 1,$$

$$\tilde{e}_{6,6} = J_1 + J_2 + J_5 + l_c^2 m_1 + x_5^* s_{\bar{x}_4}\left(x_5^* s_{\bar{x}_4} - 2x_2^*\right)m_5 + x_2^{*2}\left(m_2 + m_5\right),$$

$$\tilde{e}_{6,8} = x_5^* c_{\bar{x}_4}\left(x_2^* - x_5^* s_{\bar{x}_4}\right)m_5,\ \tilde{e}_{7,7} = m_2 + m_5,\ \tilde{e}_{7,9} = -x_5^* c_{\bar{x}_4} m_5\ ,\ \tilde{e}_{7,10} = -s_{\bar{x}_4} m_5,$$

$$\tilde{e}_{8,6} = x_5^* c_{\bar{x}_4}\left(x_2^* - x_5^* s_{\bar{x}_4}\right)m_5,$$

$$\tilde{e}_{8,8} = J_5 + x_5^{*2} c_{\bar{x}_4}^2 m_5,\ \tilde{e}_{9,7} = -x_5^* c_{\bar{x}_4} m_5\ \ \tilde{e}_{9,9} = J_5 + x_5^{*2} m_5,\ \tilde{e}_{10,7} = -s_{\bar{x}_4} m_5,\ \tilde{e}_{10,10} = m_5$$

$$,\ \tilde{e}_{11,11} = \tilde{e}_{12,12} = \tilde{e}_{13,13} = \tilde{e}_{13,13} = 1,\ \tilde{e}_{14,14} = \tilde{e}_{15,15} = \tilde{e}_{16,16} = 1,$$

$$\tilde{a}_{7,2} = \omega^2\left(m_2 + m_5\right) - \gamma_2 f_{D,2} - f_{P,2},\ \tilde{a}_{9,2} = -x_5^*\omega^2 c_{\bar{x}_4} m_5,\ \tilde{a}_{10,2} = -\omega^2 s_{\bar{x}_4} m_5,$$

$$\tilde{a}_{14,2} = -1,\ \tilde{a}_{8,3} = x_5^* c_{\bar{x}_4}\left(x_5^*\omega^2 c_{\bar{x}_4} - g\right)m_5,\ \tilde{a}_{7,4} = -x_5^*\omega^2 c_{\bar{x}_4} m_5,$$

$$\tilde{a}_{9,4} = x_5^*\left[\omega^2\left(x_5^* c_{2\bar{x}_4} + x_2^* s_{\bar{x}_4}\right) - g c_{\bar{x}_4}\right]m_5,\ \tilde{a}_{10,4} = \left[\omega^2 c_{\bar{x}_4}\left(2x_5^* s_{\bar{x}_4} - x_2^*\right) - g s_{\bar{x}_4}\right]m_5,$$

$$\tilde{a}_{7,5} = -\omega^2 s_{\bar{x}_4} m_5,\ \tilde{a}_{9,5} = \left[\omega^2 c_{\bar{x}_4}\left(2x_5^* s_{\bar{x}_4} - x_2^*\right) - g s_{\bar{x}_4}\right]m_5,$$

$$\tilde{a}_{10,5} = \omega^2 s_{\bar{x}_4}^2 m_5 - \gamma_3 f_{D,3} - f_{P,3},\ \tilde{a}_{16,5} = -1,\ \tilde{a}_{1,6} = 1,\ \tilde{a}_{6,6} = -\gamma_1 f_{D,1} - f_{P,1},$$

$$\tilde{a}_{7,6} = 2\omega\left[x_2^*\left(m_2 + m_5\right) - x_5^* s_{\bar{x}_4} m_5\right],\ \tilde{a}_{9,6} = 2x_5^*\omega c_{\bar{x}_4}\left(x_5^* s_{\bar{x}_4} - x_2^*\right)m_5,$$

$$\tilde{a}_{10,6} = 2\omega s_{\bar{x}_4}\left(x_5^* s_{\bar{x}_4} - x_2^*\right)m_5,\ \tilde{a}_{12,6} = -1,\ \tilde{a}_{2,7} = 1,$$

$$\tilde{a}_{6,7} = 2x_5^*\omega s_{\bar{x}_4} m_5 - 2x_2^*\omega\left(m_2 + m_5\right),\ \tilde{a}_{8,7} = -2x_5^*\omega c_{\bar{x}_4} m_5,\ \tilde{a}_{3,8} = 1,$$

$$\tilde{a}_{7,8} = 2x_5^*\omega c_{\bar{x}_4} m_5,\ \tilde{a}_{9,8} = -\omega\left(J_5 + 2x_5^{*2} c_{\bar{x}_4}^2 m_5\right),\ \tilde{a}_{10,8} = -2x_5^*\omega c_{\bar{x}_4} s_{\bar{x}_4} m_5,\ \tilde{a}_{4,9} = 1,$$

$$\tilde{a}_{6,9} = 2x_5^*\omega c_{\bar{x}_4}\left(x_2^* - x_5^* s_{\bar{x}_4}\right)m_5\ ,\ \tilde{a}_{7,9} = \omega\left(J_5 + 2x_5^{*2} c_{\bar{x}_4}^2 m_5\right),\ \tilde{a}_{5,10} = 1,$$

$$\tilde{a}_{6,10} = 2\omega s_{\bar{x}_4}\left(x_2^* - x_5^* s_{\bar{x}_4}\right)m_5,\ \tilde{a}_{8,10} = x_5^*\omega s_{2\bar{x}_4} m_5,\ \tilde{a}_{6,11} = \gamma_1 f_{I,1},\ \tilde{a}_{6,12} = -\gamma_1^2 f_{D,1} + f_{I,1},$$

$$\tilde{a}_{11,12} = 1,\ \tilde{a}_{12,12} = -\gamma_1,\ \tilde{a}_{7,13} = \gamma_2 f_{I,2},\ \tilde{a}_{7,14} = -\gamma_2^2 f_{D,2} + f_{I,2},\ \tilde{a}_{13,14} = 1,\ \tilde{a}_{14,14} = -\gamma_2,$$

$$\tilde{a}_{10,15} = \gamma_3 f_{I,3},\ \tilde{a}_{10,16} = -\gamma_3^2 f_{D,3} + f_{I,3},\ \tilde{a}_{15,16} = 1,\ \tilde{a}_{16,16} = -\gamma_3,\ \tilde{b}_{6,1} = \gamma_1 f_{D,1} + f_{P,1},$$

$$\tilde{b}_{7,2} = \gamma_2 f_{D,2} + f_{P,2},\ \tilde{b}_{10,3} = \gamma_3 f_{D,3} + f_{P,3},\ \tilde{b}_{12,1} = 1,\ \tilde{b}_{14,2} = 1,\ \tilde{b}_{16,3} = 1$$

The nonzero elements of C are

$$c_{1,6} = 1,\ c_{2,2} = 1\ ,\ c_{2,4} = -x_5^* c_{\bar{x}_4}\ ,\ c_{2,5} = -s_{\bar{x}_4}\ ,\ c_{3,4} = x_5^* s_{\bar{x}_4}\ \text{and}\ c_{3,5} = -c_{\bar{x}_4}\ .$$

3.2.3 Accuracy of the Linear Approximant

Here, it will be investigated via series of computational experiments if the linear

approximant (3.3) of the tower crane performs similarly to the nonlinear model (3.1). At first, assume that the model (3.1) operates on certain operating conditions. In particular, let $\overline{w}_1$, $\overline{w}_2$ and $\overline{w}_3$ be the nominal values of the external commands of the approximate PID controllers yielding the respective operating trajectories for the state variables, let $\overline{x}_1\left(t\right)$ and $\overline{x}_j$ for $j=2,\ldots,16$. In what follows, small variations of the model will be considered. To this end, the external commands are chosen to be of the form

$$w_i\left(t\right)=\overline{w}_i+\hat{w}_i\rho\left(t,\tau_1,\tau_2,T_1,T_2,T_3\right),\ i=1,2,3 \tag{3.5}$$

where $\hat{w}_i\in\left[\left(\hat{w}_i\right)_{\min},\left(\hat{w}_i\right)_{\max}\right]$ and where

$$\rho\left(t,\tau_1,\tau_2,T_1,T_2,T_3\right)=\sigma\left(t,\tau_1\right)-\sigma\left(t,\tau_2\right)+$$
$$-\frac{e^{\frac{\tau_1-t}{T_1}}T_1^2\left(T_2-T_3\right)-e^{\frac{\tau_1-t}{T_2}}T_2^2\left(T_1-T_3\right)+e^{\frac{\tau_1-t}{T_3}}T_3^2\left(T_1-T_2\right)}{\left(T_1-T_2\right)\left(T_1-T_3\right)\left(T_2-T_3\right)}\sigma\left(t,\tau_1\right)$$
$$+\frac{e^{\frac{\tau_2-t}{T_1}}T_1^2\left(T_2-T_3\right)-e^{\frac{\tau_2-t}{T_2}}T_2^2\left(T_1-T_3\right)+e^{\frac{\tau_2-t}{T_3}}T_3^2\left(T_1-T_2\right)}{\left(T_1-T_2\right)\left(T_1-T_3\right)\left(T_2-T_3\right)}\sigma\left(t,\tau_2\right)$$
$$\sigma\left(t,\tau_i\right)=\begin{cases}0 & t<\tau_i\\ 1 & t\geq\tau_i\end{cases},\ \tau_i=1,2$$

with $\tau_1<\tau_2$ and T_1, T_2, T_3 being positive different among themselves constants. The form of ρ is such that its 1st and 2nd derivatives with respect to time are smooth.

Using these input changes, the response of the nonlinear model (3.1) the system response regarding the performance outputs y_i ($i=1,2,3$) and the measurable variables ψ_k ($k=1,\ldots,5$) is computed. The responses of the linear approximant and nonlinear model are compared using a Euclidian type norm the form [28]

$$p\left(\varphi_j,\delta\varphi_j\right)=100\%\times\left\|\varphi_j\left(t\right)-\delta\varphi_j\left(t\right)-\overline{\varphi}_j\right\|_2\Big/\left\|\varphi_j\left(t\right)-\overline{\varphi}_j\right\|_2 \tag{3.6}$$

where φ_j is a signal representing the state, performance or measurable variables, $\left\|\varphi_j(t)\right\|_2 = \sqrt{\int_0^{\tau_{\max}} \left[\varphi_j(t)\right]^2 dt}$ and $\tau_{\max} \in \mathbb{R}^+$ where $\tau_{\max}$ represents a time instance, greater than the relaxation time of the argument response. To evaluate the cost criterion in (6), consider the test case presented in [29]

$$m_1 = 73.377\left[\text{Kgr}\right],\ m_2 = 2.492\left[\text{Kgr}\right],\ m_5 = 3.1415\left[\text{Kgr}\right],\ J_1 = 13.609\left[\text{Kgr m}^2\right],$$
$$J_2 = 8.572\left[\text{Kgr m}^2\right],\ J_5 = 0.01256\left[\text{Kgr m}^2\right],\ h_0 = 2.55\left[\text{m}\right],\ g = 9.81\left[\text{m/sec}^2\right],$$
$$l_c = 0.4517\left[\text{m}\right]$$

The nominal values and the controller parameters are

$$\omega = \pi / 20\left[\text{rad/sec}\right],\ q_{1,0} = 0\left[\text{rad}\right],\ \overline{x}_2^* = 0.5\left[\text{m}\right],\ \overline{x}_5^* = 0.5\left[\text{m}\right],\ \lambda_{0,1} = 4766.52,$$
$$\lambda_{1,1} = 889.21, \lambda_{2,1} = 53,\ \lambda_{0,2} = 1712.2557,\ \lambda_{1,2} = 1425.512,\ \lambda_{2,2} = 371.78,$$
$$\lambda_{3,2} = 35.2,\ \lambda_{0,3} = 122138.016,\ \lambda_{1,3} = 30449.576,\ \lambda_{2,3} = 2475.06,\ \lambda_{3,3} = 83.1,$$
$$\overline{w}_1 = \pi / 6\left[\text{rad/sec}\right],\ \overline{w}_2 = 0.5\left[\text{m}\right],\ \overline{w}_3 = 0.75\left[\text{m}\right]$$

For the above values of the system parameters, the inner controller coefficients are computed to be

$$f_{p,1} = 431.01,\ f_{i,1} = 2570.35,\ f_{d,1} = -8.13227,\ \gamma_1 = 53$$

$$f_{p,2} = 97.476,\ f_{i,2} = 121.22,\ f_{d,2} = 23.5511,\ \gamma_2 = 35.2$$

$$f_{p,3} = 1095.58,\ f_{i,3} = 4617.42,\ f_{d,3} = 80.3857,\ \gamma_3 = 83.1$$

while the operating trajectories for the state variables and performance outputs are evaluated to be

$$\overline{x}_1(t) = \pi t / 20\left[\text{rad}\right],\ \overline{x}_2 = 0.5\left[\text{m}\right]\ \overline{x}_3 = 0\left[\text{rad}\right],\ \overline{x}_4 = -0.00125918\left[\text{rad}\right],$$
$$\overline{x}_5 = 0.5\left[\text{m}\right],\ \overline{x}_6 = \pi / 20\left[\text{rad/sec}\right],\ \overline{x}_7 = 0\left[\text{m/sec}\right], \overline{x}_8 = 0\left[\text{rad/sec}\right],$$

$$\overline{x}_9 = 0\left[\text{rad/sec}\right],\ \overline{x}_{10} = 0\left[\text{m/sec}\right],\ \overline{x}_{11} = 0\left[\text{-}\right],\ \overline{x}_{12} = 0\left[\text{-}\right],\ \overline{x}_{13} = 0\left[\text{-}\right],\ \overline{x}_{14} = 0\left[\text{-}\right],$$
$$\overline{x}_{15} = 0\left[\text{-}\right],\ \overline{x}_{16} = 0\left[\text{-}\right],\ \overline{y}_1 = \pi / 20\left[\text{rad/sec}\right],\ \overline{y}_2 = 0.5006\left[\text{m}\right],\ \overline{y}_3 = 2.05016\left[\text{m}\right]$$

To evaluate the accuracy of the linear approximant through the cost criterion (3.6) for the measurable and performance variables of the plant, the external commands are considered to deviate from their nominal values about 15%, i.e. $\left|\hat{w}_i / \overline{w}_i\right| < 0.15$ $(i = 1,2,3)$. Here, the level of accuracy of the linear approximant is considered to be the maximum of p for all performance and measurable variables. After computing the level of accuracy for all combinations in the aforementioned indicative deviation bounds of the external commands, it has been shown that a level of accuracy of 10.16% is derived, i.e. for all combinations of the external commands in $\left|\hat{w}_i / \overline{w}_i\right| < 0.15$, the maximum of $p\left(\varphi_j, \delta\varphi_j\right)$ for $\varphi_j \in \left\{y_1, y_2, y_3, \psi_1, \ldots, \psi_5\right\}$ is less than or equal to 10.16%. Hence, it can be stated that that the linear approximant (3.3) is an accurate representation of the nonlinear model (1) and so a controller can be designed based on it.

3.2.4 Wireless Controller Implementation

Wireless control overcomes mobility limitations and enhances the system's flexibility especially for the case of controlling simultaneously multiple mechanisms. However, wireless control necessitates the use of high-fidelity equipment. For our purposes, neither data storage limitations, transmission rate nor long distances are crucial factors to consider. A major limitation to consider is the need for a telecommunication signal resisting to noise and other users' interference. This is an inherent situation to any industrial environment.

3.2.5 Measurable Variables

Since a wireless controller must be designed, a transmission delay is expected between the sensors and the controller base. Furthermore, this transmission delay is in general time varying. Hence, the vector of the system's measurable outputs $\psi\left(t\right)$ is truly $\psi\left(t\right) = Lx\left(t - \tau_1\left(t\right)\right)$. Note that the delay $\tau_1\left(t\right)$ stands for the

transmission/reconstruction delay taking place between the sensors and the controller. Without loss of generality, this delay is assumed to be the same for all measurable variables. In the following subsections, an appropriate transmission/reconstruction algorithm will be proposed in order to eliminate delay variations. Elimination of the delay variations will clearly facilitate controller design and implementation.

3.2.6 Controller Configuration

With respect to the controller configuration, it is considered that the setup consists of two separates Networks (see Fig.3.2)

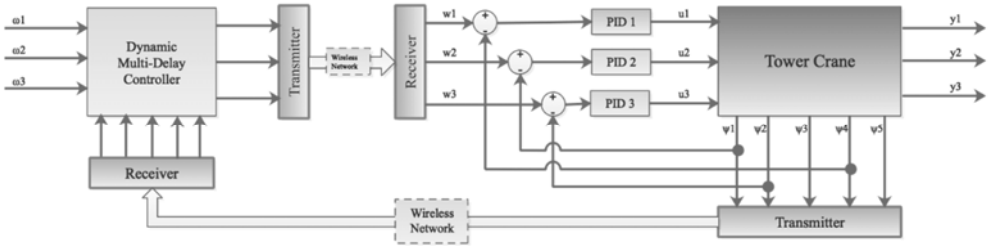

Fig. 3.2 Block diagram of the closed loop system.

The 1st network is dedicated to the transmission of the measurable outputs from the sensors to the controller, while the 2nd network is dedicated to the transmission of the inner PID external commands to the preinstalled PIDs on the tower crane. Each network consists of a single transmitter and a single receiver. The transmitter and receiver of the tower crane are assumed to be located at the highest point of the mast while the 2nd transmitter / receiver system is located at the controller base at the ground. It is important to point out that since the inner PID external commands are transmitted to the local preinstalled controllers, a transmission delay is expected between the base and the crane. Furthermore, this transmission delay, denoted by $\tau_2(t)$, is time varying. Consequently, the nonlinear model in (1) takes on the form

$$\frac{dx(t)}{dt} = \left[E(x(t))\right]^{-1} f\left(x(t), w\left(t - \tau_2(t)\right)\right) \tag{3.7}$$

Clearly, the signals of each network cannot be transmitted simultaneously, and an appropriate synchronization algorithm is needed. As already mentioned, this algorithm must satisfy the specification of equal delay for all signals.

3.2.7 Communication Protocol

With the aforementioned factors in mind, the Wi-Fi, the Bluetooth and the ZigBee protocols were recognized as suitable candidates. The connectivity of Bluetooth is practically limited to a several meters distance. Moreover, its activation latency, typically about three seconds, was considered rather large for the present application. ZigBee as compared to Wi-Fi is cheaper, easier to implement, more robust from a networking topology perspective and less power consuming. Further-on, the robustness of both systems' direct sequence spread spectrum (ds-ss) modulation is evaluated and compared, since it constitutes the most determining factor against interference. To account for ZigBee's IEEE 802.15.4 Mac/Physical layer, a 31 chips Gold sequence is used. For the Wi-Fi case, the known 11-chip Barker pn-sequence '110110111000' is used. At both cases, a zero-mean average white Gaussian noise is added using a uniform random number generator. According to the emulation test results, the comparison between ZigBee and Wi-Fi clearly demonstrated the effectiveness of the 802.15.4 modulation type, in terms of signal to noise ratio.

3.2.8 Elimination of the Transmission Delay Variations

As mentioned in the previous subsections, time varying delays appear during wireless communication between the base and the tower crane. Furthermore, due to the system's configuration, the signals cannot be transmitted simultaneously. In the present section a signal transmission/ synchronization approach will be proposed to synchronize the transmitted signals and eliminate delay variations.

To this end, assume that a set of n_s signals, let $\varphi_i (i = 1,\ldots,n_s)$, needs to be transmitted. Furthermore, define a base clock period, let T_s, upon which signal transmission changes take place. The synchronization algorithm is proposed to be:

Synchronization Algorithm

Step 1: At $t = t_0$ sample and hold $\varphi_i\left(t_0\right)$ for $i = 1,\ldots,n_s$.

Step 2: Let $i = 1$.

Step 3: For the time period $t_0 + T_s\left(i-1\right) \le t < t_0 + T_s i$ the transmitter is triggered to transmit the value $\varphi_i\left(t_0\right)$. Within the above time period, triggering takes place multiple times at a sub period T_s / r_p where $r_p \ge 2$. The receiver holds the value $\varphi_i\left(t_0\right)$.

Step 4: Let $i = i + 1$.

Step 5: If $i \le n_s$ go to ***Step 3*** else go to ***Step 6***.

Step 6: For the time period $t_0 + T_s n_s \le t < t_0 + T_s\left(n_s + 1\right)$ the transmitter is triggered to transmit a "loop completion" signal to the receiver. Within the above time period, triggering takes place multiple times at a sub period T_s / r_p where $r_p \ge 2$. As soon as the receiver gets the "loop completion" signal releases as output $\varphi_i\left(t_0\right)$ ($i = 1,\ldots,n_s$).

Step 7: Let $t_0 = t_0 + T_s\left(n_s + 1\right)$.

Step 8: Go to ***Step 1***.

Although in the above procedure multiple transmissions of the same signal take place, it guaranties from the practical point of view that all transmitted signals are synchronized, while a constant delay transmission of $T_s\left(n_s + 1\right)$ time units is achieved.

3.2.9 Signal Reconstruction

The final task in the signal transmission scheme lies in the reconstruction of the continuous time signal at the receiver, using discrete time signal data. To this end, there exist several well-established procedures, such as “zero order hold” (ZOH) and “first order hold” (FOH). The main disadvantage of these techniques is that they generate discontinuous non-smooth signals that may produce significant errors if used for control purposes, especially if the control schemes include derivative terms. To avoid these drawbacks, in the present work a “delayed interpolation” scheme will be proposed. The basic idea of this approach is to use past data available to the designer to reconstruct the signal at the present time. The reconstruction is accomplished by evaluating appropriate interpolating functions based upon the past data. Then the interpolating function is used to generate the signal at the present time.

The proposed procedure will be applied choosing a second order interpolation scheme. At a time instance $t = kT$, where T is the sampling period, three consecutive samples are available from a transmitted signal $\varphi(t)$, let $\varphi(kT)$, $\varphi(kT-T)$ and $\varphi(kT-2T)$. The second order interpolating function passing from all data points is of the form $\vartheta(t) = \beta_2(kT)t^2 + \beta_1(kT)t + \beta_0(kT)$. It can be verified that the polynomial coefficients $\beta_0(kT)$, $\beta_1(kT)$ and $\beta_2(kT)$ can be evaluated through the relation

$$\begin{bmatrix} (kT)^2 & kT & 1 \\ (kT-T)^2 & kT-T & 1 \\ (kT-2T)^2 & kT-2T & 1 \end{bmatrix} \begin{bmatrix} \beta_2(kT) \\ \beta_1(kT) \\ \beta_0(kT) \end{bmatrix} = \begin{bmatrix} \varphi(kT) \\ \varphi(kT-T) \\ \varphi(kT-2T) \end{bmatrix} \tag{3.8}$$

The system in (8) is solvable if and only if $T \neq 0$ which is obviously satisfied. For $t \in (kT, kT+T]$ the reconstructed signal, let $\varphi_r(t)$, becomes $\varphi_r(t) = \vartheta(t-2T)$. Clearly, this scheme does not use extrapolation of past data, thus providing accurate reconstruction. The main disadvantage is that it introduces an additional time delay to the reconstructed signals. Nevertheless, in the present work this issue is overcome using a controller that incorporates the time delays.

To demonstrate the efficiency of the proposed scheme the test signal $\varphi(t) = \sin(2t)\sin(3t) / (2 + \cos(4t))$ is considered. Different sampling periods from $0.1[\text{sec}]$ to $0.5[\text{sec}]$ are used and the sampled signal is reconstructed using ZOH, FOH and the delayed interpolation approach proposed herein. Defining a percentile error norm of the form $p(\varphi, \varphi_r) = 100\% \|\varphi(t) - \varphi_r(t)\|_2 / \|\varphi(t)\|_2$ it is observed that for all sampling periods examined, the delayed interpolation scheme provides far more accurate reconstruction than the ZOH or FOH schemes (see Figure 3.3). It is noted that in the above experiment the two sampling periods delay of the reconstructed signal produced by the delayed interpolation scheme has been considered.

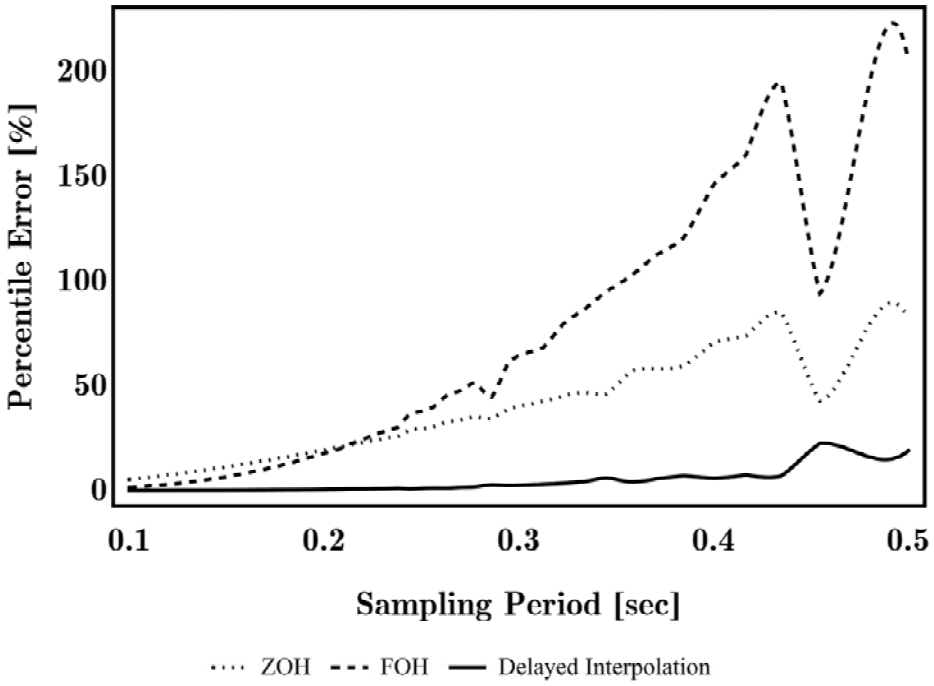

Fig. 3.3 Signal Reconstruction Error for Different Sampling Periods.

The previous algorithm of signal synchronization and signal reconstruction is depicted in the figure 3.4 above.

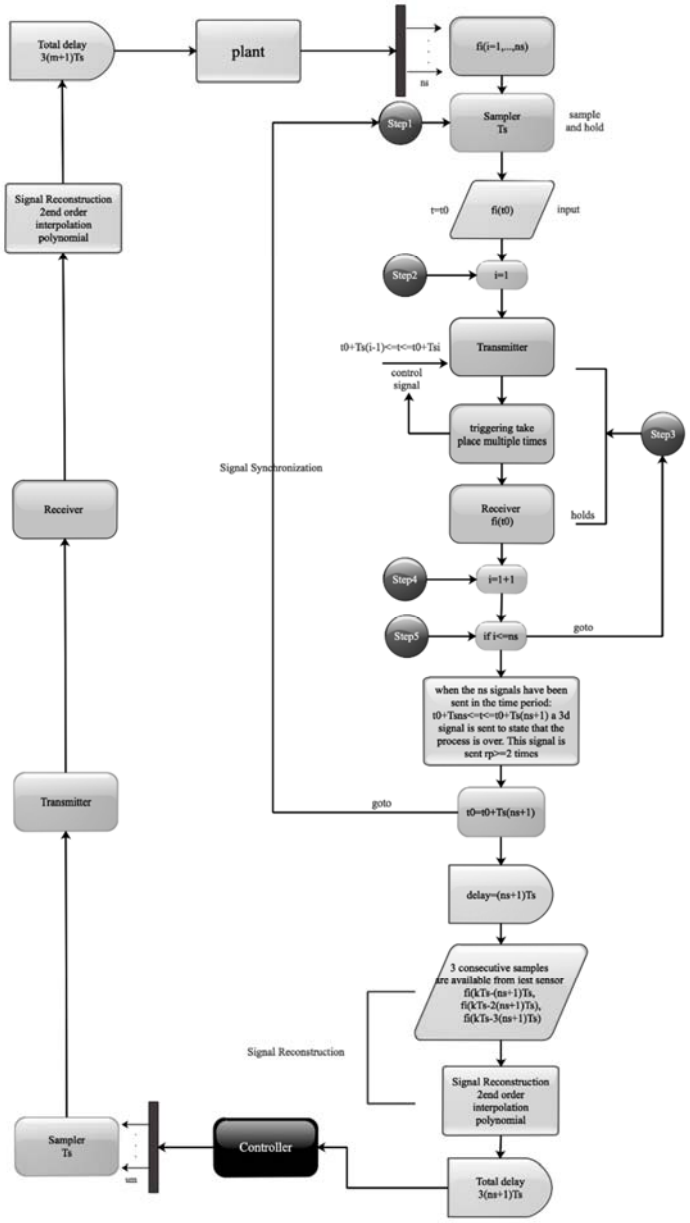

Fig. 3.4 Block diagram of a WNC n^{th} order system with m actuatable inputs where flow chart of signal synchronization/reconstruction algorithm is depicted.

3.2.10 Controller Design

In the present section a dynamic controller will be designed in order to control the performance outputs of the tower crane. In particular the design goal will be that of Input / Output (I/O) Decoupling (see [30] and [31]), where each performance output is controlled by only one external input. Using the results presented in the previous sections and considering that constant transmission / reconstruction delays exists between the controller and the actuators, the overall linear approximant of the nonlinear model takes on the form

$$\frac{d}{dt}\delta x\left(t\right) = A\delta x\left(t\right) + B\delta w\left(t-\tau_2\right) \tag{3.9a}$$

$$\delta y\left(t\right) = C\delta x\left(t\right),\ \delta\psi\left(t\right) = L\delta x\left(t-\tau_1\right) \tag{3.9b}$$

where τ_1 and τ_2 are the constant transmission/reconstruction delays between the sensors and the controller respectively and the controller and the actuators respectively. For the I/O Decoupling goal, the interest is focused on the forced behaviour of the system, i.e. for zero initial and past conditions ($x\left(t\right)=0, w\left(t\right)=0$ for $t\le 0$). The system in (9) can be described in the frequency domain by the following set of algebraic equations

$$s\delta X\left(s\right) = A\delta X\left(s\right) + z_2 B\delta W\left(s\right) \tag{3.10a}$$

$$\delta Y\left(s\right) = C\delta X\left(s\right),\ \delta\Psi\left(s\right) = z_1 L\delta X\left(s\right) \tag{3.10b}$$

where $z_1 = e^{-s\tau_1}$ and $z_2 = e^{-s\tau_2}$, $\delta X\left(s\right) = \mathbf{L}_-\left\{\delta x\left(t\right)\right\}$, $\delta W\left(s\right) = \mathbf{L}_-\left\{\delta w\left(t\right)\right\}$, $\delta Y\left(s\right) = \mathbf{L}_-\left\{\delta y\left(t\right)\right\}$ and $\delta\Psi\left(s\right) = \mathbf{L}_-\left\{\delta\psi\left(t\right)\right\}$ with $\mathbf{L}_-\left\{\bullet\right\}$ be the Laplace transform of the argument signal.

To derive a decoupled closed loop system, the feedback is proposed to be of the dynamic multi delay type (see [30]), i.e.

$$\delta W(s) = K(s, z_1, z_2)\delta\Psi(s) + G(s, z_1, z_2)\Omega(s) \tag{3.11}$$

where $\Omega(s)$ is the 3×1 vector of external inputs and where the elements of the matrices $K(s, z_1, z_2)$ and $G(s, z_1, z_2)$ are rational functions of s with coefficients being functions of z_1 and z_2. It must be noted that the implementability of the controller requires that the elements of the matrices $K(s, z_1, z_2)$ and $G(s, z_1, z_2)$ must be realizable ([30] and [31]). Substituting (3.11) to (3.10) the I/O decoupling problem is formally stated as follows (see [30] and [31]): Find $K(s, z_1, z_2)$ and $G(s, z_1, z_2)$ such that

$$z_2 C\left[sI_{16} - A - z_1 z_2 BK(s, z_1, z_2)L\right]^{-1} BG(s, z_1, z_2) = \operatorname*{diag}_{i=1,\ldots,3}\left\{h_i(s, z_1, z_2)\right\} \tag{3.12}$$

where $h_i(s, z_1, z_2)$ are appropriate different than zero rational functions of s with coefficients being functions of z_1 and z_2 and I_n is the n-dimensional unitary matrix. Equation (12) formulates the problem in a normal system form. For the equation (3.12) to be well defined the precompensator $G(s, z_1, z_2)$ must be invertible and the feedback matrix $K(s, z_1, z_2)$ is restricted to satisfy the inequality

$$\det\left[sI_{16} - A - z_1 z_2 BK(s, z_1, z_2)L\right] \not\equiv 0 \tag{3.13}$$

Let

$$L_B(s, z_1, z_2) = z_1 z_2 L\left(sI_{16} - A\right)^{-1} B \tag{3.14a}$$

$$H_B(s, z_2) = z_2 C\left(sI_{16} - A\right)^{-1} B \tag{3.14b}$$

where $L_B(s, z_1, z_2)$ is the transfer matrix mapping the actuatable inputs to the measurable variables and $H_B(s, z_2)$ is the transfer matrix mapping the actuatable inputs to the performance variables. Using the results presented in [31], it can be

verified that the solution of the controller matrices presented in (11) solving the I/O decoupling problem are,

$$K\left(s,z_1,z_2\right)\text{: arbitrary proper and realizable} \tag{3.15a}$$

$$G\left(s,z_1,z_2\right)=\left\{I_5-K\left(s,z_1,z_2\right)L_B\left(s,z_1,z_2\right)\right\}\left[H_B\left(s,z_2\right)\right]^{-1}\operatorname*{diag}_{i=1,\ldots,3}\left\{h_i\left(s,z_1,z_2\right)\right\} \tag{3.15b}$$

For $G\left(s,z_1,z_2\right)$ to be invertible and realizable, it is necessary for $h_i\left(s,z_1,z_2\right)$ ($i=1,\ldots,3$) to be different than zero and sufficiently realizable. For example the index of realizability of $h_i\left(s,z_1,z_2\right)$ should be greater than or equal to the minus of the index of realizability of the *i*-th column of $\left\{I_5-K\left(s,z_1,z_2\right)L_B\left(s,z_1,z_2\right)\right\}\left[H_B\left(s,z_2\right)\right]^{-1}$. Obviously, $L_B\left(s,z_1,z_2\right)$ is realizable. It can be proven that the index of realizability $\left[H_B\left(s,z_2\right)\right]^{-1}$ is $-\tau_2$. Thus, the index of realizability of $h_i\left(s,z_1,z_2\right)$ ($i=1,\ldots,3$) must be greater than or equal to τ_2.

The diagonal elements of the closed loop transfer matrix connecting the external commands to the respective performance outputs are selected to be of the form:

$$h_i\left(s\right)=z_2\left(1+\sum_{j=1}^{5}\alpha_j s^j\right)/\prod_{j=1}^{7}\left(\zeta_{i,j}s+1\right) \tag{3.16}$$

where $\zeta_{i,j}$ ($i=1,2,3$, $j=1,\ldots,7$) are positive numbers. The independent of the delays denominator guaranties asymptotic command following for the performance outputs of the system.

The parameters α_i ($i=1,\ldots,5$) are dedicated to cancelling out in (3.15b) possible unstable roots of $\left\{I_5-K\left(s,z_1,z_2\right)L_B\left(s,z_1,z_2\right)\right\}\left[H_B\left(s,z_2\right)\right]^{-1}$ by $h_i\left(s\right)$.

3.2.11 Performance of the Closed Loop System

To demonstrate the performance of the control scheme proposed in 3.2.10, consider the data presented in 3.2. To simulate the influence of the wireless network,

the TrueTime Simulator [32] will be used. With regard to the network parameters, the data rate is $250\left[\text{kbps}\right]$, the minimum frame size is $30\left[\text{byte}\right]$, the transmit power is $0\left[\text{dBm}\right]$, the receiver signal threshold is $-85\left[\text{dbm}\right]$, the path loss exponent is $5.5\left[-\right]$, the ACK timeout is $8.64\cdot 10^{-4}\left[\text{sec}\right]$, the retry limit is $3\left[-\right]$ and the packet size is $126\left[\text{byte}\right]$. Furthermore it is considered that $T_s = 0.01\left[\text{sec}\right]$ and $r_p = 2$. The diagonal elements of the closed loop transfer matrix are selected to be $\zeta_{i,1} = 1.0$, $\zeta_{i,2} = 1.2$, $\zeta_{i,3} = 1.4$, $\zeta_{i,4} = 1.6$, $\zeta_{i,5} = 1.8$, $\zeta_{i,6} = 2.0$, $\zeta_{i,7} = 2.2$ for $i = 1,2,3$. Furthermore, we select $\alpha_1 = -2.83721\times 10^{-22}$, $\alpha_2 = 0.000042283$, $\alpha_3 = -3.534\times 10^{-19}$, $\alpha_4 = 0.052667$ and $\alpha_5 = -6.7101156\times 10^{-18}$. The feedback matrix $K\left(s, z_1, z_2\right)$ is chosen to be static thus guaranteeing properness and realizability, i.e.

$$K = \begin{bmatrix} 1.5541576 & 2.6063396 & -0.04554566 & -0.068197 & 0.04717 \\ 0.1274696 & -0.3491352 & -0.002501128 & -0.03775 & -0.0038487 \\ -0.9324828 & 0.098935732 & -0.01374911 & -0.06254563 & 0.0151221 \end{bmatrix} \tag{3.17}$$

The above selection of the feedback matrix increases the stability margin of the closed loop system, as compared to the open loop system, to more than 50%. Using (3.15b), the precompensator is derived to be of the form:

$$G\left(s, z_1, z_2\right) = \left[\tilde{G}_{i,j}\left(s\right) + z_1 z_2 \hat{G}_{i,j}\left(s\right)\right] / \bar{G}\left(s\right),\ i, j = \left\{1,2,3\right\} \tag{3.18}$$

where $\tilde{G}_{i,j}\left(s\right)$, $\hat{G}_{i,j}\left(s\right)$ and $\bar{G}\left(s\right)$ are appropriate polynomials of s (independent of z_1 and z_2). The external commands are chosen to be unit step changes of the form $\omega_1\left(t\right) = 0.1\overline{y}_1$, $\omega_2\left(t\right) = 0.1\overline{y}_2$, $\omega_3\left(t\right) = -0.15\overline{y}_3$. To demonstrate the performance of the proposed control scheme when applied to the nonlinear model of the plant (3.1), Figures 3.5 to 3.10 are presented. In Figures 3.5 to 3.7 the closed loop responses of the performance outputs for both the linear (dotted line) and the nonlinear (continuous line) closed loop systems are presented, while in Figures 3.8 to 3.10 the actuator forces are presented. With respect to the performance outputs (Figures 3.5 to 3.7), it can

readily be observed that the closed loop responses follow accurately (being almost visually identical) the reference responses. With respect to the actuator forces (Figures 3.8 to 3.10), it is observed that they do not present significant fluctuations, especially for the mast rotation and cart position actuators. With respect to the cable length actuator (Figure 3.8), fast varying changes can be observed. Nevertheless, their amplitude is small, thus not imposing any significant difficulty in the implementation. With respect to the state variables of the system it is mentioned that they all remain within acceptable limits. Finally, it is important to mention that the accuracy range of the linear approximant of the closed loop system as compared to the nonlinear one is preserved.

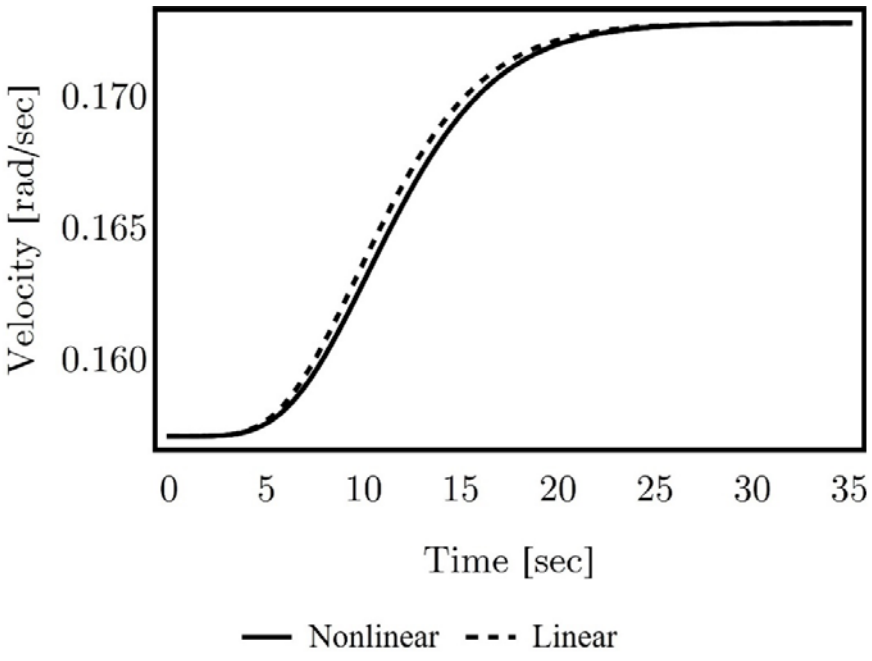

Fig. 3.5 Nonlinear and Linear Closed Loop Response for $y_1(t)$.

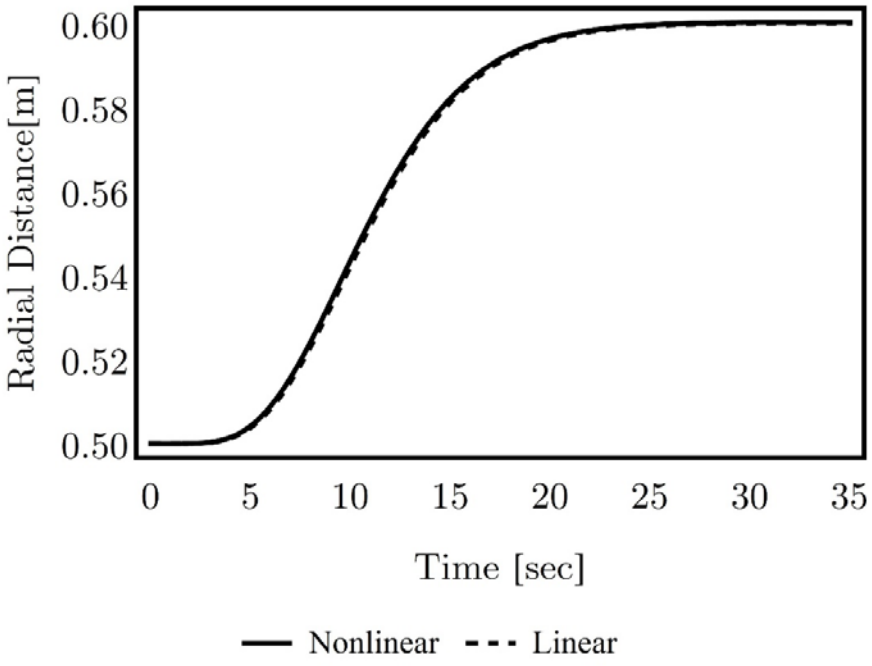

Fig. 3.6 Nonlinear and Linear Closed Loop Response for $y_2(t)$.

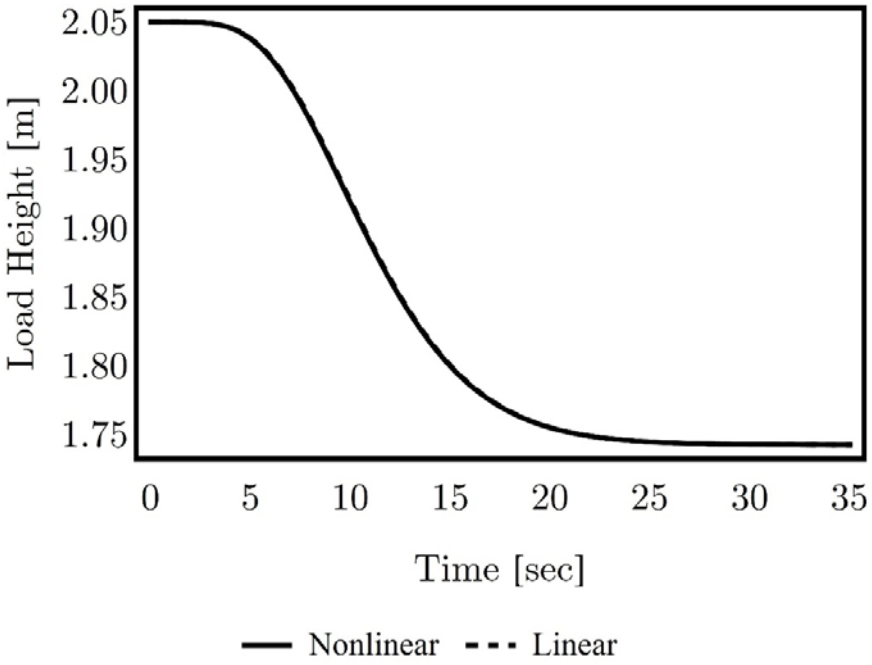

Fig. 3.7 Nonlinear and Linear Closed Loop Response for $y_3(t)$.

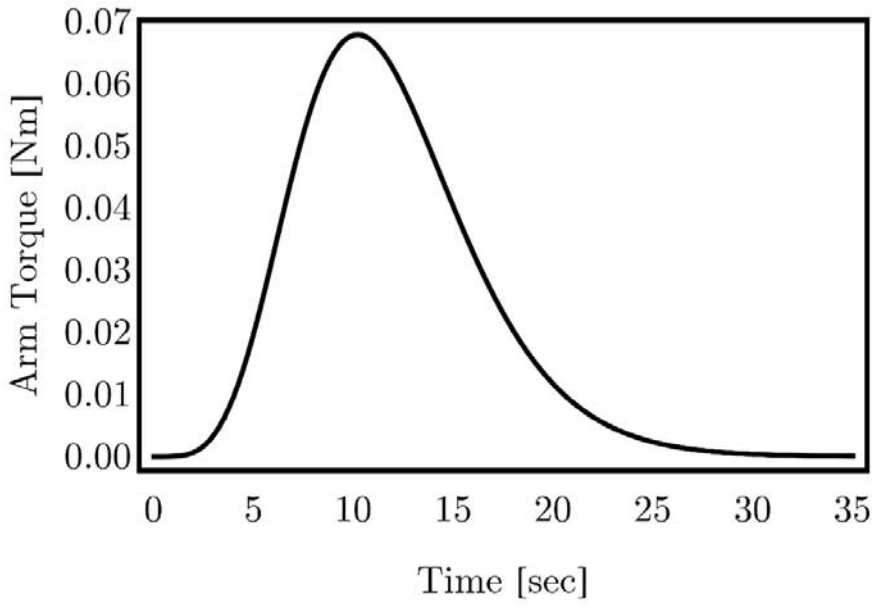

Fig. 3.8 Nonlinear Closed Loop Response for the Arm Actuator Torque.

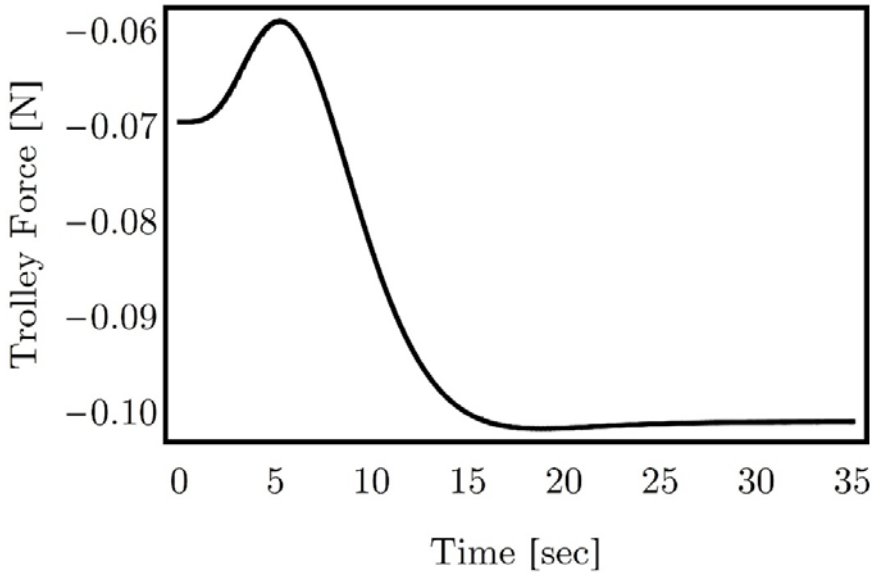

Fig. 3.9 Nonlinear Closed Loop Response for the Trolley Actuator Force.

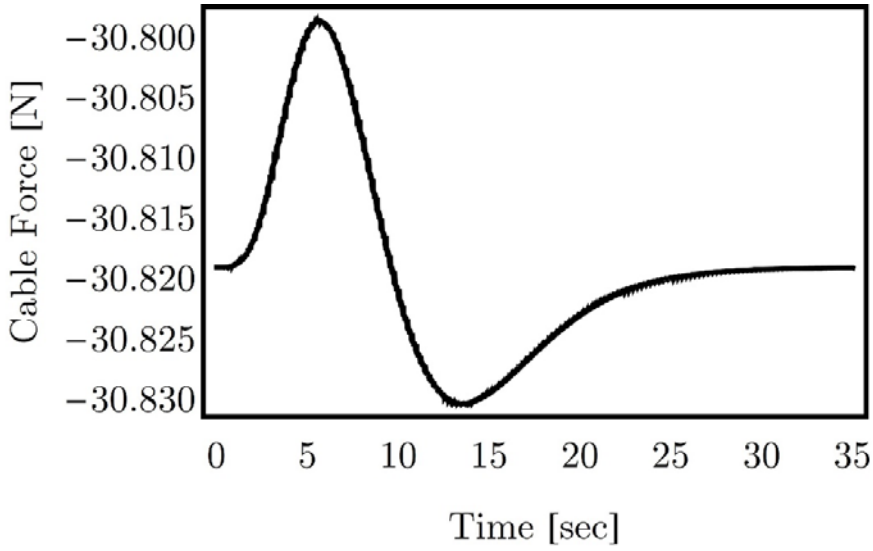

Fig. 3.10 Nonlinear Closed Loop Response for the Cable Actuator Force.

The influence of the presence of the delays to the controller performance and the necessity for the design of a delay dependent controller is a very important issue. To investigate this issue, consider the case where the controller $\delta W\left(s\right) = K\delta\Psi\left(s\right) + G\left(s,1,1\right)\Omega\left(s\right)$ is used where K and $G\left(s,z_1,z_2\right)$ are given in (3.17)-(3.18). The nonlinear closed loop response for this case will be compared to the respective one using the delay dependent controller presented in the previous paragraph. To compare the responses, consider the percentile error of the form (3.6) with $\tau_{\max} = 30\left[\sec\right]$. It is observed that the percentile error for the first performance variable using the proposed controller in 3.2.10 as compared to the one using the delayless controller is 96.23% smaller. For the second performance variable the respective error is 91.45% smaller while for the third performance variable the respective error is 78.62% smaller. Clearly, the proposed delay dependent controller approach produces far more accurate results.

The final issue that needs to be addressed is whether the use of the delayed interpolation scheme (for the analogue signal reconstruction from the transmitted signals) is advantageous as compared to the use of classical reconstruction approaches such as the ZOH approach, especially after recalling that the delayed interpolation scheme as used in the present work increases the transmission delay by two cycles. With respect to the accuracy of the signal reconstruction, the issue has been examined

in 3.2.9 where it has been observed that the reconstructed signal using the delayed interpolation technique is far more accurate. With respect to the performance outputs it can be observed that using the ZOH approach the results are similar to those using the delayed interpolation approach. The main advantage of the delayed interpolation approach lies in the fact that it produces smooth responses for the state variables in the sense that the acceleration of the state variables x_1 to x_5 does not present high oscillatory behavior. Furthermore, the peak values in the zero order hold case are significantly larger as compared to the respective ones in the delayed interpolation approach. The variation ranges for $\dot{x}_6(t)$, $\dot{x}_7(t)$, $\dot{x}_8(t)$, $\dot{x}_9(t)$ and $\dot{x}_{10}(t)$ are 12.91, 250.85, 282.7, 9713.9 and 426.88 times greater in the ZOH case than in the delayed interpolation case. High variations in the accelerations of the system motion variables may lead to destructive conditions to the system and reveal flexible structure characteristics that should be included in the model (3.1), thus producing a more complex mathematical model to describe the system's dynamics and consequently requiring the design of a much more complex controller. Similar conclusions can be drawn for the implementation of the actuator forces where an additional issue regarding the implementability of these forces arises. Indeed, in the ZOH case, the variation ranges for the actuator forces are 10.85, 47.76 and 426.37 times greater than in the delayed interpolation case.

3.3 SUMMARY

In this work, the standard model of the crane was modified to include variable cable length as well as include all coupling terms in the system dynamics. In addition, the nonlinear dynamics of the plant were accurately linearized. An appropriate realizable multi-delay dynamic controller has been designed based on the linear approximant of the crane and applied on the realistic nonlinear model. The variability of the time delays in the communication between sensors to controller and controller to actuators, which is generally induced by wireless network has a significant impact on the stability and robustness of the controller, was successfully handled with the development of a synchronization algorithm. At the same time, a signal reconstruction algorithm ensures the accurate signal transmission between the plant and the controller. The proposed controller, that depends on constant communication delays, provides stability and I/O decoupling. The efficiency of our algorithms has been

demonstrated with appropriate computer simulation. This approach is particularly useful for industrial purposes where remote operation via wireless communication network can be severely hindered by communication delays.

REFERENCES

[1] W. Singhose, J. Lawrence, K. Sorensen, and K. Dooroo, "Applications and educational uses of crane oscillation control," *FME Transactions,* vol. 34, pp. 175-183, 2006.

[2] G. G. Parker, A. P. Smith, and K. P. Hogan, "Access to the upper forest canopy with a large tower crane," *BioScience*, vol. 42, pp. 664-670, 1992.

[3] E. M. Abdel-Rahman, A. H. Nayfeh, and Z. N. Masoud, "Dynamics and control of cranes: A review," *Journal of Vibration and Control,* vol. 9, pp. 863-908, 2003.

[4] N. Zrnić and S. Bošnjak, "Comments on "Modeling of system dynamics of a slewing flexible beam with moving payload pendulum"," *Mechanics Research Communications,* vol. 35, pp. 622-624, 2008.

[5] S. Kang and E. Miranda, "Physics based model for simulating the dynamics of tower cranes," *International Conference on Computing in Civil and Building Engineering (ICCCBE)*, Weimar, Bauhaus-University, Germany, 2004, pp. 248-253.

[6] R. Ghigliazza and P. Holmes, "On the dynamics of cranes, or spherical pendula with moving supports,» *International Journal of Non-Linear Mechanics,* vol. 37, pp. 1211-1221, 2002.

[7] F. Altaf, "Modeling and event-triggered control of multiple 3d tower cranes over WSNs," Master's thesis, Royal Institute of Technology (KTH), Nov. 2010.

[8] M. Bock and A. Kugi, "Real-time Nonlinear Model Predictive Path-Following Control of a Laboratory Tower Crane," *IEEE Transactions on Control Systems Technology*, vol. 22, no. 4, pp. 1461-1473, 2014.

[9] T. Arampatzis, J. Lygeros, and S. Manesis, "A survey of applications of wireless sensors and wireless sensor networks," in *Proceedings of the 2005 IEEE International Symposium on Intelligent Control, Mediterrean Conference on Control and Automation*, 2005, pp. 719-724.

[10] J. V. Capella, A. Bonastre, and R. Ors, "Industrial applications of wireless networks: a bridge crane distributed control system based on Bluetooth," in *IEEE International Conference on Industrial Technology (ICIT 04)*, 2004, pp. 824-829.

[11] F. Altaf, J. Araújo, A. Hernandez, H. Sandberg, and K. H. Johansson, “Wireless event-triggered controller for a 3D tower crane lab process,” in *19th Mediterranean Conference on Control & Automation (MED 2011)*, 2011, pp. 994-1001.

[12] F. Altaf, “Modeling and Event-Triggered Control of Multiple 3D Tower Cranes over WSNs,” 2010.

[13] M. A. Ahmad, “Active sway suppression techniques of a gantry crane system,” *European journal of scientific research,* vol. 27, pp. 322-333, 2009.

[14] N. Armstrong and P. Moore, “A distributed control architecture for intelligent crane automation,” *Automation in construction,* vol. 3, pp. 45-53, 1994.

[15] J. Auernig and H. Troger, “Time optimal control of overhead cranes with hoisting of the load,” *Automatica,* vol. 23, pp. 437-447, 1987.

[16] A. Benhidjeb and G. Gissinger, “Fuzzy control of an overhead crane performance comparison with classic control,” *Control Engineering Practice,* vol. 3, pp. 1687-1696, 1995.

[17] C.-C. Cheng and C.-Y. Chen, “Controller design for an overhead crane system with uncretainty,” *Control Engineering Practice,* vol. 4, pp. 645-653, 1996.

[18] J. Kłosiński, “Swing-free stop control of the slewing motion of a mobile crane,” *Control Engineering Practice,* vol. 13, pp. 451-460, 2005.

[19] D. Lewis, G. G. Parker, B. Driessen, and R. D. Robinett, “Command shaping control of an operator-in-the-loop boom crane,” *Proceedings of the 1998 American Control Conference*, pp. 2643-2647, 1998.

[20] J. Lin, Z. Huang, and P. Huang, “An active damping control of robot manipulators with oscillatory bases by singular perturbation approach,” *Journal of sound and vibration,* vol. 304, pp. 345-360, 2007.

[21] K. Nakazono, K. Ohnishi, H. Kinjo, and T. Yamamoto, “Vibration control of load for rotary crane system using neural network with GA-based training,” *Artificial Life and Robotics,* vol. 13, pp. 98-101, 2008.

[22] J. Neupert, E. Arnold, K. Schneider, and O. Sawodny, “Tracking and anti-sway control for boom cranes,” *Control Engineering Practice,* vol. 18, pp. 31-44, 2010.

[23] H. M. Omar and A. H. Nayfeh, "Gantry cranes gain scheduling feedback control with friction compensation," *Journal of sound and vibration,* vol. 281, pp. 1-20, 2005.

[24] K. Terashima, Y. Shen, and K. i. Yano, “Modeling and optimal control of a rotary crane using the straight transfer transformation method,” *Control Engineering Practice,* vol. 15, pp. 1179-1192, 2007.

[25] W. He, S. Zhang and S. S. Ge, “Adaptive control of a flexible crane system with the boundary output constraint,” *IEEE Transactions on Industrial Electronics*, vol. 61, no. 8, pp. 4126-4133, 2014.

[26] L.-H. Lee, C.-H. Huang, S.-C. Ku, Z.-H. Yang and C.-Y. Chang, “Efficient visual feedback method to control a three-dimensional overhead crane,” *IEEE Transactions on Industrial Electronics*, vol. 61, no. 8, pp. 4073-4083, 2014.

[27] K. Tsujita, K. Tsuchiya and A. Onat, “Decenrtalized autonomous control of a quadrupedal locomotion robot using oscillators,” *Artificial Life Robotics*, vol. 5, no. 3, pp. 153-158, 2001.

[28] F. Koumboulis, N. Kouvakas, and P. Paraskevopoulos, “Linear approximant-based metaheuristic proportional-integral-derivative controller for a neutral time delay central heating system,” *Proceedings of the Institution of Mechanical Engineers, Part I: Journal of Systems and Control Engineering,* vol. 223, pp. 605-618, 2009.

[29] H. M. Pearce, “*The Design and Construction of an Intelligent Power Assist Jib Crane*,” MSc Theses, Northwestern University, 1999.

[30] F. Koumboulis, N. Kouvakas, and P. Paraskevopoulos, “Dynamic Controllers for I/O Decoupling of Neutral Time Delay Systems with Application to a Coupled Core Nuclear Reactor,” *Proceedings of the European Control Conference (ECC 2007)*, 2005.

[31] F.N. Koumboulis and N. D. Kouvakas, “I/O Decoupling with simultaneous Disturbance Rejection of general neutral time delay systems via a measurement output feedback dynamic controller,” in *Control & Automation (MED), 2013 21st Mediterranean Conference on*, 2013, pp. 890-895.

[32] A. Cervin, D. Henriksson, B. Lincoln, J. Eker, K.E. Årzén, “How Does Control Timing Affect Performance? Analysis and Simulation of Timing Using Jitterbug and TrueTime,” *IEEE Control Systems Magazine*, vol. 23, pp. 16–30, 2003.

Chapter 4: Towards Remote Control of Planar Redundant Robotic Manipulator

4.1 INTRODUCTION

Due to the dexterity arising from the increased number of degrees of freedom, the use of redundant robots is significantly increasing. Typical applications are met in robotic surgery, cutting and assembly (see [1]-[3] and the references therein). Nevertheless a tradeoff has to be made to address the much greater structural complexity of redundant robots as well as the complicated algorithms needed for the solution of the inverse kinematics problems and the motion control. For such robots, teleoperation is of special interest, especially for the case of hazardous environments (see indicatively [4]-[6]). During teleoperation, special attention must be paid to the problem of having time varying communication delays (see [7]-[14] and the references therein).

The main contribution of the present work lies in the design of a linear dynamic remote controller that includes time delays in its representation and achieves accurate control for the performance variables, despite the presence of communcation delays and disturbances. The mathematical model (including disturbance forces at the end effector) of a planar 3dof Cartesian robot moving on a level being perpendicular to the gravitational acceleration is derived. The robot manipulator is considered to be controlled through a wireless network using the ZigBee protocol imposing time varying communication delays between the sensors and the controller, as well as between the controller and the actuators. The transmission-reception-reconstruction protocol proposed in [15] is used. According to [15] the communication/signal reconstruction delays can become constant. The performance variables of the systems are the coordinates of the end effector of the robot. For the regulation of the performance variables, a static feedback controller with a dynamic precompensator including constant time delays is proposed. Based on the above, the following design goals are imposed a) I/O non-square decoupling, namely diagonalization of the transfer

matrix mapping the external commands to the performance outputs, b) D/O diagonalization, namely diagonalization of the transfer matrix mapping the disturbances to the performance outputs, c) attenuation of the influence of the disturbances to the performance output through inequalities of the infinity norm of the D/O transfer matrix, and d) balanced allotment of the redundant degrees of freedom of the robot through allotment of the steady state gains of the transfer matrices mapping the external inputs to the redundant joint variables. The design goals are proven to be satisfied. Analytic expressions of the controller matrices are derived for the design goals (a), (b) and (d), while for the design goal (c) a metaheuristic algorithm similar to that in [16] is proposed to compute the remaining degrees of freedom of the controller. The good performance of the proposed control scheme is demonstrated through computational experiments. In particular, two scenarios for the external commands are examined. In the first scenario the external commands are chosen such that the end effector "draws" a meander while in the second scenario the external commands are chosen such that the end effector "draws" an Archimedean Spiral.

4.2 MATHEMATICAL MODEL OF THE ROBOT

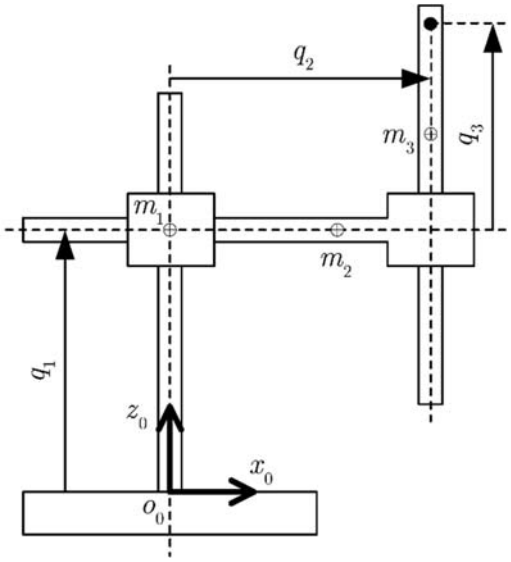

Fig. 4.1 Planar Cartesian Robot.

Consider the planar Cartesian robot presented in Figure 4.1. Using an Euler-Lagrange approach and considering the gravitational acceleration to be perpendicular to the $x_0 - z_0$ plane, the dynamic model of the robot can be described as follows:

$$\dot{x}(t) = Ax(t) + Bu(t) + J\xi(t) \tag{4.1a}$$

where $A \in \mathbb{R}^{6\times6}$, $B \in \mathbb{R}^{6\times3}$, $J \in \mathbb{R}^{6\times2}$

$$x(t) = \begin{bmatrix} x_1(t) & x_2(t) & x_3(t) & x_4(t) & x_5(t) & x_6(t) \end{bmatrix}^T =$$
$$= \begin{bmatrix} q_1(t) & q_2(t) & q_3(t) & \dot{q}_1(t) & \dot{q}_2(t) & \dot{q}_3(t) \end{bmatrix}^T$$
$$u(t) = \begin{bmatrix} u_1(t) & u_2(t) & u_3(t) \end{bmatrix}^T = \begin{bmatrix} r_1(t) & r_2(t) & r_3(t) \end{bmatrix}^T$$
$$\xi(t) = \begin{bmatrix} \xi_1(t) & \xi_2(t) \end{bmatrix}^T = \begin{bmatrix} f_x(t) & f_z(t) \end{bmatrix}^T$$

where q_1, q_2 and q_3 are the robot joint variables, r_1, r_2 and r_3 are the respective actuator forces and f_x and f_z are unknown external disturbances, in the x_0 and z_0 direction respectively, exerted at the end effector. The nonzero elements of A, B and J are computed to be

$$a_{1,4} = a_{2,5} = a_{3,6} = 1, a_{4,4} = \frac{c_1}{m_1 + m_2}, a_{4,6} = \frac{c_3}{m_1 + m_2}$$
$$a_{5,5} = -\frac{c_2}{m_2 + m_3}, a_{6,4} = -a_{4,4}, a_{6,6} = -\frac{c_3\left(m_1 + m_2 + m_3\right)}{\left(m_1 + m_2\right)m_3}$$
$$b_{4,1} = \frac{1}{m_1 + m_2}, b_{4,3} = b_{6,1} = -b_{4,1}, b_{5,2} = \frac{1}{m_2 + m_3}$$
$$b_{6,3} = \frac{m_1 + m_2 + m_3}{\left(m_1 + m_2\right)m_3}, j_{5,1} = b_{5,2}, j_{6,2} = \frac{1}{m_3}$$

where m_1, m_2 and m_3 are the first, second and third link masses respectively and c_1, c_2 and c_3 are the viscous damping coefficients for the first, second and third joint respectively. It is important to mention that the viscus forces appear either due to friction in the joints or due to the presence of local preinstalled controllers used to achieve weak stability for the system. The performance outputs of the system are the x_0 and z_0 coordinates of the end effector, i.e. it holds that

$$y(t) = Cx(t) \tag{4.1b}$$

where

$$C = \begin{bmatrix} 0 & 1 & 0 & 0 & 0 & 0 \\ 1 & 0 & 1 & 0 & 0 & 0 \end{bmatrix}$$

Only position and speed sensors are considered. The state vector is measurable while the disturbances are not considered to be measurable.

The robot manipulator is controlled through a wireless network using the ZigBee protocol due to the effectiveness of the 802.15.4 modulation type, in terms of signal to noise ratio as compared to other approaches (e.g. Wi-Fi or Bluetooth). The wireless network is used to transmit measurable variables signals from the robot sensors to the remote controller as well as from the remote controller to the robot's actuators imposing time varying communication delays. Following the modifications of the transmission-reception protocol proposed in [15], the communication delays (including signal reconstruction), become approximately constant in both ways of transmission (see [15] and [17]). Based on the above, the mathematical model of the system takes on the form

$$\dot{x}(t) = Ax(t) + Bu(t - \tau_1) + J\xi(t) \tag{4.2a}$$

$$y(t) = Cx(t), \psi(t) = x(t - \tau_2) \tag{4.2b,c}$$

where $\psi(t) \in \mathbb{R}^{6\times 1}$ is the vector of the measurable outputs of the system while τ_1 and τ_2 are the transmission/reconstruction delays of the actuatable inputs and the measurable outputs of the system respectively.

4.3 CONTROLLER DESIGN

The forced response of the mathematical model (4.2) is expressed in the frequency domain by the following set of equations

$$X(s) = z_1(sI_6 - A)^{-1} BU(s) + (sI_6 - A)^{-1} J\Xi(s) \tag{4.3a}$$

$$Y(s) = CX(s), \Psi(s) = z_2 X(s) \tag{4.3b,c}$$

where I_6 is the 6×6 identity matrix, $z_1 = e^{-s\tau_1}$, $z_2 = e^{-s\tau_2}$, $X(s) = \mathcal{L}\{x(t)\}$, $U(s) = \mathcal{L}\{u(t)\}$, $\Xi(s) = \mathcal{L}\{\xi(t)\}$, $Y(s) = \mathcal{L}\{y(t)\}$, $\Psi(s) = \mathcal{L}\{\psi(t)\}$ and where $\mathcal{L}\{\bullet\}$ denotes the Laplace transform of the argument signal.

The controller is considered to be of the static feedback type with a dynamic precompensator including delays, i.e. to be of the form

$$U(s) = K\Psi(s) + G(s, z_1, z_2)\Omega(s) \tag{4.4}$$

where $\Omega(s) = \mathcal{L}\{\omega(t)\}$ is the Laplace transform of the 2×1 vector of external inputs, $G(s, z_1, z_2) \in \mathbb{R}^{3\times 2}(s, z_1, z_2)$ and $K \in \mathbb{R}^{3\times 6}$. The elements of the precompensator matrix $G(s, z_1, z_2)$ are rational functions of s. The respective numerator and denominator polynomial coefficients are multivariable rational function of z_1 and z_2. Substituting controller (4.4) to the open loop system (4.3), the performance outputs are related to the external inputs and the disturbances as follows

$$Y(s) = H_{\Omega}(s, z_1, z_2)\Omega(s) + H_{\Xi}(s, z_1, z_2)\Xi(s) \tag{4.5}$$

where

$$H_{\Omega}(s, z_1, z_2) = z_1 C\left(sI_6 - A - z_1 z_2 BK\right)^{-1} BG(s, z_1, z_2) \tag{4.6a}$$

$$H_{\Xi}(s, z_1, z_2) = C\left(sI_6 - A - z_1 z_2 BK\right)^{-1} J \tag{4.6b}$$

The design goals are:

1. non-square I/O decoupling
2. D/O diagonalization
3. disturbance attenuation
4. balanced allotment of the redundant degrees of freedom of the robot

The design goal of non-square I/O decoupling is translated to that of finding appropriate controller matrices such that

$$H_{\Omega}(s,z_1,z_2) = \mathrm{d}iag\left\{h_i(s,z_1,z_2)\right\}; i = 1,2 \tag{4.7}$$

where $h_1(s,z_1,z_2)$ and $h_2(s,z_1,z_2)$ are different than zero rational functions of s while the respective numerator and denominator polynomial coefficients are multivariable rational function of z_1 and z_2. The design goal of D/O diagonalization is translated to that of finding appropriate K such that the transfer matrix mapping the disturbances to the performance outputs is of the form

$$H_{\Xi}(s,z_1,z_2) = \mathrm{d}iag\left\{\left(h_{\Xi}\right)_i(s,z_1,z_2)\right\}; i = 1,2 \tag{4.8}$$

The design goal of disturbance attenuation is translated to that of finding appropriate K such that (see [16])

$$\max\left\{\left\|\left(h_{\Xi}\right)_1(s,z_1,z_2)\right\|_{\infty}, \left\|\left(h_{\Xi}\right)_2(s,z_1,z_2)\right\|_{\infty}\right\} < e_{\max} \tag{4.9}$$

where $e_{\max} \in \mathbb{R}^+$ which is specified by the designer to meet closed loop performance specifications.

From relation (4.1b) it can readily be observed that the response of the second performance variable is the sum of the responses of q_1 and q_3. In order to keep q_1 and q_3 appropriately bounded so that the joint variables remain within appropriate limitations imposed by the robot geometry, balanced allotment of the redundant DOFs of the robot must be achieved. Let $\left(h_x\right)_{1,2}(s,z_1,z_2)$ and $\left(h_x\right)_{3,2}(s,z_1,z_2)$ be the transfer functions mapping the external command that regulates the z_0 coordinate of the end effector to q_1 and q_3 respectively. The balanced allotment design requirement is translated to the introduction of an appropriate algebraic constraint for the steady state gains of $\left(h_x\right)_{1,2}(s,z_1,z_2)$ and $\left(h_x\right)_{3,2}(s,z_1,z_2)$, i.e. to hold that

$$\left(h_x\right)_{1,2}(0,1,1) = \mu\left(h_x\right)_{3,2}(0,1,1) \tag{4.10}$$

where $\mu \in \mathbb{R}$.

4.3.1 I/O Non-Square Decoupling Controller

Using the results presented in [18], the design requirement (4.7) is satisfied by selecting

$$\begin{aligned} G(s,z_1,z_2) = &\left[I_3 - z_1 z_2 K (sI_6 - A)^{-1} B \right] \left[\hat{H}(s,z_1,z_2) \right]^{-1} \times \\ &\left[\mathrm{diag}\left\{ h_i(s,z_1,z_2) \right\} \quad N(s,z_1,z_2)^T \right]^T \end{aligned} \tag{4.11}$$

where

$$\hat{H}(s,z_1,z_2) = \begin{bmatrix} z_1 C (sI_6 - A)^{-1} B \\ H^{\dagger}(s,z_1,z_2) \end{bmatrix}$$

$$H^{\dagger}(s,z_1,z_2) = \left[H_1^{\dagger}(s,z_1,z_2) \quad H_2^{\dagger}(s,z_1,z_2) \quad H_3^{\dagger}(s,z_1,z_2) \right]$$

$$N(s,z_1,z_2) = \left[N_1(s,z_1,z_2) \quad N_2(s,z_1,z_2) \right]$$

where $H_j^{\dagger}(s,z_1,z_2)$ ($j = 1,2,3$) are selected such that $\hat{H}(s,z_1,z_2)$ is invertible while $N_i(s,z_1,z_2)$ ($i = 1,2$) are arbitrary rational functions of s with coefficients being rational functions of z_1 and z_2. Note that choosing $N_i(s,z_1,z_2)$ and $h_i(s,z_1,z_2)$ to be realizable enough, the realizability of the precompensator is guaranteed. The feedback matrix K is arbitrary but is restricted to be realizable and to satisfy the solvability of the closed loop system, i.e. $\det\left[sI_6 - A - z_1 z_2 BK \right] \neq 0$. It is obvious that since the feedback matrix is static, this inequality is satisfied. Furthermore, in order to simplify the form of the precompensator, choose

$$N_1(s,z_1,z_2) = 0, N_2(s,z_1,z_2) = 0, H_1^{\dagger}(s,z_1,z_2) = \lambda_1,$$

$$H_2^{\dagger}(s,z_1,z_2) = \lambda_2, H_3^{\dagger}(s,z_1,z_2) = \lambda_3$$

where $\lambda_j \in \mathbb{R}$ ($j = 1,2,3$). Applying elementary computations, it can be observed that

$$\left|\hat{H}\left(s, z_1, z_2\right)\right| = \frac{\beta_1 s + \beta_0}{s^5 + a_4 s^4 + a_3 s^3 + a_2 s^2}, \qquad \text{where} \qquad \alpha_4 = \frac{c_1 + c_2}{m_1 + m_2} + \frac{c_3}{m_3} + \frac{c_2}{m_2 + m_3},$$

$$\alpha_3 = \frac{c_2 c_3 \left(m_1 + m_2\right) + c_2 \left(c_1 + c_3\right) m_3 + c_1 c_3 \left(m_2 + m_3\right)}{\left(m_1 + m_2\right) m_3 \left(m_2 + m_3\right)}, \qquad \alpha_2 = \frac{c_1 c_2 c_3}{\left(m_1 + m_2\right) m_3 \left(m_2 + m_3\right)},$$

$\beta_1 = \dfrac{z_1^2 \lambda_1}{m_3 \left(m_2 + m_3\right)}$, $\beta_0 = \dfrac{z_1^2 \left(c_1 \lambda_1 - c_3 \lambda_3\right)}{\left(m_1 + m_2\right) m_3 \left(m_2 + m_3\right)}$. Clearly, if $\lambda_1 \neq 0$ or $\lambda_3 \neq \dfrac{c_1}{c_3} \lambda_1$, then $\hat{H}\left(s, z_1, z_2\right)$ is invertible. Let

$$h_i\left(s, z_1, z_2\right) = \frac{z_1}{\left(T_{i,1} s + 1\right)\left(T_{i,2} s + 1\right)\left(T_{i,3} s + 1\right)} \tag{4.12}$$

where $T_{i,j} \in \mathbb{R}^+$. Clearly, asymptotic command following is achieved for the performance outputs. Substituting relation (4.12) in (4.11) and using the above selections of $N_i\left(s, z_1, z_2\right)$ and $H_j^{\dagger}\left(s, z_1, z_2\right)$ as well as the specification of having a static feedback matrix, the precompensator takes on the form

$$G\left(s, z_1, z_2\right) = \begin{bmatrix} \dfrac{\tilde{g}_{1,1}\left(s, z_1, z_2\right)}{\tilde{p}_1\left(s\right)} & \dfrac{\tilde{g}_{1,2}\left(s, z_1, z_2\right)}{\tilde{p}_2\left(s\right)} \\ \dfrac{\tilde{g}_{2,1}\left(s, z_1, z_2\right)}{\tilde{p}_1\left(s\right)} & \dfrac{\tilde{g}_{2,2}\left(s, z_1, z_2\right)}{\tilde{p}_2\left(s\right)} \\ \dfrac{\tilde{g}_{3,1}\left(s, z_1, z_2\right)}{\tilde{p}_1\left(s\right)} & \dfrac{\tilde{g}_{3,2}\left(s, z_1, z_2\right)}{\tilde{p}_2\left(s\right)} \end{bmatrix} \tag{4.13}$$

where

$$\tilde{p}_i\left(s\right) = \left(T_{i,1} s + 1\right)\left(T_{i,2} s + 1\right)\left(T_{i,3} s + 1\right)\left[s + \frac{c_1 \lambda_1 - c_3 \lambda_3}{\left(m_1 + m_2\right) \lambda_1}\right]$$

$$\tilde{g}_{j,i}\left(s, z_1, z_2\right) = \left(\gamma_{j,i}\right)_3 s^3 + \left(\gamma_{j,i}\right)_2 s^2 + \left(\gamma_{j,i}\right)_1 s^1 + \left(\gamma_{j,i}\right)_0$$

$$\left(\gamma_{1,1}\right)_3 = -\frac{\left(m_2 + m_3\right) \lambda_2}{\lambda_1},$$

$$\left(\gamma_{1,1}\right)_2 = -k_{1,5}z - \frac{\left[c_2\left(m_1+m_2\right)+\left(m_2+m_3\right)\left(c_1-k_{1,4}z+k_{1,6}z\right)\right]\lambda_2}{\left(m_1+m_2\right)\lambda_1}$$

$$\left(\gamma_{1,1}\right)_1 = -\left\{c_1\left(k_{1,5}\lambda_1 z + c_2\lambda_2\right) + z\left[k_{1,2}\left(m_1+m_2\right)\lambda_1 + \right.\right.$$

$$\left.\left. + c_2\left(k_{1,6}-k_{1,4}\right)\lambda_2 - \left(k_{1,1}-k_{1,3}\right)\left(m_2+m_3\right)\lambda_2 - c_3k_{1,5}\lambda_3\right]\right\} / \left[\left(m_1+m_2\right)\lambda_1\right]$$

$$\left(\gamma_{1,1}\right)_0 = \frac{z\left[c_2\left(k_{1,1}-k_{1,3}\right)\lambda_2 + c_3k_{1,2}\lambda_3 - c_1k_{1,2}\lambda_1\right]}{\left(m_1+m_2\right)\lambda_1}$$

$$\left(\gamma_{1,2}\right)_3 = -\frac{m_3\lambda_3}{\lambda_1}$$

$$\left(\gamma_{1,2}\right)_2 = -\frac{c_1m_3\lambda_3 + c_3\left(m_1+m_2+m_3\right)\lambda_3}{\left(m_1+m_2\right)\lambda_1} +$$

$$\frac{z\left[m_3\left(\lambda_1+\lambda_3\right)\left(k_{1,4}-k_{1,6}\right) - \left(m_1+m_2\right)\lambda_1k_{1,6}\right]}{\left(m_1+m_2\right)\lambda_1}$$

$$\left(\gamma_{1,2}\right)_1 = -\frac{c_1\left[m_3\left(\lambda_1+\lambda_3\right)\left(k_{1,1}-k_{1,3}\right) - \left(m_1+m_2\right)\lambda_1k_{1,3} + c_3\lambda_3k_{1,4}\right]}{\left(m_1+m_2\right)\lambda_1} +$$

$$\frac{z\left[m_3\left(\lambda_1+\lambda_3\right)\left(k_{1,1}-k_{1,3}\right) - \left(m_1+m_2\right)\lambda_1k_{1,3} + c_3\lambda_3k_{1,4}\right]}{\left(m_1+m_2\right)\lambda_1}$$

$$\left(\gamma_{1,2}\right)_0 = \frac{z\left(c_3\lambda_3k_{1,1} - c_1\lambda_1k_{1,3}\right)}{\left(m_1+m_2\right)\lambda_1}, \left(\gamma_{2,1}\right)_3 = m_2+m_3$$

$$\left(\gamma_{2,1}\right)_2 = \left[c_2\left(m_1+m_2\right)\lambda_1 + c_1\left(m_2+m_3\right)\lambda_1 - c_3m_2\lambda_3 - \right.$$

$$c_3m_3\lambda_3 + zm_2\lambda_2k_{2,4} + zm_3\lambda_2k_{2,4} - zm_1\lambda_1k_{2,5} -$$

$$\left. - zm_2\lambda_1k_{2,5} - z\left(m_2+m_3\right)\lambda_2k_{2,6}\right] / \left[\left(m_1+m_2\right)\lambda_1\right]$$

$$\left(\gamma_{2,1}\right)_1 = \left\{z\left(m_2+m_3\right)\lambda_2k_{2,1} + c_1\lambda_1\left(c_2 - zk_{2,5}\right) - \right.$$

$$z\left[\left(m_1+m_2\right)\lambda_1k_{2,2} + \left(m_2+m_3\right)\lambda_2k_{2,3} - c_3\lambda_3k_{2,5}\right] -$$

$$\left. - c_2\left[c_3\lambda_3 + z\lambda_2\left(-k_{2,4}+k_{2,6}\right)\right]\right\} / \left[\left(m_1+m_2\right)\lambda_1\right]$$

$$\left(\gamma_{2,1}\right)_0 = \frac{z\left[\left(c_3\lambda_3 - c_1\lambda_1\right)k_{2,2} + c_2\lambda_2\left(k_{2,1}-k_{2,3}\right)\right]}{\left(m_1+m_2\right)\lambda_1}$$

$$\left(\gamma_{2,2}\right)_2 = \frac{zm_3\left(\lambda_1+\lambda_3\right)\left(k_{2,4}-k_{2,6}\right) - z\left(m_1+m_2\right)\lambda_1k_{2,6}}{\left(m_1+m_2\right)\lambda_1}$$

$$\left(\gamma_{2,2}\right)_1 = z\left\{m_3\left(\lambda_1+\lambda_3\right)\left(k_{2,1}-k_{2,3}\right) + c_3\lambda_3k_{2,4} - \right.$$

$$\left.\lambda_1\left[\left(m_1+m_2\right)k_{2,3} + c_1k_{2,6}\right]\right\} / \left[\left(m_1+m_2\right)\lambda_1\right]$$

$$\left(\gamma_{2,2}\right)_0 = \frac{z\left(c_3\lambda_3k_{2,1} - c_1\lambda_1k_{2,3}\right)}{\left(m_1+m_2\right)\lambda_1}$$

$$\left(\gamma_{3,1}\right)_3 = \left(\gamma_{2,2}\right)_3 = 0, \left(\gamma_{3,2}\right)_3 = m_3$$

$$\left(\gamma_{3,1}\right)_2 = \left\{\left(m_2+m_3\right)\lambda_2\left[c_3+z\left(k_{3,4}-k_{3,6}\right)\right]-z\left(m_1+m_2\right)\lambda_1 k_{3,5}\right\}/\left[\left(m_1+m_2\right)\lambda_1\right]$$

$$\left(\gamma_{3,1}\right)_1 = \left(z\left\{-m_1\lambda_1 k_{3,2}+m_2\left[\lambda_2\left(k_{3,1}-k_{3,3}\right)-\lambda_1 k_{3,2}\right]+\right.\right.$$

$$\left.\left.m_3\lambda_2\left(k_{3,1}-k_{3,3}\right)+\left(c_3\lambda_3-c_1\lambda_1\right)k_{3,5}\right\}++c_2\lambda_2\left[c_3+z\left(k_{3,4}-k_{3,6}\right)\right]\right)/\left[\left(m_1+m_2\right)\lambda_1\right]$$

$$\left(\gamma_{3,1}\right)_0 = \frac{z\left[\left(c_3\lambda_3-c_1\lambda_1\right)k_{3,2}+c_2\lambda_2\left(k_{3,1}-k_{3,3}\right)\right]}{\left(m_1+m_2\right)\lambda_1}$$

$$\left(\gamma_{3,2}\right)_2 = \left\{c_1 m_3\lambda_1+c_3\left(m_1+m_2+m_3\right)\lambda_1+\right.$$

$$\left.z\left[m_3\left(\lambda_1+\lambda_3\right)\left(k_{3,4}-k_{3,6}\right)-\left(m_1+m_2\right)\lambda_1 k_{3,6}\right]\right\}/\left[\left(m_1+m_2\right)\lambda_1\right]$$

$$\left(\gamma_{3,2}\right)_1 = \left\{z\left[m_3\left(\lambda_1+\lambda_3\right)\left(k_{3,1}-k_{3,3}\right)-\left(m_1+m_2\right)\lambda_1 k_{3,3}+\right.\right.$$

$$\left.\left.+c_3\lambda_3 k_{3,4}\right]+c_1\lambda_1\left(c_3-zk_{3,6}\right)\right\}/\left[\left(m_1+m_2\right)\lambda_1\right]$$

$$\left(\gamma_{3,2}\right)_0 = \frac{z\left(c_3\lambda_3 k_{3,1}-c_1\lambda_1 k_{3,3}\right)}{\left(m_1+m_2\right)\lambda_1}$$

where $k_{i,j}$ is the $\{i,j\}$ element of the feedback matrix K and $z = z_1 z_2$.

4.3.2 D/O Diagonalization

If $k_{1,2} = k_{1,5} = k_{2,1} = k_{2,3} = k_{2,4} = k_{2,6} = k_{3,2} = k_{3,5} = 0$, the design requirement (4.8) is satisfied

4.3.3 Disturbance Attenuation

Considering the complexity of the problem of deriving analytic formulae for the selection of the remaining feedback matrix elements, a metaheuristic algorithm similar to that presented in [16] will be used in order to produce a controller parameter set that satisfies condition (4.9) while simultaneously preserves the stability of the closed loop system. The main idea is to define an initial search area for the controller parameters. After a number of sets the area gradually contracts providing at the end a suboptimal solution of the controller parameters. It is important to mention that given a set of controller parameters that produce a stable delayless closed loop system, a stability margin with respect to the delays can easily be evaluated using for example the algorithm presented in [19]. Considering that the sum of time delays imposed by the wireless network may change due to different network settings, a lower desired bound,

let $\overline{\tau}$, greater than $\tau_1 + \tau_2$ may be imposed during the metaheuristic algorithm in order to preserve stability for the closed loop system for different values of the delays. The metaheuristic algorithm is:

Initial Data and Performance Criterion

1. Center values and half widths for the initial search area of the controller parameters $\left(k_{i,j}\right)_c$ and $\left(k_{i,j}\right)_w$.

2. Performance criterion $J\left(k_{i,j}\right) = \max\left\{\left\|\left(h_{\Xi}\right)_1\left(s, z_1, z_2\right)\right\|_{\infty}, \left\|\left(h_{\Xi}\right)_2\left(s, z_1, z_2\right)\right\|_{\infty}\right\}$.

3. Iteration parameters n_{loop} , n_{rep}, $n_{total} \in \mathrm{N}$.

4. Search algorithm threshold $\lambda_{k_{i,j}}$.

Algorithm

Step 0: Set the numbering index $i_{\max} = 0$.

Step 1: Determine a search area $\Im$ for the controller parameters according to the inequalities $\left(k_{i,j}\right)_c - \left(k_{i,j}\right)_w \le k_{i,j} \le \left(k_{i,j}\right)_c + \left(k_{i,j}\right)_w$.

Step 2: Set the numbering index $i_1 = 0$.

Step 3: Set the numbering index $i_1 = i_1 + 1$.

Step 4: Set the numbering index $i_2 = 0$.

Step 5: Set the numbering index $i_{\max} = i_{\max} + 1$. If $i_{\max} > n_{total}$ go to ***Step 15***.

Step 6: Set the numbering index $i_2 = i_2 + 1$.

Step 7: Select randomly a set of controller parameters within the search area $\Im$, let $\left(k_{i,j}\right)_{i_2}$. Check if stability conditions are satisfied. If yes, proceed to the next step. If not repeat ***Step 7***.

Step 8: Evaluate $J_{i_2} = J\left(\left(k_{i,j}\right)_{i_2}\right)$.

Step 9: If $J_{i_2} < e_{\max}$ go to ***Step 15***.

Step 10: If $i_2 < n_{loop}$ go to ***Step 5***.

Step 11: Find $\left(J_{\min}\right)_{i_2} = \min\left\{J_i, i = 1,\ldots,n_{loop}\right\}$ as well as the corresponding controller parameters, let $\left(k_{i,j}\right)_{i_1}$

Step 12: If $i_1 \geq n_{rep}$ then find the controller parameters, $\left(k_{i,j}\right)_{\min}$ and $\left(k_{i,j}\right)_{\max}$ corresponding to $J_{\min} = \min\left\{\left(J_{\min}\right)_i, i = 1,\ldots,n_{rep}\right\}$ and $J_{\max} = \max\left\{\left(J_{\min}\right)_i, i = 1,\ldots,n_{rep}\right\}$. Else go to ***Step 3***.

Step 13: Define $\left(k_{i,j}\right)_c = \left(\left(k_{i,j}\right)_{\min} + \left(k_{i,j}\right)_{\max}\right)/2$ and $\left(k_{i,j}\right)_w = \left|\left(k_{i,j}\right)_{\min} - \left(k_{i,j}\right)_{\max}\right|/2$

Step 14: If there exists at least one $\left(k_{i,j}\right)_w$ such that $\left(k_{i,j}\right)_w > \lambda_{k_{i,j}}$ go to ***Step 2***.

Step 15: If $J_{i_2} < e_{\max}$ then set $k_{i,j} = \left(k_{i,j}\right)_{i_2}$ (determined in Step 8), else set $k_{i,j} = \left(k_{i,j}\right)_{\min}$ (determined in ***Step 12***).

4.3.4 Balanced Allotment of the Redundant DOFs of the Robot

Applying series of computations it can be verified that the condition in (4.10) is satisfied if $\lambda_1 = -\dfrac{c_3\lambda_3}{c_1\mu_1}$. This selection results in responses for q_1 and q_3 being independent from the values of the elements of the feedback matrix K that are specified in 4.3.3. Hence, the the ballance allotment requirement is independent from the results of the metaheuristic algorithm presented in 4.3.3. The regulation of the transient phenomenon can only be achieved by appropriate setting of $T_{2,1}$, $T_{2,2}$ and $T_{2,3}$.

4.4 SIMULATION RESULTS

Let $m_1 = 0.93[\text{kg}]$, $m_2 = 11.54[\text{kg}]$, $m_3 = 11.54[\text{kg}]$, $e_{\max} = 0.6$, $c_1 = 2[\text{N}s/m]$, $c_2 = 2[\text{N}s/m]$, $c_3 = 2[\text{N}s/m]$, $T_{1,1} = 0.5$, $T_{1,2} = 0.6$, $T_{1,3} = 0.7$, $T_{2,1} = 0.5$, $T_{2,2} = 0.6$, $T_{2,3} = 0.7$, $\lambda_1 = 1$, $\lambda_2 = 0.5$, $\lambda_3 = -1$, $\tau_1 = 0.12[\text{s}]$, $\tau_2 = 0.21[\text{s}]$.

The metaheuristic algorithm parameters are selected to be $(k_{1,1})_c = 0$, $(k_{1,3})_c = 0$ $(k_{1,4})_c = 0$, $(k_{1,6})_c = 0$, $(k_{2,2})_c = 0$, $(k_{2,5})_c = 0$, $(k_{3,1})_c = 0$, $(k_{3,3})_c = 0$, $(k_{3,4})_c = 0$, $(k_{3,6})_c = 0$, $(k_{1,1})_w = 5$, $(k_{1,3})_w = 5$, $(k_{1,4})_w = 5$, $(k_{1,6})_w = 5$, $(k_{2,2})_w = 5$, $(k_{2,5})_w = 5$, $(k_{3,1})_w = 5$, $(k_{3,3})_w = 5$, $(k_{3,4})_w = 5$, $(k_{3,6})_w = 5$, $\lambda_{k_{1,1}} = 0.01$, $\lambda_{k_{1,3}} = 0.01$, $\lambda_{k_{1,4}} = 0.01$ $\lambda_{k_{1,6}} = 0.01$, $\lambda_{k_{2,2}} = 0.01$, $\lambda_{k_{2,5}} = 0.01$, $\lambda_{k_{3,1}} = 0.01$, $\lambda_{k_{3,3}} = 0.01$, $\lambda_{k_{3,4}} = 0.01$, $\lambda_{k_{3,6}} = 0.01$, $n_{loop} = 100$, $n_{rep} = 10$, $n_{total} = 10^9$.

Implementation of the metaheuristic algorithm using the above parameters yields

$k_{1,1} = -3.1501$, $k_{1,3} = 2.6512$, $k_{1,4} = 0.664$, $k_{1,6} = -4.4848$, $k_{2,2} = -5.5564$, $k_{2,5} = -3.4635$, $k_{3,1} = 2.2635$, $k_{3,3} = -4.2886$, $k_{3,4} = 7.1497$, $k_{3,6} = -4.8208$.

The above set of controller parameters produces a cost criterion $J = 0.5642$ that obviously satisfies the condition (4.9). The simulation of the closed loop system will

be performed using Matlab/Simulink software while simulation of the wireless network will be carried out using the TrueTime 2.0 add-on (see [20]). For simulation purposes, the disturbances will be considered to be random satisfying $\left|\xi_1(t)\right| < 0.1[\mathrm{N}]$ and $\left|\xi_2(t)\right| < 0.1[\mathrm{N}]$ while two scenarios of external commands will be used. In the first scenario it holds that

$$\omega_1(t) = \begin{cases} 0.2[\mathrm{m}] & t \in [0,5)[\mathrm{s}] \\ 0.45[\mathrm{m}] & t \in [5,15)[\mathrm{s}] \\ 0.325[\mathrm{m}] & t \in [15,25)[\mathrm{s}] \\ 0.3875[\mathrm{m}] & t \in [25,\infty)[\mathrm{s}] \end{cases}$$

$$\omega_2(t) = \begin{cases} 0.25[\mathrm{m}] & t \in [0,10)[\mathrm{s}] \\ 0.125[\mathrm{m}] & t \in [10,20)[\mathrm{s}] \\ 0.1875[\mathrm{m}] & t \in [20,\infty)[\mathrm{s}] \end{cases}$$

The above selection of the external commands is translated to a meander path following for the end effector. In the second scenario we will assume that

$$\omega_1(t) = 0.0979 + 0.005(6.5\pi - t)\sin(6.5\pi - t)(1 - u_s(t - 6.5\pi))$$

$$\omega_2(t) = 0.4 + 0.005(6.5\pi - t)\sin(6.5\pi - t)(1 - u_s(t - 6.5\pi))$$

where $u_s(t)$ is the unit step signal. The second selection of the external commands is translated to an Archimedean Spiral path following for the end effector. In both cases (see Figures 4.2 and 4.5), the end effector follows accurately the desired paths. For both scenarios, the maximum distance error between the end effector response and the model response is small and does not exceed $0.0025[\mathrm{m}]$. With respect to the actuatable inputs (see Figures 4.6 and 4.7) they remain within acceptable limits being easily implementable by common robotic actuators. Finally, in both cases, the robot joint variables remain appropriately bounded (see Figures 4.4 and 4.7).

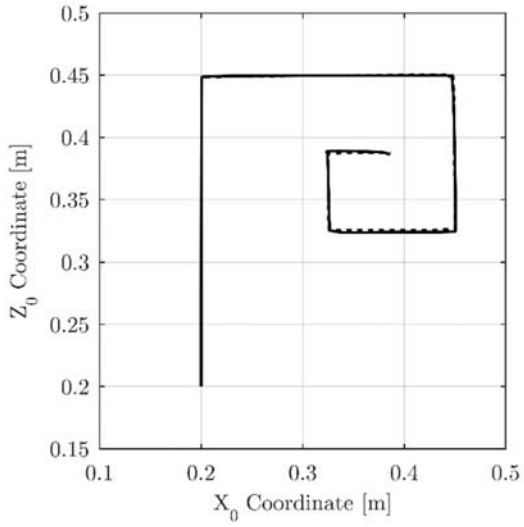

Fig. 4.2 Position of the end effector for the first scenario (continuous response, dashed model).

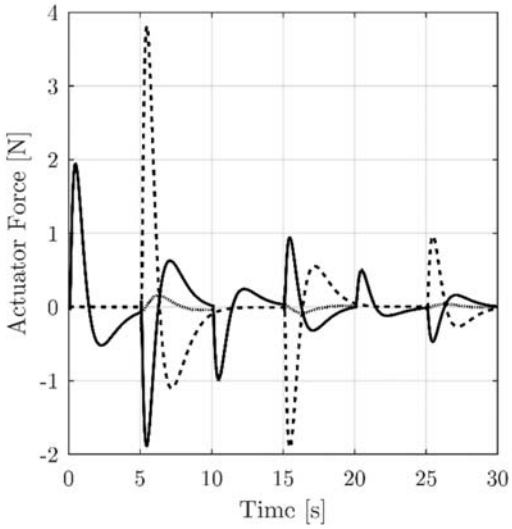

Fig. 4.3 Actuatable inputs for the first scenario (continuous 1st, dashed - 2nd, dotted - 3rd).

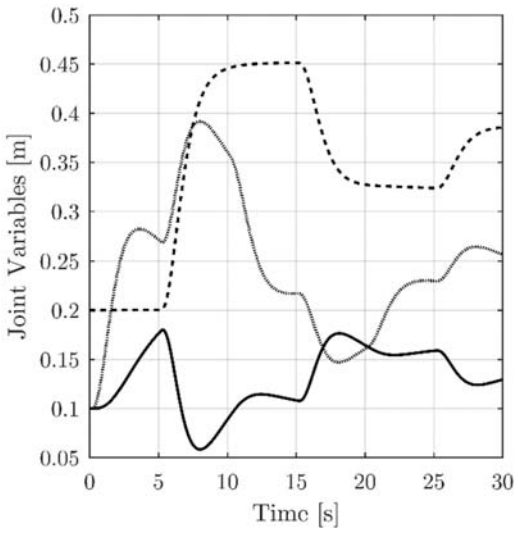

Fig. 4.4 Joint variables for the first scenario (continuous 1st, dashed - 2nd, dotted - 3rd).

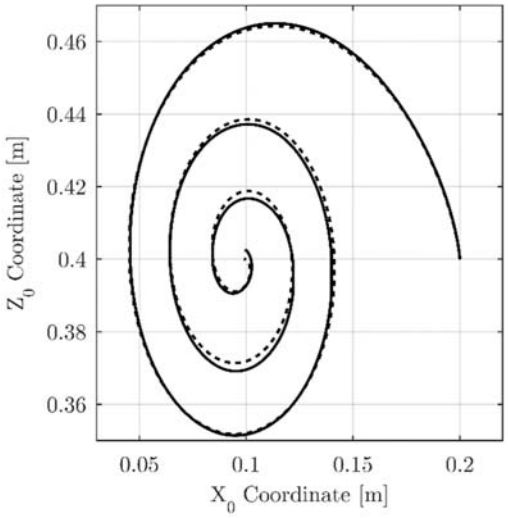

Fig. 4.5 Position of the end effector for the second scenario (continuous response, dashed model).

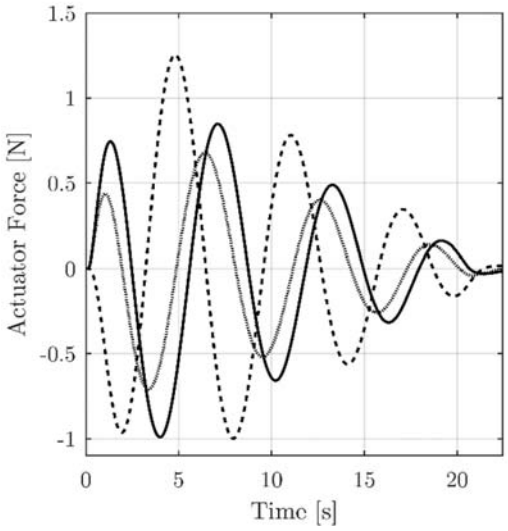

Fig. 4.6 Actuatable inputs for the second scenario (continuous 1st, dashed - 2nd, dotted - 3rd).

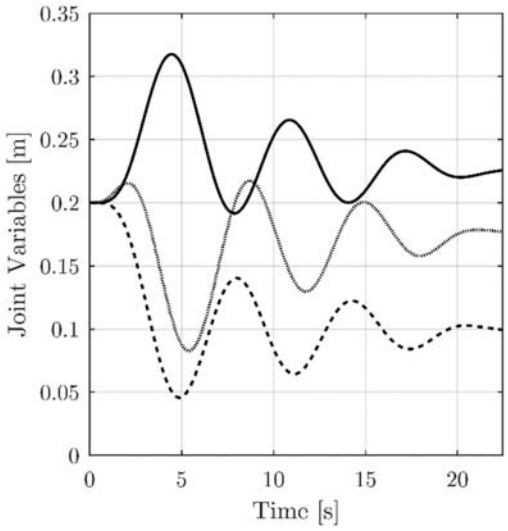

Fig. 4.7 Joint variables for the second scenario (continuous1st, dashed - 2nd, dotted - 3rd).

4.5 SUMMARY

In this work the problem of remote control of a planar redundant manipulator has been studied. Using a static feedback with dynamic precompensator including time delays the following design requirements have been satisfied a) I/O non-square decoupling, b) D/O diagonalization, c) attenuation of the influence of the disturbances

to the performance output, and d) balanced allotment of the redundant degrees of freedom of the robot. The performance of the proposed control scheme has been demonstrated through computational experiments where it has been shown that the planar trajectory of the end effector followed accurately the desired path.

REFERENCES

[1] Y. Li and Y. Chen, "The ultimate hyper redundant robotic arm based on omnidirectional joints," in *Proceedings of the 2015 IEEE International Conference on Mechatronics and Automation (ICMA)*, Beijing, 2-5 August, 2015.

[2] H. Parzer, H. Gattringer and M. Neubauer, "Dynamic modeling and force control of a redundant robot for polishing applications," in *Proceedings in Applied Mathematics and Mechanics*, vol. 14, no. 1, pp. 77-78, 2014.

[3] J. Funda, R. H. Taylor, B. Eldridge, S. Gomory and K. G. Gruben, "Constrained Cartesian Motion Control for Teleoperated Surgical Robots," in *IEEE Transactions on Robotics and Automation*, vol. 12, no. 3, pp. 453-465, 1996.

[4] N. Nath, E. Tatlicioglu and D. M. Dawson, "Teleoperation with Kinematically Redundant Robot Manipulators with Sub-Task Objectives," in *Proceedings of the 47th IEEE Conference on Decision and Control*, Cancun, Mexico, Dec. 9-11, 2008.

[5] P. Malysz and S. Sirouspour, "Trilateral teleoperation control of kinematically redundant robotic manipulators," in *The International Journal of Robotics Research*, vol. 30, no. 13, pp. 1643-1664, 2011.

[6] D.-Y. Hwang and B. Hannaford, "Teleoperation Performance with a Kinematically Redundant Slave Robot," in *The International Journal of Robotics Research*, vol. 17, no. 6, pp. 579-597, 1998.

[7] D.-H. Zhai and Y. Xia, "Adaptive Control of Semi-Autonomous Teleoperation System With Asymmetric Time-Varying Delays and Input Uncertainties," in *IEEE Transactions on Cybernetics*, *to appear*

[8] D. D. Santiago, E. Slawiñski and V. A. Mut, "Stable Delayed Bilateral Teleoperation of Mobile Manipulators," in *Asian Journal of Control*, *to appear*

[9] X. Wang, C. Yang and Z. Li, "Development of a TouchX based teleoperation approach using wave variable technique," in *Proceedings of the International Conference on Advanced Robotics and Mechatronics (ICARM)*, 18-20 Aug. 2016, Macau, China.

[10] Y. Kang, Z. Li, X. Cao and D. Zhai, "Robust Control of Motion/Force for Robotic Manipulators With Random Time Delays," in *IEEE Transactions on Control Systems Technology*, vol. 21, no. 5, pp. 1708 - 1718, 2013.

[11] Y.-C. Liu and N. Chopra, "Control of Robotic Manipulators under Input/Output Communication Delays: Theory and Experiments," in *IEEE Transactions on Robotics*, vol. 28, no. 3, pp. 742-751, 2012.

[12] L. M. Capisani, T. Facchinetti and A. Ferrara, "Real-time networked control of an industrial robot manipulator via discrete-time second-order sliding modes," in *International Journal of Control*, vol. 83, no. 8, pp. 1595-1611, 2010.

[13] L. M. Capisani, T. Facchinetti and A. Ferrara, "Second Order Sliding Mode Real-Time Networked Control of a Robotic Manipulator," in *Proceedings of the IEEE Conference on Emerging Technologies and Factory Automation (ETFA)*, Patras, Greece, 25-28 Septempber 2007.

[14] C.-C. Chen, S. Hirche and M. Buss, "Stability, Stabilization and Experiments for Networked Control Systems with Random Time Delay," in *Proceedings of the 2008 American Control Conference*, pp. 1552-1557, Seattle, Washington, USA, June 11-13, 2008.

[15] Fotis N. Koumboulis, N. D. Kouvakas, G. L. Giannaris and D. Vouyioukas, "Independent motion control of a tower crane through wireless sensor and actuator networks," in *ISA Transactions*, vol. 60, pp. 312-320, 2016.

[16] F. N. Koumboulis and N. D. Kouvakas, "A three term controller for ride comfort improvement," in *Proceedings of the 19th Mediterranean Conference on Control and Automation (MED2011)*, pp. 114-119, Corfu, Greece, 20-23 June, 2011.

[17] N. D. Kouvakas, F. N. Koumboulis, G. L. Giannaris and D. Vouyioukas, "Towards Wireless Control for a Permanent Magnet Synchronous Motor," in *Proceedings of the IEEE International Conference on Emerging Technologies and Factory Automation (ETFA 2014)*, Barcelona, Spain, 16-19 September, 2014.

[18] F. N. Koumboulis, N. D. Kouvakas and P. N. Paraskevopoulos, "On the Morgan's problem for neutral time delay systems via dynamic controllers with application to a test case central heating system," in *Proceedings of the 18th IEEE International Conference on Control Applications*, pp. 1195-1202, Saint Petersburg, Russia, 8-10 July, 2009.

[19] N. Olgac and R. Sipahi, "An exact Method for the Stability Analysis of Time-Delayed Linear Time-Invariant (LTI) Systems," in *IEEE Transactions on Automatic Control*, vol. 47, no. 5, pp. 793-797, 2002.

[20] A. Cervin, D. Henriksson, B. Lincoln, J. Eker and K.-E. Årzén, "How Does Control Timing Affect Performance? Analysis and Simulation of Timing Using Jitterbug and TrueTime," in *IEEE Control Systems Magazine*, vol. 23, no. 3, pp. 16–30, 2003.

Chapter 5: Wireless Longitudinal Motion Controller Design for Quadrotors

5.1 INTRODUCTION

Multi-rotor aerial vehicles have a wide and increasing range of applications (e.g. traffic surveillance, aerial photography, package delivery). The success of their missions depends greatly upon control. Several control approaches have been proposed, ranging from PID type controllers (see [1]-[5] and the references therein) to optimal type controllers ([6]-[8]). Of particular importance appears to be the design goal of I/O decoupling since it improves the manoeuvrability of the quadrotors and provides safe and reliable trajectory following (indicatively see [9]-[13]). Towards improved manoeuvrability, the compensation of the external disturbance is of significant importance (indicatively see [14]-[21] and the references therein).

In the majority of practical cases, the quadrotors are remotely controlled through a wireless communication channel. The performance of a remote controller depends greatly upon the communication errors. The issue has been addressed in [22]-[26] where communication delays of the signals in the control loop are considered. In [23], discrete time models are used. The proposed tracking controller designed for the zero-delay case is successfully tested to the communication delay case. In [24], unknown time varying communication delays are considered together with event triggered controllers. In [25], the models include time delays together with a waiting time. Satisfactory asymptotic behaviour of the closed loop is achieved. In [26], packet delays are included in the model and a procedure for the estimation of the delays is proposed to achieve average consensus. The approaches in [23]-[26] are not oriented to I/O decoupling. Due to the presence of significant delays, existing I/O decoupling approaches for delayless systems (e.g. [27] and the references therein) cannot be used. The compensation of the influence of the communication errors is a goal of the present work in the sense that communication delays being noisy and time varying are handled via appropriate synchronization and signal reconstruction

In this work, the problem of remotely controlling the longitudinal motion of a quadrotor in the presence of atmospheric disturbances and a remote-control loop with communication errors, is studied. Here, two design goals are aimed to be satisfied, despite the presence of communication errors: a) the independent control of the horizontal and vertical velocity of the quadrotor, and b) the attenuation of the influence of the atmospheric disturbances on the performance outputs. Towards the two goals, using the linear approximant of the nonlinear model of the longitudinal motion of the quadrotor, a realizable dynamic controller with two-time delays that provides I/O decoupling with simultaneous disturbance attenuation, is designed. The delays are constant communication delays imposed by an appropriate synchronization/signal reconstruction algorithm. The performance of the proposed control scheme is illustrated through computational experiments for the case of a climbing manoeuvre. It is important to mention that, although the controller is based upon the linear approximant around an operating point, it behaves satisfactorily when applied to the nonlinear model of the quadrotor for a wide range of external commands and a wide range of atmospheric disturbances.

A key point of the approach is the artificial increase of the communication delays in the control loop till constant values. These constant values are used by the controller that aims to satisfy I/O decoupling and disturbance attenuation. Although the increase requires significant computational resources of the earth controller, it compensates the influence of the communication errors to the performance of the closed loop system.

5.2 THE QUADROTOR MODEL

The longitudinal flight of a quadrotor with aerodynamic disturbances is considered. The longitudinal motion of air vehicles is of significant importance providing a wide range of useful flight envelopes (see [13] and [28] - [30]). The disturbance-free model in [13] is augmented to consider aerodynamic disturbances. After appropriate modifications, the mathematical model of the system takes the form:

$$\dot{x}(t) = f(x, u, \xi) \tag{5.1a}$$

$$y(t) = Cx(t) \tag{5.1b}$$

where

$$
\begin{aligned}
x(t) &= \begin{bmatrix} x_1(t) & x_2(t) & x_3(t) & x_4(t) & x_5(t) & x_6(t) \end{bmatrix}^T \\
&= \begin{bmatrix} \theta(t) & v_x(t) & v_z(t) & q(t) & \omega_f(t) & \omega_r(t) \end{bmatrix}^T \\
u(t) &= \begin{bmatrix} u_1(t) & u_2(t) \end{bmatrix}^T = \begin{bmatrix} V_f(t) & V_r(t) \end{bmatrix}^T \\
\xi(t) &= \begin{bmatrix} \xi_1(t) & \xi_2(t) \end{bmatrix}^T = \begin{bmatrix} v_{a,x}(t) & v_{a,z}(t) \end{bmatrix}^T \\
y(t) &= \begin{bmatrix} y_1(t) & y_2(t) \end{bmatrix}^T = \begin{bmatrix} v_x(t) & v_z(t) \end{bmatrix}^T
\end{aligned}
$$

where x , u , ξ and y are the state, input, disturbance and performance output vectors of the system. The variables in the above vectors are: the pitch angle of the quadrotor θ, the horizontal and vertical velocities of the quadrotor v_x and v_z respectively, the pitch rate q, the front and rear motor velocities ω_f and ω_r respectively, the front and rear motor voltage supplies V_f and V_r (actuatable inputs) and the horizontal and vertical velocities of the ambient air $v_{a,x}$ and $v_{a,z}$ (nonmeasurable disturbances). The non-zero elements of C and $f(x,u,\xi)$ are

$$
\begin{aligned}
c_{1,2} = 1, c_{2,3} = 1, f_1(x,u,\xi) &= x_4 \\
f_2(x,u,\xi) &= \left[2s_{x_1}K_l\left(x_5^2 + x_6^2\right) - \left(x_2 - \xi_1\right)k_{dt,x}\right] / m_q \\
f_3(x,u,\xi) &= \left[2c_{x_1}K_l\left(x_5^2 + x_6^2\right) - \left(x_3 - \xi_2\right)k_{dt,z} - gm_q\right] / m_q \\
f_4(x,u,\xi) &= \left[\sqrt{2}dK_l\left(x_6^2 - x_5^2\right) - x_4k_{a,y}\right] / J_{q,y} \\
f_5(x,u,\xi) &= -a_0 + bu_1 - a_1x_5 - a_2x_5^2 \\
f_6(x,u,\xi) &= -a_0 + bu_2 - a_1x_6 - a_2x_6^2
\end{aligned}
$$

where $s_{x_1} = \sin(x_1)$, $c_{x_1} = \cos(x_1)$, m_q is the mass of the quadrotor, $k_{dt,x}$ and $k_{dt,z}$ are the translation drag coefficients in the x and z directions of the earth reference frame, g is the gravitational acceleration, K_l is the lift coefficient of the propellers, d is the distance between the quadrotor center of mass and the rotation axis of the propellers, $k_{a,y}$ is the rotational aerodynamic friction coefficient around the y axis, $J_{q,y}$

is the quadrotor moment of inertia and a_0, a_1, a_2 and b are electric motor parameters. All state variables are considered to be measurable.

To complete the presentation of the model, the linear approximant of the nonlinear model (5.1) will be produced around nominal values corresponding to horizontal cruising with constant speed and zero disturbances. Let $\overline{u}_1$ and $\overline{u}_2$ be the nominal points of u_1 and u_2 respectively, $\overline{\xi}_1$ and $\overline{\xi}_2$ be the nominal points of ξ_1 and ξ_2 respectively and $\overline{x}_i$ be the nominal points of x_i $i=(1,...,6)$. The respective vectors of the nominal values are denoted by $\overline{u}$, $\overline{\xi}$ and $\overline{x}$. Similarly to [13], the nominal points are determined to be

$$\overline{x}_1 = \tan^{-1}\left(\overline{x}_2 k_{dt,x} g^{-1} m_q^{-1}\right), \overline{x}_2 = \overline{x}_2^*, \overline{x}_3 = 0, \overline{x}_4 = 0,$$
$$\overline{x}_5 = \overline{x}_6 = \left(g^2 m_q^2 + \overline{x}_2^2 k_{dt,x}^2\right)^{1/4} \left(2\sqrt{K_l}\right)^{-1}$$
$$\overline{u}_1 = \overline{u}_2 = \left[4a_0 K_l + 2a_1\sqrt{K_l}\left(g^2 m_q^2 + \overline{x}_2^2 k_{dt,x}^2\right)^{1/4} + a_2\sqrt{g^2 m_q^2 + \overline{x}_2^2 k_{dt,x}^2}\right] / \left(4bK_l\right),$$
$$\overline{\xi}_1 = 0, \overline{\xi}_2 = 0$$

where $\overline{x}_2^*$ is the horizontal cruising velocity of the quadrotor. The deviations around the nominal vectors of the inputs, the disturbances, the state and the performance variables are

$\Delta u(t) = u(t) - \overline{u}$, $\Delta\xi(t) = \xi(t) - \overline{\xi}$, $\Delta x(t) = x(t) - \overline{x}$ and $\Delta y(t) = y(t) - \overline{y}$ respectively, where $\overline{y}^T = \left[\overline{x}_2 \quad \overline{x}_3\right]$.

The linear approximant of the model (5.1) is of the form

$$\delta\dot{x}(t) = A\delta x(t) + B\delta u(t) + Q\delta\xi(t) \tag{5.2a}$$

$$\delta y(t) = C\delta x(t) \tag{5.2b}$$

where $\delta u(t) = \Delta u(t)$ and $\delta\xi(t) = \Delta\xi(t)$. The variables $\delta x(t)$ and $\delta y(t)$ are the responses of the linear system (2). Clearly, they approximate $\Delta x(t)$ and $\Delta y(t)$,

respectively. The approximation is accurate around an operating point $o(t)=\bar{o}$ where $o(t)=\left(u(t),\xi(t),x(t),y(t)\right)$ and $\bar{o}=\left(\bar{u},\bar{\xi},\bar{x},\bar{y}\right)$.

The system matrices in (2) are

$$\begin{bmatrix} A & B & Q \end{bmatrix}=\left[\frac{\partial}{\partial x} \quad \frac{\partial}{\partial u} \quad \frac{\partial}{\partial \xi}\right] f\left(x,u,\xi\right)\Big|_{o=\bar{o}} \tag{5.3}$$

The nonzero elements of A, B and Q are

$$a_{1,4}=1, a_{2,1}=g, a_{2,2}=-k_{dt,x}m_q^{-1}$$
$$a_{2,5}=a_{2,6}=4\bar{x}_6 s_{\bar{x}_1} K_l m_q^{-1}, a_{3,1}=-4\bar{x}_6^2 s_{\bar{x}_1} K_l m_q^{-1}$$
$$a_{3,3}=-k_{dt,z}m_q^{-1}, a_{3,5}=a_{3,6}=4c_{\bar{x}_1}\bar{x}_6 K_l m_q^{-1}$$
$$a_{4,4}=-k_{a,y}J_{q,y}^{-1}, a_{4,5}=-2\sqrt{2}d\bar{x}_6 K_l J_{q,y}^{-1}$$
$$a_{4,6}=-a_{4,5}, a_{5,5}=a_{6,6}=-a_1-2\bar{x}_6 a_2$$
$$b_{5,1}=b_{6,2}=b, q_{2,1}=k_{dt,x}m_q^{-1}, q_{3,2}=k_{dt,z}m_q^{-1}$$

5.3 WIRELESS CONTROL DESIGN

In the present section, a remote dynamic controller is designed in order to achieve the desired flight performance. The quadrotor is controlled through a wireless network. The ZigBee protocol is used due to its effectiveness in terms of signal-to-noise ratio, range, power consumption and implementation cost (see [31]). The wireless network is used to transmit signals from the quadrotor sensors to the remote controller as well as from the remote controller to the quadrotor's motors thus imposing time varying communication delays. Following the modifications of the transmission/reception protocol proposed in [31], the communication delays become constant in both ways of transmission. This approach is based on the repetitive transmission of sampled data and reconstruction of the continuous time signals through appropriate interpolation based on passed values of the data. The approach increases the communication time delay till a constant value and the reconstructed signals are smooth facilitating the use of controllers including derivative terms. Note that following the approach presented in [31], the communication delays become constant independently of the selected wireless transmission protocol. Using the above wireless

scheme, the linear approximant of the nonlinear model is in the following time delay dynamic system form

$$\delta\dot{x}(t) = A\delta x(t) + B\delta u(t-\tau_1) + Q\delta\xi(t) \tag{5.4a}$$

$$\delta y(t) = C\delta x(t) \tag{5.4b}$$

where τ_1 is the transmission / reconstruction delay of the control commands at the actuatable inputs. The forced response of the linear system (5.4) is expressed in the frequency domain as follows

$$\delta X(s) = z_1 (sI_6 - A)^{-1} B\delta U(s) + (sI_6 - A)^{-1} Q\delta\Xi(s) \tag{5.5a}$$

$$\delta Y(s) = C\delta X(s) \tag{5.5b}$$

where I_6 is the 6×6 identity matrix, $z_1 = e^{-s\tau_1}$, $\delta X(s) = \mathcal{L}\{\delta x(t)\}$, $\delta U(s) = \mathcal{L}\{\delta u(t)\}$, $\delta\Xi(s) = \mathcal{L}\{\delta\xi(t)\}$, $\delta Y(s) = \mathcal{L}\{\delta y(t)\}$ and where $\mathcal{L}\{\bullet\}$ denotes the Laplace transform of the argument signal. The controller is of the proportional delayed feedback type with dynamic precompensator including delays, i.e.

$$\delta U(s) = z_2 K\delta X(s) + G(s, z_1, z_2)\delta\Omega(s) \tag{5.6}$$

where $z_2 = e^{-s\tau_2}$, τ_2 is the transmission / reconstruction delay of the measurable state variables at the controller and $\delta\Omega(s) = \mathcal{L}\{\delta\omega(t)\}$ is the Laplace transform of the 2×1 vector of external inputs, $G(s, z_1, z_2) \in \mathbb{R}(s, z_1, z_2)^{2\times 2}$ and $K \in \mathbb{R}^{2\times 6}$. The elements of the precompensator matrix $G(s, z_1, z_2)$ are rational functions of s where the numerator and denominator polynomial coefficients are multivariable rational function of z_1 and z_2. Following the procedure in [30], the delays τ_1 and τ_2 upper bounds of the respective communication delays plus the required processing time.

Substitution of the controller in (6) to the open loop system (5.5) yields

$$\delta Y(s) = H_{\Omega}(s, z_1, z_2)\delta\Omega(s) + H_{\Xi}(s, z_1, z_2)\delta\Xi(s) \tag{5.7a}$$

where

$$H_{\Omega}(s, z_1, z_2) = z_1 C\left(sI_6 - A - z_1 z_2 BK\right)^{-1} BG(s, z_1, z_2) \tag{5.7b}$$

$$H_{\Xi}(s, z_1, z_2) = C\left(sI_6 - A - z_1 z_2 BK\right)^{-1} Q \tag{5.7c}$$

The design goals are: a) I/O decoupling and b) attenuation of the influence of the disturbances to the performance outputs. I/O decoupling, being one of the most attractive design requirements in flight control, is formulated as

$$H_{\Omega}(s, z_1, z_2) = \underset{i=1,2}{\operatorname{diag}}\left\{h_i(s, z_1, z_2)\right\} \tag{5.8}$$

Where $h_1(s, z_1, z_2)$ and $h_2(s, z_1, z_2)$ are nonzero rational functions of s with the numerator and denominator polynomial coefficients being multivariable rational function of z_1 and z_2. The design goal of attenuation of the influence of the atmospheric disturbances to the outputs is translated to the following cost criterion

$$J(K) = \max_{i,j\in\{1,2\}}\left\{\left\|\left(h_{\Xi}\right)_{i,j}(s, z_1, z_2)\right\|_{\infty}\right\} \le e_{\max} \tag{5.9}$$

Where $e_{\max} \in \mathbb{R}^{+}$ is set by the designer to be enough small.

It is mentioned that the controller is designed using the linear approximant of the quadrotor model and so it is efficient around the operating point. To achieve manoeuvres extending far from the operating point the safe switching approach in [32] and [33] can be used.

5.3.1 I/O Decoupling

Using the approach in [34] it can be observed that the solvability conditions for I/O decoupling are satisfied. The equality (8) is satisfied by

$$G(s, z_1, z_2) = \tilde{G}(s, z_1, z_2)\operatorname{diag}\left\{h_i(s, z_1, z_2)\right\} \tag{5.10}$$

where $\tilde{G}(s,z_1,z_2)=\left[I_2-z_1z_2K\left(sI_6-A\right)^{-1}B\right]\left[H(s,z_1,z_2)\right]^{-1}$ and $H(s,z_1,z_2)=z_1C\left(sI_6-A\right)^{-1}B$. Note that by choosing $h_i(s,z_1,z_2)$, $(j=1,2)$ to be realizable enough, the realizability of the precompensator matrix is guaranteed. For now, we assume that the feedback matrix K is not specified. The matrix $\tilde{G}(s,z_1,z_2)$ is of the form

$$\tilde{G}(s,z_1,z_2)=\begin{bmatrix}\tilde{g}_{1,1}(s,z_1,z_2) & \tilde{g}_{1,2}(s,z_1,z_2)\\ \tilde{g}_{2,1}(s,z_1,z_2) & \tilde{g}_{2,2}(s,z_1,z_2)\end{bmatrix} \tag{5.11}$$

Its elements are derived to be in a 4-th order polynomial form with respect to s with homogeneous polynomial coefficients of 1^{st} order with respect to z_1^{-1} and z_2^{-1} i.e.

$$\tilde{g}_{i,j}(s,z_1,z_2)=\left(32bdK_l^2\bar{x}_6^3\right)^{-1}z_1^{-1}\times\sum_{k=0}^{4}\left[\left(\tilde{\gamma}_{i,j}\right)_k+z_1z_2\left(\hat{\gamma}_{i,j}\right)_k\right]s^k,(i,j=1,2)$$

and where

$$\left(\tilde{\gamma}_{1,1}\right)_0=4dK_ls_{\bar{x}_1}\bar{x}_6^2\left(a_1+2a_2\bar{x}_6\right)k_{dt,x}$$
$$\left(\tilde{\gamma}_{1,1}\right)_1=-\sqrt{2}c_{\bar{x}_1}\left(a_1+2a_2\bar{x}_6\right)k_{a,y}k_{dt,x}+4dK_ls_{\bar{x}_1}\bar{x}_6^2\left[m_q\left(a_1+2a_2\bar{x}_6\right)+k_{dt,x}\right]$$
$$\left(\tilde{\gamma}_{1,1}\right)_2=4dK_lm_qs_{\bar{x}_1}\bar{x}_6^2-$$
$$\sqrt{2}c_{\bar{x}_1}\left[a_1m_qk_{a,y}+a_1J_{q,y}k_{dt,x}+k_{a,y}k_{dt,x}+2a_2\bar{x}_6\left(m_qk_{a,y}+J_{q,y}k_{dt,x}\right)\right]$$
$$\left(\tilde{\gamma}_{1,1}\right)_3=-\sqrt{2}c_{\bar{x}_1}\left\{m_qk_{a,y}+J_{q,y}\left[m_q\left(a_1+2a_2\bar{x}_6\right)+k_{dt,x}\right]\right\}$$
$$\left(\tilde{\gamma}_{1,1}\right)_4=-\sqrt{2}c_{\bar{x}_1}m_qJ_{q,y}$$
$$\left(\tilde{\gamma}_{1,2}\right)_0=4dc_{\bar{x}_1}K_l\bar{x}_6^2\left(a_1+2a_2\bar{x}_6\right)k_{dt,z}$$
$$\left(\tilde{\gamma}_{1,2}\right)_1=\sqrt{2}s_{\bar{x}_1}\left(a_1+2a_2\bar{x}_6\right)k_{a,y}k_{dt,z}+4dK_lc_{\bar{x}_1}\bar{x}_6^2\left[m_q\left(a_1+2a_2\bar{x}_6\right)+k_{dt,z}\right]$$
$$\left(\tilde{\gamma}_{1,2}\right)_2=4dK_lm_qc_{\bar{x}_1}\bar{x}_6^2+$$
$$\sqrt{2}s_{\bar{x}_1}\left[a_1m_qk_{a,y}+a_1J_{q,y}k_{dt,z}+k_{a,y}k_{dt,z}+2a_2\bar{x}_6\left(m_qk_{a,y}+J_{q,y}k_{dt,z}\right)\right]$$
$$\left(\tilde{\gamma}_{1,2}\right)_3=\sqrt{2}s_{\bar{x}_1}\left\{m_qk_{a,y}+J_{q,y}\left[m_q\left(a_1+2a_2\bar{x}_6\right)+k_{dt,z}\right]\right\}$$
$$\left(\tilde{\gamma}_{1,2}\right)_4=\sqrt{2}m_qs_{\bar{x}_1}J_{q,y},\left(\tilde{\gamma}_{2,1}\right)_0=4ds_{\bar{x}_1}K_l\bar{x}_6^2\left(a_1+2a_2\bar{x}_6\right)k_{dt,x}$$
$$\left(\tilde{\gamma}_{2,1}\right)_1=\sqrt{2}c_{\bar{x}_1}\left(a_1+2a_2\bar{x}_6\right)k_{a,y}k_{dt,x}+4dK_ls_{\bar{x}_1}\bar{x}_6^2\left[m_q\left(a_1+2a_2\bar{x}_6\right)+k_{dt,x}\right]$$
$$\left(\tilde{\gamma}_{2,1}\right)_2=4dK_lm_qs_{\bar{x}_1}\bar{x}_6^2+$$
$$\sqrt{2}c_{\bar{x}_1}\left[a_1m_qk_{a,y}+a_1J_{q,y}k_{dt,x}+k_{a,y}k_{dt,x}+2a_2\bar{x}_6\left(m_qk_{a,y}+J_{q,y}k_{dt,x}\right)\right]$$

$$\left(\tilde{\gamma}_{2,1}\right)_3 = \sqrt{2}c_{\bar{x}_1}\left\{m_q k_{a,y} + J_{q,y}\left[m_q\left(a_1 + 2a_2\bar{x}_6\right) + k_{dt,x}\right]\right\}$$

$$\left(\tilde{\gamma}_{2,1}\right)_4 = \sqrt{2}m_q c_{\bar{x}_1} J_{q,y}, \left(\tilde{\gamma}_{2,2}\right)_0 = 4dc_{\bar{x}_1} K_l \bar{x}_6^2\left(a_1 + 2a_2\bar{x}_6\right)k_{dt,z}$$

$$\left(\tilde{\gamma}_{2,2}\right)_1 = -\sqrt{2}s_{\bar{x}_1}\left(a_1 + 2a_2\bar{x}_6\right)k_{a,y}k_{dt,z} + 4dK_l c_{\bar{x}_1}\bar{x}_6^2\left[m_q\left(a_1 + 2a_2\bar{x}_6\right) + k_{dt,z}\right]$$

$$\left(\tilde{\gamma}_{2,2}\right)_2 = 4dK_l m_q c_{\bar{x}_1}\bar{x}_6^2 -$$

$$\sqrt{2}s_{\bar{x}_1}\left[a_1 m_q k_{a,y} + a_1 J_{q,y}k_{dt,z} + k_{a,y}k_{dt,z} + 2a_2\bar{x}_6\left(m_q k_{a,y} + J_{q,y}k_{dt,z}\right)\right]$$

$$\left(\tilde{\gamma}_{2,2}\right)_3 = \sqrt{2}s_{\bar{x}_1}\left\{m_q k_{a,y} + J_{q,y}\left[m_q\left(a_1 + 2a_2\bar{x}_6\right) + k_{dt,z}\right]\right\}$$

$$\left(\tilde{\gamma}_{2,2}\right)_4 = -\sqrt{2}m_q s_{\bar{x}_1} J_{q,y}$$

$$\left(\hat{\gamma}_{1,1}\right)_0 = -4bdK_l\bar{x}_6\left\{2c_{\bar{x}_1}k_{1,1}k_{dt,x} + \bar{x}_6\left[8K_l\bar{x}_6 k_{1,2} + s_{\bar{x}_1}\left(k_{1,5} + k_{1,6}\right)k_{dt,x}\right]\right\}$$

$$\left(\hat{\gamma}_{1,1}\right)_1 = b\left\{-4dK_l m_q s_{\bar{x}_1}\bar{x}_6^2\left(k_{1,5} + k_{1,6}\right) +\right.$$

$$\left. c_{\bar{x}_1}\left[\sqrt{2}k_{1,5}k_{a,y}k_{dt,x} - \sqrt{2}k_{1,6}k_{a,y}k_{dt,x} - 8dK_l\bar{x}_6\left(m_q k_{1,1} + k_{1,4}k_{dt,x}\right)\right]\right\}$$

$$\left(\hat{\gamma}_{1,1}\right)_2 = bc_{\bar{x}_1}\left[-8dK_l m_q\bar{x}_6 k_{1,4} + \sqrt{2}m_q\left(k_{1,5} - k_{1,6}\right)k_{a,y} + \sqrt{2}J_{q,y}\left(k_{1,5} - k_{1,6}\right)k_{dt,x}\right]$$

$$\left(\hat{\gamma}_{1,1}\right)_3 = \sqrt{2}bc_{\bar{x}_1}m_q J_{q,y}\left(k_{1,5} - k_{1,6}\right)$$

$$\left(\hat{\gamma}_{1,1}\right)_4 = 0, \left(\hat{\gamma}_{1,2}\right)_0 = -4bdK_l\bar{x}_6\left[8K_l\bar{x}_6^2 k_{1,3} - 2s_{\bar{x}_1}k_{1,1}k_{dt,z} + c_{\bar{x}_1}\bar{x}_6\left(k_{1,5} + k_{1,6}\right)k_{dt,z}\right]$$

$$\left(\hat{\gamma}_{1,2}\right)_1 = b\left\{-4dc_{\bar{x}_1}K_l m_q\bar{x}_6^2\left(k_{1,5} + k_{1,6}\right) + s_{\bar{x}_1}\left[\sqrt{2}k_{1,6}k_{a,y}k_{dt,z}\right.\right.$$

$$\left.\left. -\sqrt{2}k_{1,5}k_{a,y}k_{dt,z} + 8dK_l\bar{x}_6\left(m_q k_{1,1} + k_{1,4}k_{dt,z}\right)\right]\right\}$$

$$\left(\hat{\gamma}_{1,2}\right)_2 = -bs_{\bar{x}_1}\left[-8dK_l m_q\bar{x}_6 k_{1,4} + \sqrt{2}m_q\left(k_{1,5} - k_{1,6}\right)k_{a,y} + \sqrt{2}J_{q,y}\left(k_{1,5} - k_{1,6}\right)k_{dt,z}\right]$$

$$\left(\hat{\gamma}_{1,2}\right)_3 = \sqrt{2}bm_q s_{\bar{x}_1}J_{q,y}\left(k_{1,6} - k_{1,5}\right)$$

$$\left(\hat{\gamma}_{1,2}\right)_4 = 0$$

$$\left(\hat{\gamma}_{2,1}\right)_0 = -4bdK_l\bar{x}_6\left\{2c_{\bar{x}_1}k_{2,1}k_{dt,x} + \bar{x}_6\left[8K_l\bar{x}_6 k_{2,2} + s_{\bar{x}_1}\left(k_{2,5} + k_{2,6}\right)k_{dt,x}\right]\right\}$$

$$\left(\hat{\gamma}_{2,1}\right)_1 = b\left\{-4dK_l m_q s_{\bar{x}_1}\bar{x}_6^2\left(k_{2,5} + k_{2,6}\right) + c_{\bar{x}_1}\left[\sqrt{2}k_{2,5}k_{a,y}k_{dt,x} -\right.\right.$$

$$\left.\left. -\sqrt{2}k_{2,6}k_{a,y}k_{dt,x} - 8dK_l\bar{x}_6\left(m_q k_{2,1} + k_{2,4}k_{dt,x}\right)\right]\right\}$$

$$\left(\hat{\gamma}_{2,1}\right)_2 = bc_{\bar{x}_1}\left[-8dK_l m_q\bar{x}_6 k_{2,4} + \sqrt{2}m_q\left(k_{2,5} - k_{2,6}\right)k_{a,y} + \sqrt{2}J_{q,y}\left(k_{2,5} - k_{2,6}\right)k_{dt,x}\right]$$

$$\left(\hat{\gamma}_{2,1}\right)_3 = \sqrt{2}bc_{\bar{x}_1}m_q J_{q,y}\left(k_{2,5} - k_{2,6}\right)$$

$$\left(\hat{\gamma}_{2,1}\right)_4 = 0$$

$$\left(\hat{\gamma}_{2,2}\right)_0 = -4bdK_l\bar{x}_6\left[8K_l\bar{x}_6^2 k_{2,3} - 2s_{\bar{x}_1}k_{2,1}k_{dt,z} + c_{\bar{x}_1}\bar{x}_6\left(k_{2,5} + k_{2,6}\right)k_{dt,z}\right]$$

$$\left(\hat{\gamma}_{2,2}\right)_1 = b\left\{-4dc_{\bar{x}_1}K_l m_q\bar{x}_6^2\left(k_{2,5} + k_{2,6}\right) + s_{\bar{x}_1}\left[\sqrt{2}k_{2,6}k_{a,y}k_{dt,z}\right.\right.$$

$$\left.\left. -\sqrt{2}k_{2,5}k_{a,y}k_{dt,z} + 8dK_l\bar{x}_6\left(m_q k_{2,1} + k_{2,4}k_{dt,z}\right)\right]\right\}$$

$$\left(\hat{\gamma}_{2,2}\right)_2 = -bs_{\bar{x}_1}\left[-8dK_l m_q\bar{x}_6 k_{2,4} + \sqrt{2}m_q\left(k_{2,5} - k_{2,6}\right)k_{a,y} + \sqrt{2}J_{q,y}\left(k_{2,5} - k_{2,6}\right)k_{dt,z}\right]$$

$$\left(\hat{\gamma}_{2,2}\right)_3 = \sqrt{2}bm_q s_{\bar{x}_1}J_{q,y}\left(k_{2,6} - k_{2,5}\right)$$

$$\left(\hat{\gamma}_{2,2}\right)_4 = 0$$

Where $k_{i,j}$ is the $\{i,j\}$ element of the feedback matrix K. The symbols $s_{\bar{x}_1} = \sin\left(\bar{x}_1\right)$ and $c_{\bar{x}_1} = \cos\left(\bar{x}_1\right)$ have been used. In order to have a realizable precompensator and a strictly proper and stable closed loop transfer matrix with steady state gain the 2×2 matrix identity matrix, the diagonal elements of the closed loop transfer matrix are chosen to be $h_i\left(s, z_1, z_2\right) = z_1 / \prod_{j=1}^{5}\left(T_{i,j}s + 1\right), \left(i = 1,2\right)$, where $T_{i,j}$ are positive real numbers. This implies asymptotic command following. The elements of the feedback matrix K are chosen to satisfy closed loop stability and disturbance attenuation.

5.3.2 Disturbance Attenuation

In order to accomplish disturbance attenuation, the feedback matrix elements are selected so that a) The closed loop system is stable for $0 \le \tau_1 + \tau_2 < \tau_{\max}$ and b) The condition in (5.9) is satisfied. To this end, a mixed analytic - heuristic approach is proposed. In the analytic part of the approach, the elements $k_{1,j}$ $(j = 1,\ldots,6)$ are chosen in terms of $k_{2,i}$ such that when $\tau_1 + \tau_2 = 0$, the delayless closed loop characteristic polynomial is of the form

$$p_c\left(s\right) = \prod_{j=0}^{5}\left(s + \rho + j\delta\rho\right)$$

where ρ and $\delta\rho$ are positive real numbers. The above selection guarantees stability for the closed delayless case with system poles being equally distanced. In order to determine the values of $k_{2,i}$ $(i = 1,\ldots,6)$ as well as ρ and $\left(\delta\rho\right)$ achieving disturbance attenuation, a metaheuristic algorithm similar to that presented in [35] and [36] is proposed. The key point of the algorithm is to define an initial search area for the controller parameters and after several loops to contract to a suboptimal solution for the controller parameters that satisfy the stability and the disturbance attenuation conditions, for the nonzero delay case. The metaheuristic algorithm is:

Initial Data and Performance Criterion

1) Center values and half widths for the initial search area $\left(k_{2,j}\right)_c$, $\left(\rho\right)_c$, $\left(\delta\rho\right)_c$, $\left(k_{2,j}\right)_w$, $\left(\rho\right)_w$ and $\left(\delta\rho\right)_w$.

2) Performance criterion $J\left(k_{2,j},\rho,\delta\rho\right)$.

3) Iteration parameters n_{loop}, n_{rep}, $n_{total} \in \mathrm{N}$.

4) Search algorithm threshold λ.

Algorithm

Step 0: Set the numbering index $i_{\max} = 0$.

Step 1: Determine a search area $\Im$ for the controller parameters according to the inequalities

$$\left(k_{2,j}\right)_c - \left(k_{2,j}\right)_w \le k_{2,j} \le \left(k_{2,j}\right)_c + \left(k_{2,j}\right)_w$$

$$\left(\rho\right)_c - \left(\rho\right)_w \le \rho \le \left(\rho\right)_c + \left(\rho\right)_w$$

$$\left(\delta\rho\right)_c - \left(\delta\rho\right)_w \le \delta\rho \le \left(\delta\rho\right)_c + \left(\delta\rho\right)_w$$

Step 2: Set the numbering index $i_1 = 0$.

Step 3: Set the numbering index $i_1 = i_1 + 1$.

Step 4: Set the numbering index $i_2 = 0$.

Step 5: Set the numbering index $i_{\max} = i_{\max} + 1$. If $i_{\max} > n_{total}$ go to ***Step 15***.

Step 6: Set the numbering index $i_2 = i_2 + 1$.

Step 7: Select randomly a set of controller parameters within the search area $\Im$, let $\left(k_{2,j}\right)_{i_2}$, $\left(\rho\right)_{i_2}$ and $\left(\delta\rho\right)_{i_2}$ and evaluate the respective controller parameters $\left(k_{1,j}\right)_{i_2}$. Check if stability conditions for the nonzero delay case are satisfied. If yes, proceed to the next step. If not, repeat Step 7.

***Step 8*:** Evaluate $J_{i_2} = J\left(\left(k_{2,j}\right)_{i_2},\left(\rho\right)_{i_2},\left(\delta\rho\right)_{i_2}\right)$

Step 9: If $J_{i_2} < e_{\max}$ go to ***Step 15***.

Step 10: If $i_2 < n_{loop}$ go to ***Step 5***.

Step 11: Find $\left(J_{\min}\right)_{i_2} = \min\left\{J_i, i = 1,\ldots,n_{loop}\right\}$ and the respective controller parameters $\left(k_{2,j}\right)_{i_1}$, $\left(\rho\right)_{i_1}$ and $\left(\delta\rho\right)_{i_1}$.

Step 12: If $i_1 \geq n_{rep}$ then find the controller parameters, $\left(k_{2,j}\right)_{\min}$, $\left(\rho\right)_{\min}$, $\left(\delta\rho\right)_{\min}$ and $\left(k_{2,j}\right)_{\max}$, $\left(\rho\right)_{\max}$, $\left(\delta\rho\right)_{\max}$ corresponding to $J_{\min} = \min\left\{\left(J_{\min}\right)_i, i = 1,\ldots,n_{rep}\right\}$ and $J_{\max} = \max\left\{\left(J_{\min}\right)_i, i = 1,\ldots,n_{rep}\right\}$. Else go to ***Step 3***.

Step 13: Define

$$\left(k_{2,j}\right)_c = \left(\left(k_{2,j}\right)_{\min} + \left(k_{2,j}\right)_{\max}\right)/2$$

$$\left(\rho\right)_c = \left(\left(\rho\right)_{\min} + \left(\rho\right)_{\max}\right)/2$$

$$\left(\delta\rho\right)_c = \left(\left(\delta\rho\right)_{\min} + \left(\delta\rho\right)_{\max}\right)/2$$

$$\left(k_{2,j}\right)_w = \left|\left(k_{2,j}\right)_{\min} - \left(k_{2,j}\right)_{\max}\right|/2$$

$$(\rho)_w = \left|(\rho)_{\min} - (\rho)_{\max}\right| / 2$$

$$(\delta\rho)_w = \left|(\delta\rho)_{\min} - (\delta\rho)_{\max}\right| / 2$$

Step 14: If $\left(k_{2,j}\right)_w > \lambda$ or $(\rho)_w > \lambda$ or $(\delta\rho)_w > \lambda$, go to ***Step 2***.

Step 15: If $J_{i_2} < e_{\max}$ then set $k_{2,j} = \left(k_{2,j}\right)_{i_2}$, $\rho = (\rho)_{i_2}$ and $\delta\rho = (\delta\rho)_{i_2}$ (determined in Step 7), else set $k_{2,j} = \left(k_{2,j}\right)_{\min}$, $\rho = (\rho)_{\min}$ and $\delta\rho = (\delta\rho)_{\min}$ (determined in ***Step 12***).

5.4 SIMULATION RESULTS

To demonstrate the performance of the above proposed control scheme for a climbing manoeuvre, the linear controller (5.6) is used in the form $\Delta U(s) = z_2 K \Delta X(s) + G(s, z_1, z_2)\delta\Omega(s)$ where $\Delta X(s) = \mathcal{L}\{\Delta x(t)\}$. Upon adding the nominal values of the inputs to the variations of the inputs, the result is applied to the nonlinear system (1).

Consider the parameters of the quadrotor model in [13] and [37]:

$$m_q = 0.4[\text{kg}], J_{q,y} = 3.8278 \cdot 10^{-3}\left[\text{N}m / rad / s^2\right]$$
$$g = 9.81\left[\text{m} / s^2\right], d = 0.205[\text{m}], k_{dt,x} = 0.032[\text{N} / m / s]$$
$$k_{dt,z} = 0.048[\text{N} / m / s], k_{a,y} = 5.567 \cdot 10^{-4}[\text{N} / m / s]$$
$$K_l = 2.9842 \cdot 10^{-5}[\text{N} / rad / s], \alpha_0 = 189.63, \alpha_1 = 6.0612$$
$$\alpha_2 = 0.0122, \beta = 280.19, \bar{x}_2 = 1[\text{m} / s]$$

Furthermore, let

$$e_{\max} = 0.2, \left(k_{2,1}\right)_c = 0, \left(k_{2,2}\right)_c = 0, \left(k_{2,3}\right)_c = 0$$
$$\left(k_{2,4}\right)_c = 0, \left(k_{2,5}\right)_c = 0, \left(k_{2,6}\right)_c = 0, (\rho)_c = 0.5$$
$$(\delta\rho)_c = 0.5, \left(k_{2,1}\right)_w = 1, \left(k_{2,2}\right)_w = 1, \left(k_{2,3}\right)_w = 1$$

$$\left(k_{2,4}\right)_w = 1, \left(k_{2,5}\right)_w = 1, \left(k_{2,6}\right)_w = 1, \left(\rho\right)_w = 0.5$$
$$\left(\delta\rho\right)_w = 0.5, \lambda = 0.01, n_{loop} = 10, n_{rep} = 30$$
$$n_{total} = 3 \cdot 10^4, T_{1,1} = 0.1, T_{1,2} = 0.2, T_{1,3} = 0.3$$
$$T_{1,4} = 0.4, T_{1,5} = 0.5, T_{2,1} = 0.1, T_{2,2} = 0.2, T_{2,3} = 0.3$$
$$T_{2,4} = 0.4, T_{2,5} = 0.5, \tau_1 = 0.21[\mathrm{s}], \tau_2 = 0.09[\mathrm{s}]$$
$$\tau_{\max} = 0.3[\mathrm{s}]$$

Using the above parameters, execution of the metaheuristic algorithm yields

$$\rho = 0.8615, \delta\rho = 0.7612, k_{2,1} = -2.1102,$$
$$k_{2,2} = -0.3553, k_{2,3} = -0.4750, k_{2,4} = -0.8488,$$
$$k_{2,5} = -0.2222, k_{2,6} = 0.2370$$

resulting in

$$k_{1,1} = -1.9777, k_{1,2} = -0.3511, k_{1,3} = -0.4755$$
$$k_{1,4} = -0.7356, k_{1,5} = -0.2202, k_{1,6} = 0.2351$$

Using the the above set of values, the cost criterion is computed to be $J = 0.1959$. Thus the condition (5.9) is satisfied.

Simulation of the closed loop system is accomplished using Matlab/Simulink software while simulation of the wireless network is carried out using the TrueTime 2.0 add-on (see [38]). Let

$$\beta_1 = \sup_{t \in \mathbb{R}_{\geq 0}} \left|\xi_1(t)\right|, \beta_2 = \sup_{t \in \mathbb{R}_{\geq 0}} \left|\xi_2(t)\right|$$

For simulation purposes, the disturbances will be considered to be random with $\beta_1 = \beta_2 = 0.1[\mathrm{m/s}]$. The implementation of the disturbance signals is carried out through random discrete time signal generators, satisfying the above inequalities, with a sampling period of $0.1[\mathrm{s}]$. The signal is fed through a zero-order-hold and the 3rd order filter

$$H_f(s) = \frac{1}{(0.002s+1)(0.003s+1)(0.004s+1)}$$

The external commands are

$$\delta\omega_1(t) = \alpha_1\left(1 - 2e^{-5t} + 9e^{-10t/3} - 8e^{-5t/2}\right)$$
$$\delta\omega_2(t) = \alpha_2\left(1 - 2e^{-5t} + 9e^{-10t/3} - 8e^{-5t/2}\right)$$

where $\alpha_1 = \alpha_2 = 0.5[\mathrm{m}/s]$. Using the above presented data and the controller given in 5.3, the closed loop response of the nonlinear model of the quadrotor is presented in Figures 5.1 to 5.8. In particular, the actuatable inputs are presented in Figures 5.1 and 5.2 while the state variable responses are presented in Figures 5.3 to 5.8. From Figures 5.1 and 5.2 it can be observed that the actuatable inputs remain appropriately bounded, thus being easily implementable. With respect to the performance variables (see Figures 5.4 and 5.5), it can be observed that the nonlinear responses follow accurately the reference model presenting small deviations due to the presence of disturbances, the application of the linear controller to the nonlinear model and the presence of the wireless network. As for the remaining state variables (see Figures 5.3, and 5.6 to 5.8), it is observed that they are sufficiently bounded thus providing satisfactory flight conditions.

In order to further demonstrate the good performance of the proposed control scheme, the responses of the performance variables $x_2(t)$ and $x_3(t)$ of the nonlinear closed loop system, using the wireless network controller proposed in 5.3, will be examined for various values of α_1, α_2, β_1 and β_2 inside a time frame ($t \le T_{\max}$). These responses will be compared to the respective responses $\delta x_2(t) + \bar{x}_2$ and $\delta x_3(t) + \bar{x}_3$ of the linear closed system (4) and (6) for the same set of α_1, α_2, β_1 and β_2. Similarly to [39], in order to execute this comparison define the percentile errors

$$\varepsilon_1 = \frac{\left\| x_2(t) - \delta x_2(t) - \bar{x}_2 \right\|_2}{\left\| \delta x_2(t) \right\|_2} \times 100\%$$

$$\varepsilon_2 = \frac{\left\| x_3(t) - \delta x_3(t) - \bar{x}_3 \right\|_2}{\left\| \delta x_3(t) \right\|_2} \times 100\%$$

where $\left\|x_i(t)\right\|_2 = \int_0^{T_{max}} x_i^2(t)\,dt$. After performing series of computational experiments, it is verified that the design goal of I/O decoupling with simultaneous disturbance attenuation is satisfied for a wide range of α_1, α_2, β_1 and β_2. The design goal is satisfied despite the presence of the wireless network and the nonlinearities of the model of the quadrotor. Indicatively, in Figures 5.9 and 5.10, contour plots of the above percentile errors are presented for $\alpha_1 = 0.5[\mathrm{m}/s]$, $\alpha_2 = 0.5[\mathrm{m}/s]$, $0[\mathrm{m}/s] \le \beta_1 \le 1[\mathrm{m}/s]$, $0[\mathrm{m}/s] \le \beta_2 \le 1[\mathrm{m}/s]$ and $T_{\max} = 7[\mathrm{s}]$. In Figures 5.11 and 5.12 contour plots of the above percentile errors are presented for $-2[\mathrm{m}/s] \le \alpha_1 \le 2[\mathrm{m}/s]$, $-2[\mathrm{m}/s] \le \alpha_2 \le 2[\mathrm{m}/s]$, $\beta_1 = 0[\mathrm{m}/s]$, $\beta_2 = 0[\mathrm{m}/s]$ and again $T_{\max} = 7[\mathrm{s}]$.

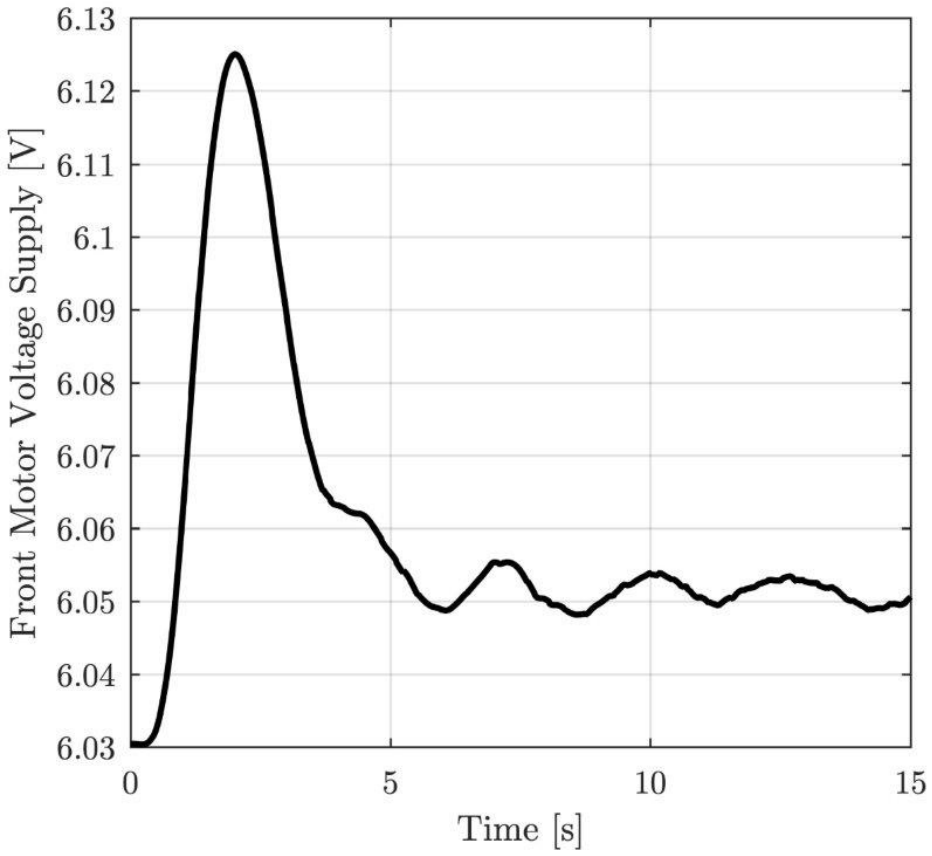

Fig. 5.1 Voltage supplies to the front motors.

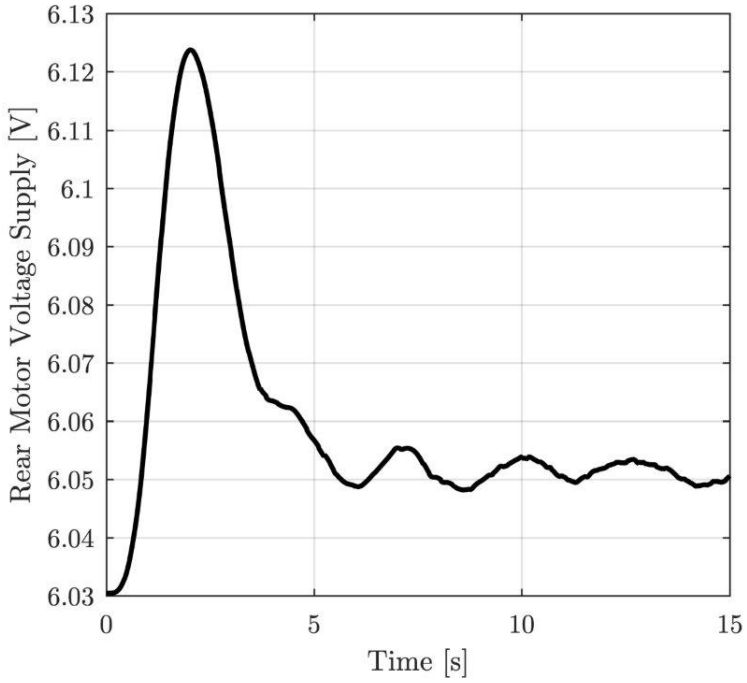

Fig. 5.2 Voltage supplies to the rear motors.

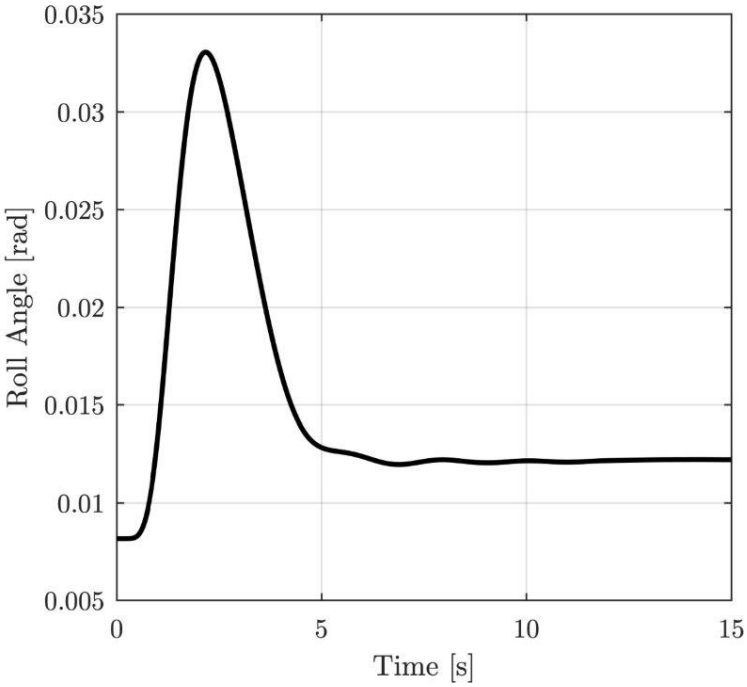

Fig. 5.3 Pitch angle of the quadrotor.

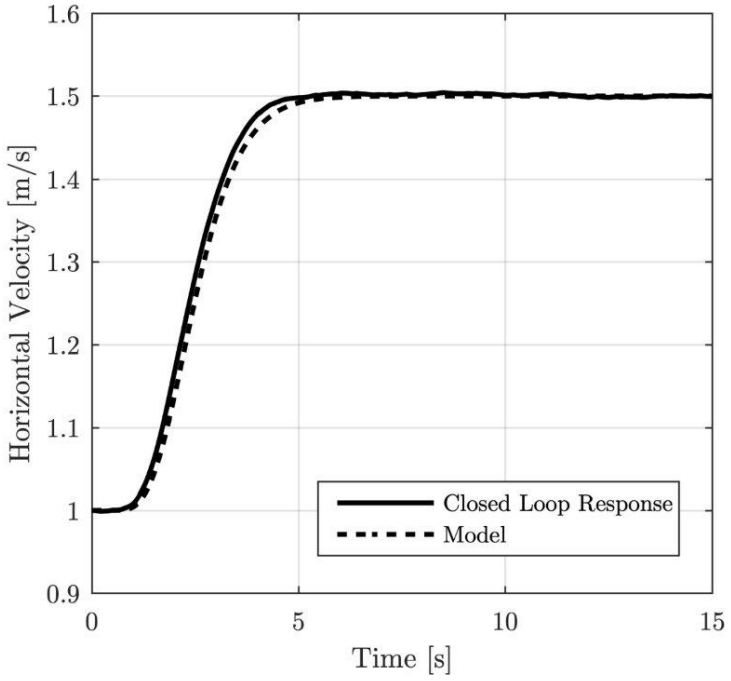

Fig. 5.4 Horizontal velocity of the quadrotor vs model response.

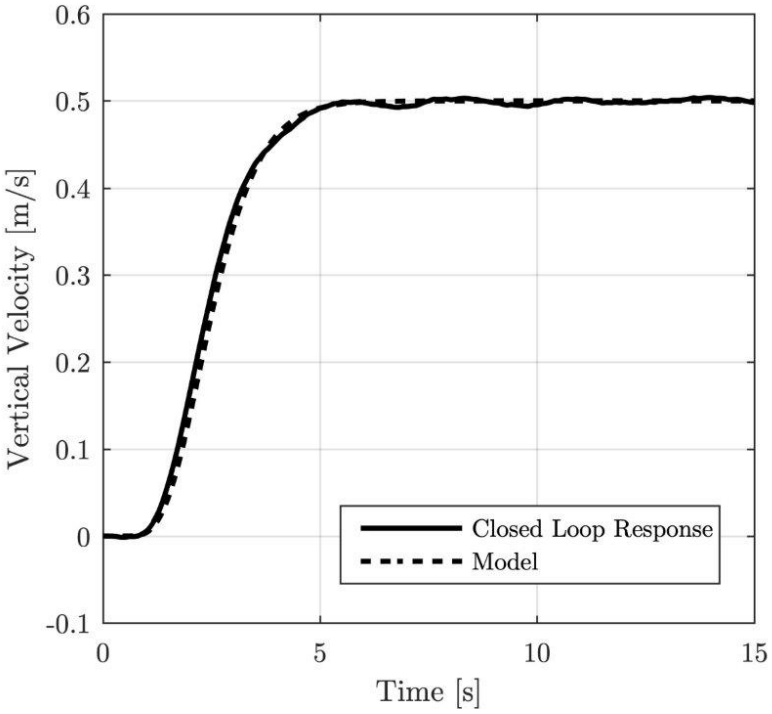

Fig. 5.5 Vertical velocity of the quadrotor vs model response.

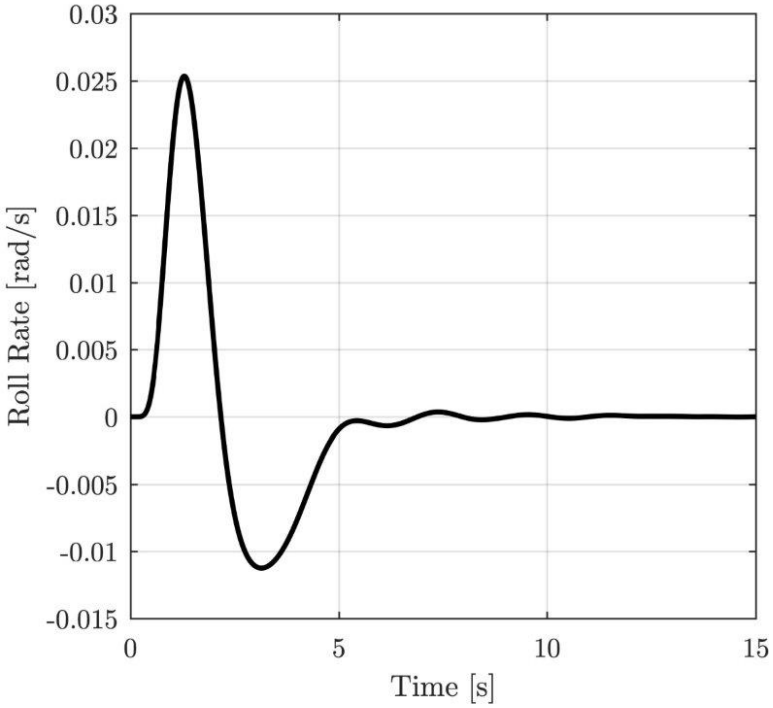

Fig. 5.6 Pitch rate.

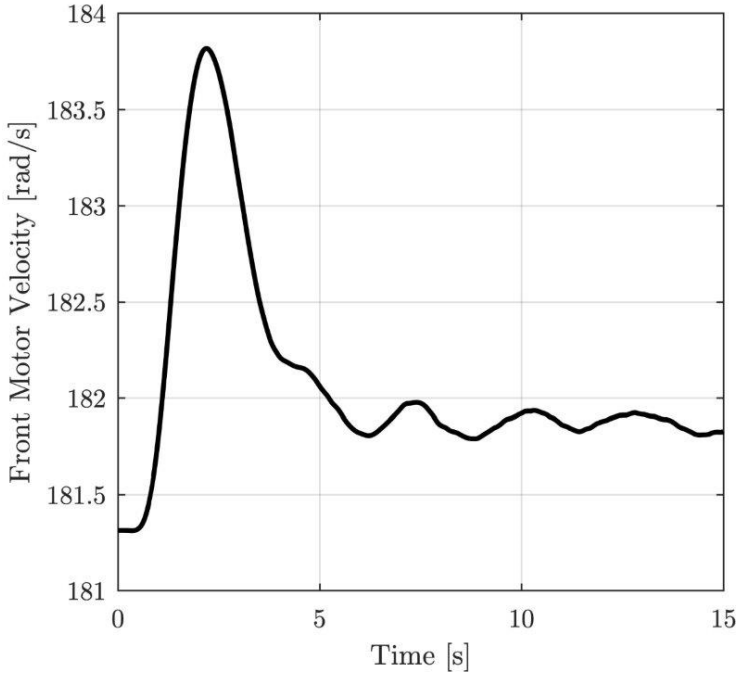

Fig. 5.7 Angular velocity of the front motors.

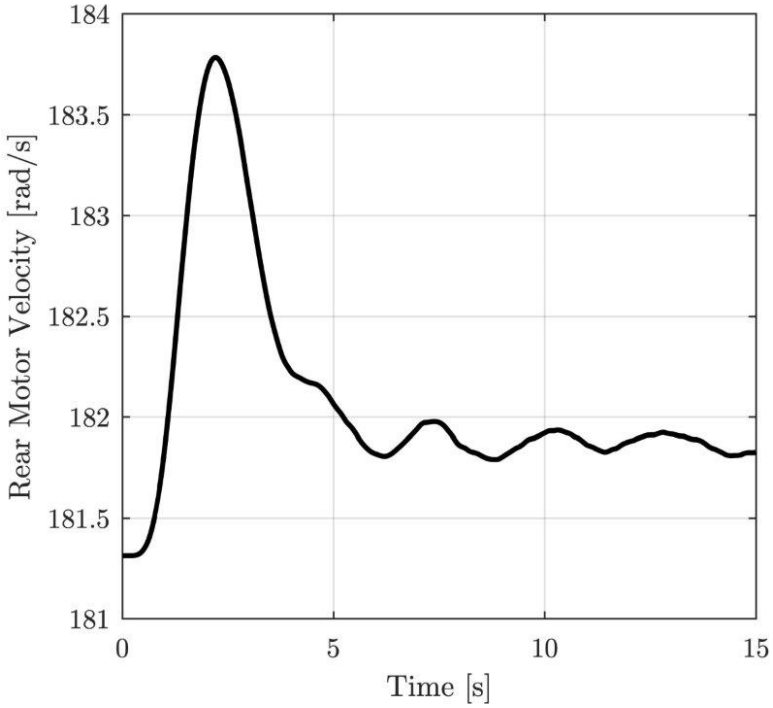

Fig. 5.8 Angluar velocity of the rear motors.

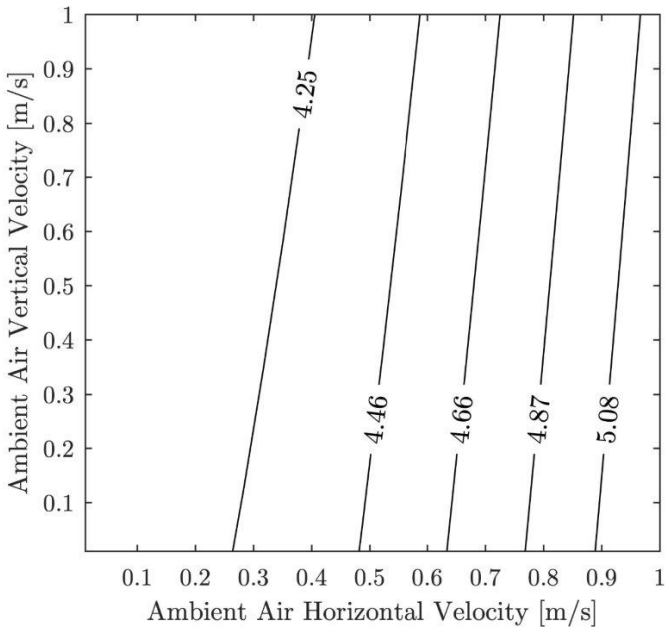

Fig. 5.9 Percentile error contour plot for the horizontal velocity.

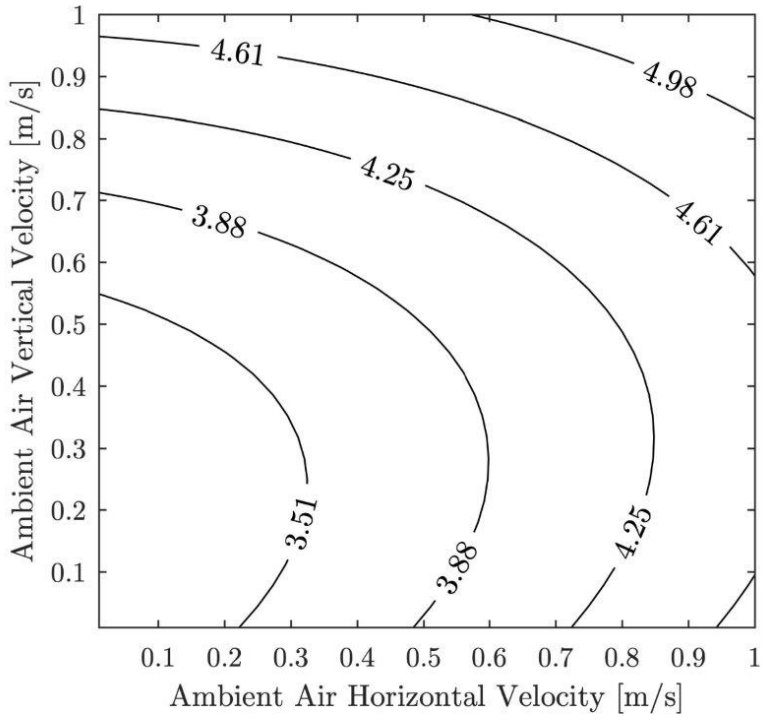

Fig. 5.10 Percentile error contour plot for the vertical velocity.

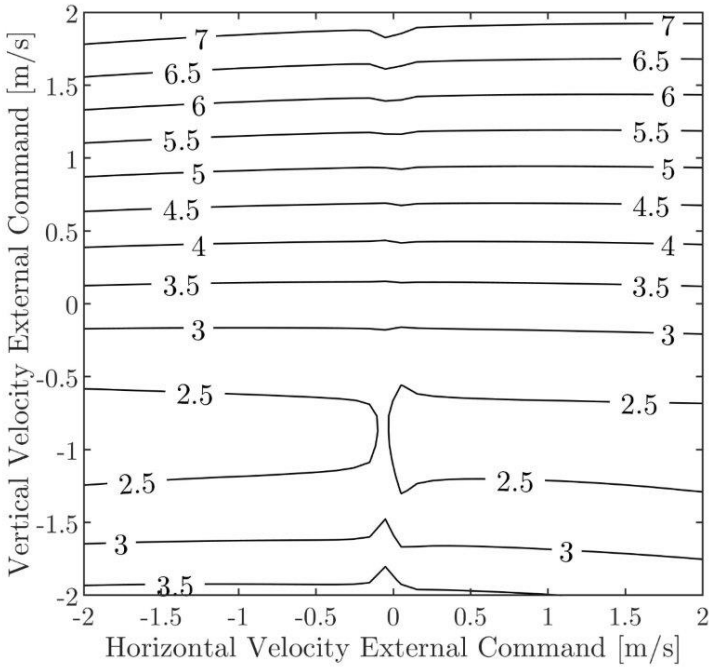

Fig. 5.11 Percentile error contour plot for the horizontal velocity.

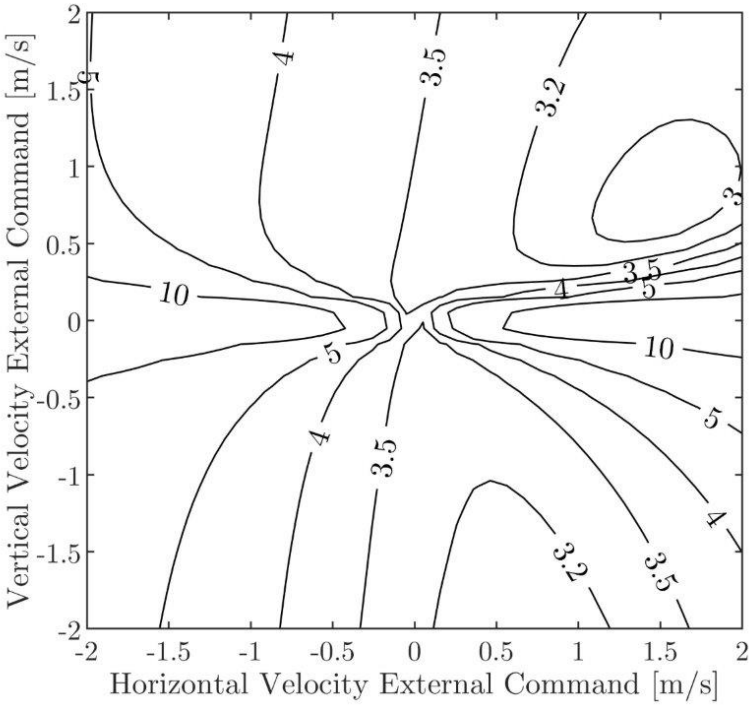

Fig. 5.12 Percentile error contour plot for the vertical velocity.

5.5 SUMMARY

In this work, the problem of I/O decoupling with simultaneous disturbance attenuation via a wireless remote controller has been studied for a quadrotor in longitudinal motion under the influence of atmospheric disturbances. Based on the linear approximant of the quadrotor model, an appropriate realizable dynamic controller depending upon constant communication delays and providing I/O decoupling with simultaneous disturbance attenuation and has been designed. Constant communication delays have been achieved using an appropriate synchronization/signal reconstruction algorithm. Using a metaheuristic algorithm, the stability of the closed loop system has been satisfying. The results have been tested to the case of a climbing manoeuvre where it has been observed that the performance of the closed loop system is satisfactory. The closed loop performance remains satisfactory even for a wide range of external commands and a wide range of disturbance amplitudes. The proposed controller provides tolerance to communication noise and package receipt delays.

[1] D. Zhang, H. Qi, X. Wu, Y. Xie, and J. Xu, “The Quadrotor Dynamic Modelling and Indoor Target Tracking Control Method”, Mathematical Problems in Engineering, 2014.

[2] G. M. Magalhaes, E. G. Santos, L. M. Borges, A. E. C. Cunha, “Com-parison and Implementation of Control Strategies for a Quadrotor”, XIII *Simpósio Brasileiro de Automação Inteligente*, Porto Alegre, 1-4October, pp. 133-138, 2017.

[3] R. A. Garcia, F. R. Rubio and M. G. Ortega, “Robust PID Control of the Quadrotor Helicopter”, IFAC Proceedings Volumes, vol. 45, no. 3, pp. 229-234, 2012.

[4] J. Moreno-Valenzuela, R. Perez-Alcocer, M. Guerrero-Medina and A. Dzul, “Nonlinear PID-Type Controller for Quadrotor Trajectory Tracking”, IEEE/ASME Transactions on Mechatronics, vol. 23, no. 5,pp. 2436-2447, 2018.

[5] M. S. Chehadeh and I. Boiko, “Design of rules for in-flight non-parametric tuning of PID controllers for unmanned aerial vehicles”, Journal of the Franklin Institute, vol. 356, pp. 474-491, 2019.

[6] P. Outeiro, C. Cardeira and P. Oliveira, “Lqr/mmae height control system of a quadrotor for constant unknown load transportation”, Proceedings of the 13th APCA International Conference on Control and Soft Computing (CONTROLO), pp. 389-394, Ponta Delgada, Portugal, June 4-6, 2018.

[7] A. Safaei and M. N. Mahyuddin, “Optimal model-free control for a generic MIMO nonlinear system with application to autonomous mobile robots”, International Journal of Adaptive Control and Signal Processing, vol. 3, pp. 792-815, 2018.

[8] O. Ozturk and H. M. Ozkan “Optimal Control of Quadrotor Un-manned Aerial Vehicles on Time Scales”, International Journal of Difference Equations, vol. 13, pp. 41-54, 2018.

[9] F. Sabatino, Quadrotor control: modelling, nonlinear control design, and simulation, Master’s Degree Project, KTH Electrical Engineering, Stockholm, Sweden, June 2015.

[10] H. Arrosida, R. Effendi, T. Agustinah, J. Pramudijanto, Design of Decoupling and Nonlinear PD Controller for Cruise Control of a Quadrotor, International Seminar on Intelligent Technology and its Applications (ISITIA), pp. 57-61, 2015.

[11] S. Leonardo, P. Zaira and M. Duque, Nonlinear Control of the Airship Cruise Flight Phase with Dynamical Decoupling, Electronics, Robotics and Autonomous Mechanics Conference, pp.473-477, 2008.

[12] G. G. Neto, F. Dos S. Barbosa, J. Genario, O. Junior, B. A. Angelico, State feedback decoupling control of a 2DoF Helicopter, XIII *Simpósio Brasileiro de Automação Inteligente*, Porto Alegre, 1-4 October, pp.398-403, 2017.

[13] N. D. Kouvakas and F. N. Koumboulis, "Independent Velocity Control of the Longitudinal Motion of Quadrotors", Proceedings of the7thInternational Conference on Systems and Control, pp. 194-200, Valencia, Spain, October 24-26, 2018.

[14] W. Cai, J. She, M. Wu and Y. Ohyama, "Disturbance suppression for quadrotor UAV using sliding-mode-observer-based equivalent-input-disturbance approach", ISA Transactions, 2019.

[15] X. Wang, S. Sun, E.-J. van Kampen and Q. Chu, "Quadrotor Fault Tolerant Incremental Sliding Mode Control driven by Sliding Mode Disturbance Observers", Aerospace Science and Technology, vol. 87,pp. 417-430, 2019.

[16] B. Wang, X. Yu, L. Mu and Y. Zhang, "Disturbance observer-based adaptive fault-tolerant control for a quadrotor helicopter subject to parametric uncertainties and external disturbances", Mechanical Systems and Signal Processing, vol. 120, pp. 727-743, 2019.

[17] H. Rios, R. Falcon, O. A. Gonzalez and A. Dzul, "Continuous Sliding-Mode Control Strategies for Quadrotor Robust Tracking: Real-Time Application", IEEE Transactions on Industrial Electronics, vol. 66, no. 2, pp. 1264-1272, 2019.

[18] M. Chen, S. Xiong and Q. Wu, "Tracking Flight Control of Quadrotor Based on Disturbance Observer", IEEE Transactions on Systems, Man, and Cybernetics: Systems, 2019.

[19] L. Qia and H. H. T. Liu, "Path Following Control of A Quadrotor UAV with A Cable Suspended Payload Unde Wind Disturbances", IEEE Transactions on Industrial Electronics, 2019.

[20] Y. Yuan, L. Cheng, Z. Wang and C. Sun, "Position tracking and attitude control for quadrotors via active disturbance rejection control method", Science China: Information Sciences, vol. 62, 2018.

[21] A. Baldini, R. Felicetti, A. Freddi, S. Longhi and A. Monteriu, "Direct position control of an octarotor unmanned vehicle under wind gust disturbance", Proceedings of the 2019 International Conference on *Unmanned Aircraft Systems (ICUAS)*, pp. 684-691, Atlanta, GA, USA, June 11-14, 2019.

[22] H. Shraim, Ali Awada and Rafic Youness, "A Survey on Quadrotors: Configurations, Modeling and Identification, Control, Collision Avoidance, Fault Diagnosis and Tolerant Control", IEEE Aerospace and Electronics Systems Magazine, vol. 33, no. 7, pp. 14-33, 2018.

[23] S. Xiong, M. Chen and Q. Wu, “Predictive control for networked switch flight system with packet dropout”, Applied Mathematics and Computation, vol. 354, pp. 444-459, 2019.

[24] A. Gonzaleza, A. Cuencab, V. Balaguerb and P. Garcia, “Event triggered predictor-based control with gain-Scheduling and extended state observer for networked control systems”, Information Sciences, vol. 491, pp. 90-108, 2019.

[25] L. He, J. Zhang, Y. Hou, X. Liang and P. Bai, “Time-Varying Formation Control for Second-Order Discrete-Time Multi-Agent Systems With Directed Topology and Communication Delay”, IEEE Access, vol. 7, pp. 33517 - 3352, 2019.

[26] J. A. Guerrero, P. C. Garcia and Y. Challal, “Quadrotors Formation Control: A Wireless Medium Access Aware Approach”, Journal of Intelligent and Robotic Systems, vol. 70, pp. 221 - 231, 2013.

[27] F. N. Koumboulis and K. G. Tzierakis, “Meeting Transfer Function Requirements via static measurement output feedback”, Journal of the Franklin Institute, vol. 335B, no. 4, pp. 661-667, 1998.

[28] I. Rosario-Gabriel and H. R. Cortes, “Aircraft Longitudinal Control based on the Lanchester’s Phugoid Dynamics Model”, Proceedings of the 2018 International Conference on Unmanned Aircraft Systems (ICUAS), pp. 924-929, 12-15 June 2018, Dallas, USA.

[29] D. D. Dhadekar and S. E. Talole, “Robust Fault Tolerant Longitudinal Aircraft Control”, IFAC-Papers OnLine, vol. 51, no. 1, pp. 604-609, 2018.

[30] F. Gossmann, F. Svaricek and A. Gabrys, “Control of Longitudinal Aircraft Motion with Loadcase Robustness using LPV-Control with Partly-Measurable Parameters”, Proceedings of the 2018 AIAA Guidance, Navigation, and Control Conference, pp. 1-13, 8–12 January 2018, Florida, USA.

[31] F. N. Koumboulis, N. D. Kouvakas, G. L. Giannaris and D. Vouyioukas, “Independent motion control of a tower crane through wireless sensor and actuator networks”, ISA Transactions, pp. 312320, vol. 60, 2016.

[32] F. N. Koumboulis, R.E. King, A. Stathaki, “Logic-Based Switching Controllers – A Stepwise Safe Switching Approach”, Information Sciences, vol. 177, no. 13, pp. 2736–2755, 2007.

[33] F. N. Koumboulis and M.P. Tzamtzi, “Multivariable Step-Wise Safe Switching Controllers”, Proceedings of the International Conference on Computational Intelligence for Modelling, Control and Automation and International Conference on Intelligent Agents, Web Technologies and Internet Commerce (CIMCA-IAWTIC’05), Vienna, Austria, November 28-30, 2005

[34] F. N. Koumboulis and N. D. Kouvakas, “I/O Decoupling with Simultaneous Disturbance Rejection of General Neutral Time Delay Systems via a Measurement Output Feedback Dynamic Controller”, Proceedings of the 21st Mediterranean Conference on Control and Automation (MED), pp. 890-895, Chania, Greece, June 25-28, 2013.

[35] G. L. Giannaris, N. D. Kouvakas, F. N. Koumboulis and D. Vouyioukas, “Towards Remote Control of Planar Redundant Robotic Manipulators”, Proceedings of the IEEE 21st International Conference on Intelligent Engineering Systems (INES 2017), pp. 231-236, Larnaca, Cyprus, October 20-23, 2017.

[36] F. N. Koumboulis and N. D. Kouvakas, “A three term controller for ride comfort improvement”, Proceedings of the 19th Mediterranean Conference on Control & Automation (MED), pp. 114-119, Corfu, Greece, June 20-23, 2011.

[37] L. Derafa, T. Madani and A. Benallegue, “Dynamic Modelling and Experimental Identification of Four Rotors Helicopter Parameters”, Proceedings of the IEEE International Conference on Industrial Technology (ICIT), Mumbai, India, December 15-17, 2006.

[38] A. Cervin, D. Henriksson, B. Lincoln, J. Eker and K.-E. Arz˚ en, “How´ Does Control Timing Affect Performance? Analysis and Simulation of Timing Using Jitterbug and True-Time”, IEEE Control Systems Magazine, vol. 23, no. 3, pp. 16–30, 2003.

[39] F. N. Koumboulis, N. D. Kouvakas and P. N. Paraskevopoulos, “Linear approximant-based metaheuristic proportional- integral-derivative controller for a neutral time delay central heating system”, Proc. IMechE Part I: J. Systems and Control Engineering, vol. 223, pp. 605-618, 2009.

Chapter 6: Switching Wireless Control for Longitudinal Quadrotor Manoeuvres

6.1 INTRODUCTION

Multi-rotor aerial vehicles (MRAVs) have a wide set of emerging applications including aerial video capture, traffic surveillance, mapping, package delivery and supportive tasks in agriculture and manufacturing. The complexity of these applications requires high maneuverability that can be accomplished through advanced control schemes. Towards this aim, PID controllers (see [1]-[5] and the references therein), optimal controllers ([6]-[8]), I/O decoupling controllers (indicatively see [9]-[13]) and disturbance attenuation controllers (see [14]-[21] and the references therein), have been proposed. From our point of view, the latter two control schemes appear to be of distinct importance.

Unmanned aerial vehicles can be remotely guided, semi-autonomous or fully autonomous (see [22]). In many applications, mainly industrial ones, the quadrotors are remotely guided. In these cases, the efficiency of the control scheme is translated to significant computer power requirements. So, the scales are tipped in favor of remote control through a wireless communication channel. The performance of such controllers depends upon communication errors, see [23]-[27] where communication delays of the signals in the control loop are considered. The communication delays are usually time varying and perturbed. Thus, I/O decoupling for delayless systems (see [28] and the references therein) is not applicable. The first effort toward the application of I/O decoupling requirement to remotely controlled quadrotors is made in [29] where the problem of controlling the longitudinal motion of a quadrotor around straight horizontal flight has been studied using the linear approximant of the nonlinear model of the quadrotor. Also, in [29] an atmospheric disturbance attenuation metaheuristic algorithm has been provided. The limits of the controller with respect to the range of the maneuver commands, the range of the atmospheric disturbances and the

performance of the nonlinear closed loop model have been investigated through simulations.

In the present work, in order to alter the aforementioned limits of external commands, a stepwise safe switching wireless control design procedure is introduced. The method of step wise safe switching was developed mainly for industrial applications (see [30] and [31] for SISO and MIMO delayless plants, respectively). To accomplish the good performance of the wireless controlled quadrotor, the method in [31] is appropriately extended and modified to cover time delay nonlinear systems.

In particular, the novelty of the present work is based on the following intermediate and terminal results:

a) The linear approximant of the longitudinal motion of the quadrotor is determined for any vertical and horizontal nominal velocity, any nominal pitch angle and of course for zero nominal disturbances. Based on this approximant, being more general than the respective in [29], the linear approximant of the model, including communication delays, is derived. Furthermore, in the present work, the controller design is based on this model. The delays of the model are derived using the synchronization/signal reconstruction algorithm in [32], imposing for the delays of the remote controller to be constant and equal to an upper bound of the time varying communication delays. This is accomplished by artificially increasing the delays in the controller platform.

b) Based on the aforementioned linear approximant with time delays, being more general than the one in [29] in the sense that it covers the case of non-zero vertical nominal velocity, a dynamic time delay controller achieving I/O decoupling, i.e., independent control of the horizontal and vertical velocity of the quadrotor is designed, together with stability and attenuation of the influence of atmospheric disturbances on the performance outputs. The latter two requirements are satisfied following the metaheuristic algorithm in [29].

c) The tolerance of the controller presented in (b) is investigated for various external commands by introducing a composite criterion that includes the infinity and H_2 norms with appropriate weighting factors, as well as hard constraints for the steady

state performance and the overshoot of the variations between the closed loop system of the time delay linear approximant and the closed loop system of the time delay nonlinear model. This criterion is advantageous as compared to that in [29], including only the H_2 of the variations, in the sense that is more representative of the desired maneuver performance.

d) The target operating areas, being the modules of the stepwise safe switching approach, are defined in terms of the operating points of the nonlinear model of the system and are determined using the composite criterion presented in (c), having a composite circular/rectangular shape. These characteristics are novelties compared to the target areas introduced in [30] and [31]. Another novelty is that there is no need for the determination of tolerance areas in the sense that the usefulness of the tolerance operating areas is covered here by the term of the composite criterion attenuating the variations around the steady state and the term attenuating the infinity norm of the variations between the nonlinear and the linear closed loop system. A third novelty, being the most important, is the definition of the target operating areas in the space of the external commands. Finally, a fourth novelty is the determination of the target areas with respect to the differences between the performance of the nonlinear closed loop time delay system and the performance of the respective linear closed loop time delay system.

e) An extended version of the MIMO stepwise safe switching algorithm is proposed with respect to the linear and nonlinear time delay closed loop systems, where the intermediate stationary points are required to belong to the intersection of two adjacent target operating areas.

f) The performance of all above results is illustrated through simulations for the case of a climbing maneuver, out of the range of the linear approximant and in the presence of atmospheric disturbances.

The material of the present work is organized as follows: In 6.2, the nonlinear model of the longitudinal motion of the quadrotor and the respective operating points are presented and the linear approximant of the general longitudinal motion with time delays is derived. In 6.3, the wireless controller for I/O decoupling, stability and disturbance attenuation, is derived. Furthermore, the performance of the nonlinear time

delay closed loop system is is illustrated using extensive simulations, introducing appropriate cost criteria. In 6.4, a new version of the stepwise safe switching algorithm based on the approximate minimization of a composite criterion for the closed loop performance, is proposed and simulation results, for a maneuver passing through different target areas, are presented.

6.2 THE NONLINEAR AND THE LINEAR MODEL OF THE QUADROTOR

In the longitudinal motion of air vehicles, a large number of flight envelopes is provided (indicatively see [13], [29] and [33]- [35]). Here, the mathematical model of the longitudinal motion of the quadrotor including atmospheric disturbances is of the following form (indicatively see [29]):

$$\dot{x}(t) = f(x,u,\xi), y(t) = Cx(t) \tag{6.1a,b}$$

where

$$\begin{aligned} x(t) &= \begin{bmatrix} x_1(t) & x_2(t) & x_3(t) & x_4(t) & x_5(t) & x_6(t) \end{bmatrix}^T \\ &= \begin{bmatrix} \theta(t) & v_x(t) & v_z(t) & q(t) & \omega_f(t) & \omega_r(t) \end{bmatrix}^T \\ u(t) &= \begin{bmatrix} u_1(t) & u_2(t) \end{bmatrix}^T = \begin{bmatrix} V_f(t) & V_r(t) \end{bmatrix}^T, \\ \xi(t) &= \begin{bmatrix} \xi_1(t) & \xi_2(t) \end{bmatrix}^T = \begin{bmatrix} v_{a,x}(t) & v_{a,z}(t) \end{bmatrix}^T \\ y(t) &= \begin{bmatrix} y_1(t) & y_2(t) \end{bmatrix}^T = \begin{bmatrix} v_x(t) & v_z(t) \end{bmatrix}^T \end{aligned}$$

where x, u, ξ and y are the state, input, disturbance and performance output vectors of the system. The state variables are the pitch angle of the quadrotor θ, the horizontal and vertical velocities of the quadrotor v_x and v_z respectively, the pitch rate q and the front and rear motor velocities ω_f and ω_r respectively. The input variables are the front and rear motor voltage supplies V_f and V_r (actuatable inputs). The disturbances are the horizontal and vertical velocities of the ambient air denoted by $v_{a,x}$ and $v_{a,z}$ (non-measurable disturbances). The non-zero elements of the performance output matrix C and the nonlinear vector function $f(x,u,\xi)$ are

$$c_{1,2}=1, c_{2,3}=1,$$
$$f_1(x,u,\xi)=x_4$$
$$f_2(x,u,\xi)=\left[2s_{x_1}K_l\left(x_5^2+x_6^2\right)-\left(x_2-\xi_1\right)k_{dt,x}\right]/m_q$$
$$f_3(x,u,\xi)=\left[2c_{x_1}K_l\left(x_5^2+x_6^2\right)-\left(x_3-\xi_2\right)k_{dt,z}-gm_q\right]/m_q$$
$$f_4(x,u,\xi)=\left[\sqrt{2}dK_l\left(x_6^2-x_5^2\right)-x_4k_{a,y}\right]/J_{q,y}$$
$$f_5(x,u,\xi)=-a_0+bu_1-a_1x_5-a_2x_5^2, f_6(x,u,\xi)=-a_0+bu_2-a_1x_6-a_2x_6^2$$

where $s_{x_1}=\sin(x_1)$, $c_{x_1}=\cos(x_1)$, m_q is the mass of the quadrotor, $k_{dt,x}$ and $k_{dt,z}$ are the translation drag coefficients in the x and z directions of the earth reference frame, g is the gravitational acceleration, K_l is the lift coefficient of the propellers, d is the distance between the quadrotor center of mass and the rotation axis of the propellers, $k_{a,y}$ is the rotational aerodynamic friction coefficient around the y axis, $J_{q,y}$ is the quadrotor moment of inertia and a_0, a_1, a_2 and b are electric motor parameters. Note that all state variables are considered to be measurable.

For the controller design that will be presented in the next section, the linear approximant of the model (6.1) will be derived. The linear approximant of the nonlinear model (6.1) will be produced around nominal values corresponding to the typical climbing/descending maneuver at constant speed and zero disturbances. Let $\bar{u}_1$ and $\bar{u}_2$ be the nominal points of u_1 and u_2 respectively, $\bar{\xi}_1$ and $\bar{\xi}_2$ be the nominal points of ξ_1 and ξ_2 respectively and $\bar{x}_i$ be the nominal points of x_i ($i=1,\ldots,6$). The respective vectors including the nominal values are denoted by $\bar{u}$, $\bar{\xi}$ and $\bar{x}$. Similarly to [29], the nominal points are analytically determined in terms of the nominal points of the performance variables by the following formulas

$$\bar{\xi}_1=0, \bar{\xi}_2=0, \bar{x}_1=\tan^{-1}(\bar{a}), \bar{x}_2=\bar{x}_2^*, \bar{x}_3=\bar{x}_3^*, \bar{x}_4=0,$$
$$\bar{x}_5=\bar{x}_6=0.5\left(\bar{a}^2+1\right)^{1/4}\left[\left(\bar{x}_3^*k_{\mathrm{dt},z}+gm_q\right)/K_l\right]^{1/2}$$
$$\bar{u}_1=\bar{u}_2=\{2a_1\left(\bar{a}^2+1\right)^{1/4}\left[K_l\left(\bar{x}_3^*k_{\mathrm{dt},z}+gm_q\right)\right]^{1/2}+$$
$$+a_2\left(\bar{a}^2+1\right)^{1/2}\left(\bar{x}_3^*k_{\mathrm{dt},z}+gm_q\right)+4a_0K_l\}(4bK_l)^{-1}$$

where $\bar{a} = \bar{x}_2^* k_{\mathrm{dt},x} / \left(\bar{x}_3^* k_{\mathrm{dt},z} + g m_q \right)$ while $\bar{x}_2^*$ and $\bar{x}_3^*$ are the horizontal and vertical nominal velocities of the quadrotor respectively. It is important to mention that in the special case where $\bar{x}_3^*$ is chosen to be equal to zero, the above nominal points and the linear approximant that follows reduces to the respective quantities derived in [29].

The deviations around the nominal vectors of the inputs, the disturbances, the states and the performance variables are $\Delta u(t) = u(t) - \bar{u}$, $\Delta \xi(t) = \xi(t) - \bar{\xi}$, $\Delta x(t) = x(t) - \bar{x}$ and $\Delta y(t) = y(t) - \bar{y}$, respectively, where $\bar{y}^T = \begin{bmatrix} \bar{y}_1 & \bar{y}_2 \end{bmatrix} = \begin{bmatrix} \bar{x}_2 & \bar{x}_3 \end{bmatrix}$. The linear approximant of the model (6.1) is of the form

$$\delta \dot{x}(t) = A \delta x(t) + B \delta u(t) + Q \delta \xi(t), \delta y(t) = C \delta x(t) \qquad (6.2a,b)$$

where $\delta u(t) = \Delta u(t)$ and $\delta \xi(t) = \Delta \xi(t)$. The variables $\delta x(t)$ and $\delta y(t)$ are the responses of the linear system (6.2). Clearly, they approximate $\Delta x(t)$ and $\Delta y(t)$, respectively. The approximation is accurate around an operating point vector, denoted by $o(t) = \bar{o}$ where $o(t) = \left(u(t), \xi(t), x(t), y(t) \right)$ and $\bar{o} = \left(\bar{u}, \bar{\xi}, \bar{x}, \bar{y} \right)$. The system matrices in (2) are derived by the following relation

$$\begin{bmatrix} A & B & Q \end{bmatrix} = \left[\frac{\partial}{\partial x} \quad \frac{\partial}{\partial u} \quad \frac{\partial}{\partial \xi} \right] f\left(x, u, \xi \right) \Big|_{o=\bar{o}} \qquad (6.3)$$

The nonzero elements of A, B and Q are determined by the following analytic formulas in terms of the operating points and the physical parameters of the nonlinear model (6.1):

$$a_{1,4} = 1, a_{2,1} = 4 \bar{x}_6^2 K_l c_{\bar{x}_1} / m_q, a_{2,2} = -k_{\mathrm{dt},x} / m_q, a_{2,5} = a_{2,6} = 4 \bar{x}_6 K_l s_{\bar{x}_1} / m_q$$
$$a_{3,1} = -4 \bar{x}_6^2 K_l s_{\bar{x}_1} / m_q, a_{3,3} = -k_{\mathrm{dt},z} / m_q, a_{3,5} = a_{3,6} = 4 \bar{x}_6 K_l c_{\bar{x}_1} / m_q$$
$$a_{4,5} = -a_{4,6} = -2\sqrt{2} d \bar{x}_6 K_l / J_{q,y}, a_{5,5} = a_{6,6} = -2 a_2 \bar{x}_6 - a_1, \; a_{4,4} = -k_{a,y} / J_{q,y}$$
$$b_{5,1} = b_{6,2} = b, q_{2,1} = k_{\mathrm{dt},x} / m_q, q_{3,2} = k_{\mathrm{dt},z} / m_q$$

6.3 THE WIRELESS LINEAR DYNAMIC CONTROLLER

The quadrotor controller is connected to the quadrotor through a wireless network. The ZigBee protocol is used due to its effectiveness in terms of signal-to-noise ratio, range, power consumption and implementation cost. The wireless network is used to transmit signals from the quadrotor sensors to the remote controller as well as from the remote controller to the quadrotor's motors. Thus, time varying communication delays are introduced to the quadrotor and the controller description. Following the modifications of the transmission-reception protocol proposed in [32], the communication delays become constant in both ways of transmission. This approach is based on the repetitive transmission of sampled data and reconstruction of the continuous time signals through appropriate interpolation, based on passed values of the data. The approach increases the communication time delays till constant values and the reconstructed signals are continuous signals thus contributing to the precision of the controller. It is important to mention that this property can be fulfilled for all wireless transmission protocol. Using the above synchronization/signal reconstruction algorithm, the linear approximant of the nonlinear model is in the following time delay dynamic system form

$$\delta\dot{x}(t) = A\delta x(t) + B\delta u(t-\tau_1) + Q\delta\xi(t),\ \delta y(t) = C\delta x(t) \qquad (6.4a,b)$$

where $\tau_1 > 0$ is the transmission / reconstruction delay of the control commands at the actuatable inputs. The forced response of the linear system (6.4) is expressed in the frequency domain as follows

$$\begin{gathered}\delta X(s) = z_1 (sI_6 - A)^{-1} B\delta U(s) + (sI_6 - A)^{-1} Q\delta\Xi(s) \\ \delta Y(s) = C\delta X(s)\end{gathered} \qquad (6.5a,b)$$

where I_6 is the 6×6 identity matrix, $z_1 = e^{-s\tau_1}$, $\delta X(s) = \mathcal{L}\{\delta x(t)\}$, $\delta U(s) = \mathcal{L}\{\delta u(t)\}$, $\delta\Xi(s) = \mathcal{L}\{\delta\xi(t)\}$, $\delta Y(s) = \mathcal{L}\{\delta y(t)\}$ and where $\mathcal{L}\{\bullet\}$ denotes the Laplace transform of the argument signal.

The controller, outlined in Figure 6.1, is of the proportional delayed feedback type with dynamic precompensator including delays, i.e., in the form

$$\delta U(s) = z_2 K \delta X(s) + G(s, z_1, z_2)\delta\Omega(s) \tag{6.6}$$

where $z_2 = e^{-s\tau_2}$, $\tau_2 > 0$ is the transmission / reconstruction delay of the measurable state variables at the controller and $\delta\Omega(s) = \mathcal{L}\{\delta\omega(t)\}$ is the Laplace transform of the 2×1 vector of external inputs, $G(s, z_1, z_2) \in R(s, z_1, z_2)^{2\times 2}$ and $K \in R^{2\times 6}$. The elements of the precompensator matrix $G(s, z_1, z_2)$ are rational functions of s where the numerator and denominator polynomial coefficients are rational function of z_1 and z_2. Following the procedure in [32], the delays τ_1 and τ_2 are upper bounds of the respective communication delays plus the required processing time.

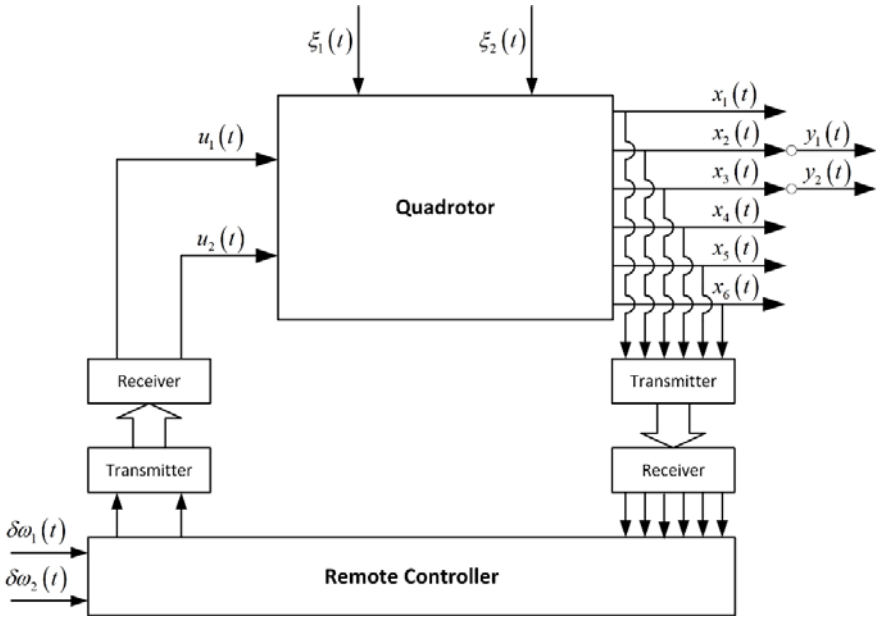

Fig. 6.1 Block diagram of the proposed control scheme

Substitution of controller in (6.6) to the open loop system (6.5), yields

$$\delta Y(s) = H_\Omega(s, z_1, z_2)\delta\Omega(s) + H_\Xi(s, z_1, z_2)\delta\Xi(s) \tag{6.7a}$$

where

$$H_\Omega(s, z_1, z_2) = z_1 C\left(sI_6 - A - z_1 z_2 BK\right)^{-1} BG(s, z_1, z_2) \tag{6.7b}$$

$$H_{\Xi}(s,z_1,z_2) = C\left(sI_6 - A - z_1 z_2 BK\right)^{-1} Q \tag{6.7c}$$

The design goals are: a) I/O decoupling, b) stability and c) attenuation of the influence of the disturbances to the performance outputs.

I/O decoupling, being one of the most attractive design requirement in flight control, is formulated as

$$H_{\Omega}(s,z_1,z_2) = \underset{i=1,2}{\mathrm{diag}}\left\{h_i(s,z_1,z_2)\right\} \tag{6.8}$$

where $h_1(s,z_1,z_2)$ and $h_2(s,z_1,z_2)$ are nonzero rational functions of s with the numerator and denominator polynomial coefficients being in general rational function of z_1 and z_2.

The design goal of attenuating the influence of the atmospheric disturbances to the outputs is translated to the preservation of small enough infinity norm of the transfer matrix mapping the disturbances to the performance outputs, i.e., satisfaction of the following inequality

$$J_d(K) = \max_{i,j\in\{1,2\}} \left\{ \left\| \left(h_{\Xi}\right)_{i,j}(s,z_1,z_2) \right\|_{\infty} \right\} < e_{d,\max} \tag{6.9}$$

where $\left(h_{\Xi}\right)_{i,j}(s,z_1,z_2)$ $(i,j=1,2)$ is the $\{i,j\}$ element of the transfer matrix $H_{\Xi}(s,z_1,z_2)$ mapping the disturbances to the performance outputs, defined in (6.7c), $\|\bullet\|_{\infty}$ denotes the infinity norm of the argument complex function of s, z_1 and z_2. The threshold $e_{d,\max} \in R^{+}$ is set by the designer.

6.3.1 I/O Decoupling

Similarly to [29] and using the approach in [36], it can be observed that the solvability conditions for I/O decoupling are satisfied. The equality (6.8) is satisfied by the following choice of the precompensator matrix

$$G(s,z_1,z_2)=\tilde{G}(s,z_1,z_2)\underset{i=1,2}{diag}\left\{h_i(s,z_1,z_2)\right\} \tag{6.10}$$

where

$$\tilde{G}(s,z_1,z_2)=\left[I_2-z_1z_2KL_B(s)\right]\left[z_1CL_B(s)\right]^{-1} \tag{6.11}$$

where $L_B(s)=[(l_B)_{i,j}(s)]=(sI_6-A)^{-1}B$ ($i=1,6;\ j=1,2$). Applying series of computations it can be observed that the non-zero elements of $L_B(s)$ are of the form

$$(l_B)_{1,1}(s)=-(l_B)_{1,2}(s)=\frac{a_{4,5}b_{5,1}}{s(s-a_{4,4})(s-a_{5,5})}$$

$$(l_B)_{2,1}(s)=\frac{b_{5,1}\left[a_{2,5}s(s-a_{4,4})+a_{2,1}a_{4,5}\right]}{s(s-a_{2,2})(s-a_{4,4})(s-a_{5,5})}$$

$$(l_B)_{2,2}(s)=\frac{b_{5,1}\left[a_{2,5}s(s-a_{4,4})+a_{2,1}a_{4,5}\right]}{s(s-a_{2,2})(s-a_{4,4})(s-a_{5,5})}$$

$$(l_B)_{3,1}(s)=\frac{b_{5,1}\left[a_{3,5}s(s-a_{4,4})+a_{3,1}a_{4,5}\right]}{s(s-a_{3,3})(s-a_{4,4})(s-a_{5,5})}$$

$$(l_B)_{3,2}(s)=\frac{b_{5,1}\left[a_{3,5}s(s-a_{4,4})+a_{3,1}a_{4,5}\right]}{s(s-a_{3,3})(s-a_{4,4})(s-a_{5,5})}$$

$$(l_B)_{4,1}(s)=-(l_B)_{4,2}(s)=\frac{a_{4,5}b_{5,1}}{(s-a_{4,4})(s-a_{5,5})}$$

$$(l_B)_{5,1}(s)=(l_B)_{6,2}(s)=\frac{b_{5,1}}{s-a_{5,5}}$$

Clearly, choosing $h_i(s,z_1,z_2)$ ($j=1,2$) to be realizable enough, the realizability of the precompensator matrix is guaranteed. For now, we assume that the feedback matrix K is not specified.

According to [29], in order to have a realizable and strictly proper precompensator and a strictly proper and stable closed loop transfer matrix with steady state gain matrix the 2×2 identity matrix, the diagonal elements of the closed loop transfer matrix are specified to be

$$h_i\left(s,z_1,z_2\right)=z_1/\prod_{j=1}^{5}\left(T_{i,j}s+1\right)\quad(i=1,2) \tag{6.12}$$

where $T_{i,j}$ are positive real parameters. The selection in (6.13) implies asymptotic command following. In the next subsection, the elements of the feedback matrix K are determined to satisfy closed loop stability and disturbance attenuation.

6.3.2 Closed Loop Stability and Disturbance Attenuation

Similarly to [29], in order to accomplish closed loop stability and disturbance attenuation, the feedback matrix elements are selected so that a) the closed loop system is stable for $0\le\tau_1+\tau_2\le\tau_{\max}$ and b) the inequality in (6.9) is satisfied. To this end, a mixed analytic - heuristic approach is proposed. In the analytic part of the approach, the elements of the 1st row of the matrix K, denoted by $k_1=\begin{bmatrix}k_{1,1} & k_{1,2} & k_{1,3} & k_{1,4} & k_{1,5} & k_{1,6}\end{bmatrix}$, are expressed in terms of the elements of the 2nd row of the matrix K, denoted by $k_2=\begin{bmatrix}k_{2,1} & k_{2,2} & k_{2,3} & k_{2,4} & k_{2,5} & k_{2,6}\end{bmatrix}$, and two positive real parameters, denoted by ρ and $\delta\rho$. In the case where $\tau_1+\tau_2\to 0$, the first parameter is the amplitude of the larger pole and the second is the distance between two neighboring poles of the closed loop characteristic polynomial, i.e.,

$$p_c\left(s\right)=\prod_{j=0}^{5}\left(s+\rho+j\delta\rho\right) \tag{6.13}$$

The above relation guarantees the stability of the closed loop system for the delayless case with equally distanced system poles. Applying series of computations it is proven here that the analytic solution for the first row of the feedback matrix is of the form

$$k_1=\left[\widetilde{A}^{-1}\left(\widetilde{B}+a_d\right)\right]^{\mathrm{T}} \tag{6.14}$$

where $\widetilde{A}=[\tilde{a}_{i,j}]\in\mathbb{R}^{6\times 6}$, $\widetilde{B}=[\tilde{b}_i]\in\mathbb{R}^{6\times 1}$ and $a_d=[a_{d,i}]\in\mathbb{R}^{6\times 1}$. The nonzero elements of $\widetilde{A}$ and $\widetilde{B}$ are expressed in terms of the physical parameters of the model, the operating points of the model and the parameters of the second row of the feedback

matrix. The analytic expressions of the nonzero elements of $\widetilde{A}$ and $\widetilde{B}$ are given in the Appendix A. The parameters $\alpha_{d,i}$ $(i=1,...,6)$ are the coefficients of the sixth order polynomial in (6.13). They are determined here to be expressed in terms of the positive real parameters ρ and $\delta\rho$ as follows: 0.5

$$\alpha_{d,1} = 120\rho\delta\rho^5 + 274\rho^2\delta\rho^4 + 225\rho^3\delta\rho^3 + 85\rho^4\delta\rho^2 + 15\rho^5\delta\rho + \rho^6$$
$$\alpha_{d,2} = 120\delta\rho^5 + 548\rho\delta\rho^4 + 675\rho^2\delta\rho^3 + 340\rho^3\delta\rho^2 + 75\rho^4\delta\rho + 6\rho^5$$
$$\alpha_{d,3} = 274\delta\rho^4 + 675\rho\delta\rho^3 + 510\rho^2\delta\rho^2 + 150\rho^3\delta\rho + 15\rho^4$$
$$\alpha_{d,4} = 225\delta\rho^3 + 340\rho\delta\rho^2 + 150\rho^2\delta\rho + 20\rho^3$$
$$\alpha_{d,5} = 85\delta\rho^2 + 75\rho\delta\rho + 15\rho^2$$
$$\alpha_{d,6} = 15\delta\rho + 6\rho$$

Using relations (6.13) and (6.14), the disturbance attenuation cost function J_d defined in (6.9), depends entirely upon k_2, ρ and $\delta\rho$. Thus it can be expressed in the following function form

$$J_d(K) = J_d(k_2, \rho, \delta\rho) \tag{6.15}$$

In order to determine the values of k_2, ρ and $\delta\rho$ achieving closed loop stability and disturbance attenuation, the metaheuristic algorithm in [29], being an extension of that in [37] and [38], will be presented. The key point of the algorithm is to define an initial search area for the controller parameters, defined by the center values, let $\left(k_{2,j}\right)_c$ ($j=1,\ldots,6$), $\left(\rho\right)_c$ and $\left(\delta\rho\right)_c$, and the respective half widths, let $\left(k_{2,j}\right)_w$ $(j=1,\ldots,6)$, $\left(\rho\right)_w$ and $\left(\delta\rho\right)_w$. Following the steps of the algorithm, this search area will be iteratively adapted and series of updated sets of controller parameters will be derived. After several iterations with appropriate loops, a suboptimal solution for the controller parameters that satisfy stability and disturbance attenuation is attempted to be derived for the nonzero delay case.

In order to produce an updated set of controller parameters, the search pattern is divided into appropriate iterations. Each iterations is divided into loops. At each loop a set of controller parameters is generated. After producing a total number of n_{loop} sets of parameters, the one corresponding to the smallest cost is selected as the temporary

suboptimal solution. This procedure is repeated for a total number of n_{rep} times. The suboptimal controller parameters derived in each iteration are used to produce an updated search area and a new set of controller parameters, center values and half widths. The procedure is repeated up till the controller parameters have converged, the maximum allowable number of controller sets of parameters, denoted by n_{total}, has been reached or an appropriate set of controller parameters, such that the performance criterion is smaller than $e_{d,\max}$, has been found. The convergence of the controller parameters is checked using a convergence threshold denoted by λ.

The metaheuristic algorithm is:

Initial Data and Performance Criterion

1) The center values and half widths for the initial search area $\left(k_{2,j}\right)_c$ $(j=1,\ldots,6))$, $\left(\rho\right)_c$, $\left(\delta\rho\right)_c$, $\left(k_{2,j}\right)_w$ $(j=1,\ldots,6)$, $\left(\rho\right)_w$ and $\left(\delta\rho\right)_w$.

2) The performance criterion $J_d(k_2,\rho,\delta\rho)$ and the threshold $e_{d,\max}$.

3) The iteration parameters n_{loop}, n_{rep}, n_{total}.

4) The search algorithm threshold λ.

Algorithm

Step 0: Set the numbering index $i_{\max}=0$.

Step 1: Determine a search area $\Im$ for the controller parameters according to the inequalities

$$\left(k_{2,j}\right)_c-\left(k_{2,j}\right)_w\le k_{2,j}\le\left(k_{2,j}\right)_c+\left(k_{2,j}\right)_w\ (j=1,\ldots,6),$$
$$\left(\rho\right)_c-\left(\rho\right)_w\le\rho\le\left(\rho\right)_c+\left(\rho\right)_w$$
$$\left(\delta\rho\right)_c-\left(\delta\rho\right)_w\le\delta\rho\le\left(\delta\rho\right)_c+\left(\delta\rho\right)_w$$

Step 2: Set the numbering index $i_1=0$.

Step 3: Set the numbering index $i_1 = i_1 + 1$.

Step 4: Set the numbering index $i_2 = 0$.

Step 5: Set the numbering index $i_{\max} = i_{\max} + 1$. If $i_{\max} > n_{total}$ go to ***Step 15***.

Step 6: Set the numbering index $i_2 = i_2 + 1$.

Step 7: Select randomly a set of controller parameters within the search area $\Im$, let $\left(k_{2,j}\right)_{i_2}$ ($j = 1,\ldots,6$), $\left(\rho\right)_{i_2}$ and $\left(\delta\rho\right)_{i_2}$ and evaluate the respective controller parameters $\left(k_{1,j}\right)_{i_2}$ ($j = 1,\ldots,6$). Check if the closed loop system is stable for $0 \le \tau_1 + \tau_2 \le \tau_{\max}$. If yes, proceed to the next step. If no, repeat ***Step 7***.

Step 8: Evaluate $J_{d,i_2} = J_d\left(\left(k_2\right)_{i_2}, \left(\rho\right)_{i_2}, \left(\delta\rho\right)_{i_2}\right)$

Step 9: If $J_{d,i_2} < e_{d,\max}$ go to ***Step 15***.

Step 10: If $i_2 < n_{loop}$ go to ***Step 5***.

Step 11: Find $\left(J_{d,\min}\right)_{i_2} = \min\left\{J_{d,i}, i = 1,\ldots,n_{loop}\right\}$ and the respective controller parameters $\left(k_{2,j}\right)_{i_1}$, $\left(\rho\right)_{i_1}$ and $\left(\delta\rho\right)_{i_1}$.

Step 12: If $i_1 \ge n_{rep}$ then find the controller parameters, $\left(k_{2,j}\right)_{\min}$ ($j = 1,\ldots,6$), $\left(\rho\right)_{\min}$, $\left(\delta\rho\right)_{\min}$ and $\left(k_{2,j}\right)_{\max}$ ($j = 1,\ldots,6$), $\left(\rho\right)_{\max}$, $\left(\delta\rho\right)_{\max}$ corresponding to

$J_{d,\min} = \min\left\{\left(J_{d,\min}\right)_i, i = 1,\ldots,n_{rep}\right\}$ and

$J_{d,\max} = \max\left\{\left(J_{d,\min}\right)_i, i = 1,\ldots,n_{rep}\right\}$. Else go to ***Step 3***.

Step 13: Define

$$\left(k_{2,j}\right)_c = \left(\left(k_{2,j}\right)_{\min} + \left(k_{2,j}\right)_{\max}\right)/2 \;\; (j = 1,\ldots,6), \quad (\rho)_c = \left((\rho)_{\min} + (\rho)_{\max}\right)/2$$

$$(\delta\rho)_c = \left((\delta\rho)_{\min} + (\delta\rho)_{\max}\right)/2, \quad \left(k_{2,j}\right)_w = \left|\left(k_{2,j}\right)_{\min} - \left(k_{2,j}\right)_{\max}\right| \;\; (j = 1,\ldots,6)$$

$$(\rho)_w = \left|(\rho)_{\min} - (\rho)_{\max}\right|, \quad (\delta\rho)_w = \left|(\delta\rho)_{\min} - (\delta\rho)_{\max}\right|$$

Step 14: If $\left(k_{2,j}\right)_w / \left(k_{2,j}\right)_c > \lambda$ $(j = 1,\ldots,6)$ or $(\rho)_w / (\rho)_c > \lambda$ or $(\delta\rho)_w / (\delta\rho)_c > \lambda$, go to ***Step 2***.

Step 15: If $J_{d,i_2} \le e_{d,\max}$ then set $k_{2,j} = \left(k_{2,j}\right)_{i_2}$ $(j = 1,\ldots,6)$, $\rho = (\rho)_{i_2}$ and $\delta\rho = (\delta\rho)_{i_2}$ (determined in Step 7), else set $k_{2,j} = \left(k_{2,j}\right)_{\min}$ $(j = 1,\ldots,6)$, $\rho = (\rho)_{\min}$ and $\delta\rho = (\delta\rho)_{\min}$ (determined in ***Step 12***).

6.4 ON THE PERFORMANCE OF THE CONTROLLER FOR THE NONLINEAR MODEL AND ARROUND A NOMINAL OPERATING POINT

6.4.1 Performance Metrics

An important issue is the performance of the controller derived in 6.3 when applied to the nonlinear constant time delay model of the quadrotor. The issue is investigated here by introducing appropriate performance criteria and executing extensive simulation tests for transitions of the closed loop system from the nominal operating point to other operating points around the nominal operating point. The variations of the inputs $\Delta u(t)$ of the nonlinear system are determined by the relation

$$\Delta U(s) = z_2 K \Delta X(s) + G(s, z_1, z_2)\Delta\Omega(s) \tag{6.16}$$

where $\Delta U(s)$ and $\Delta X(s)$ are the Laplace transforms of $\Delta u(t)$ and $\Delta x(t)$. The matrices K and $G(s, z_1, z_2)$ are those determined in Subsections 6.3.1 and 6.3.2 for the linear approximant case, using the controller in (6.6). Using the synchronization/signal reconstruction algorithm in [32], the closed loop system behaves as a nonlinear dynamic system with constant time delays.

Consider the nominal operating point $\overline{\chi} = \left[\overline{u}^T \quad \overline{y}^T\right]^T$. As already mentioned in 6.2, the nominal values of $\overline{x}$ are uniquely determined by $\overline{y}$. Also, $\overline{u}$ is uniquely determined by $\overline{y}$ and the nominal value of the disturbance vector is equal to zero. The system matrices of the linear approximant in (6.2a,b) depend upon $\overline{\chi}$. So, the linear approximant is denoted by $\mathcal{S}_L(\overline{\chi})$. The closed loop system resulting after the application of the controller in (6.6) to $\mathcal{S}_L(\overline{\chi})$ is denoted by $\mathcal{S}_{L,CL}(\overline{\chi})$. The controller defined in (6.16) is denoted by $\mathcal{C}(\overline{\chi})$. The closed loop system resulting after the application of $\mathcal{C}(\overline{\chi})$ to the nonlinear model in (1a,b) is denoted by $\mathcal{S}_{NL,CL}(\overline{\chi})$.

The response of $\mathcal{S}_{NL,CL}(\overline{\chi})$, namely the vector $y(t)$, depends upon $\delta\omega(t)$ and $\xi(t)$. For the case where $\xi(t) = 0$, the system $\mathcal{S}_{NL,CL}(\overline{\chi})$ is retained at the nominal operating point $\overline{\chi}$ only if $\delta\omega(t) = 0$. Indeed, at the point $\overline{\chi}$, it holds that $\Delta u = 0$ and $\Delta x = 0$ and thus using (6.16) , zero external commands must be applied. Also, for the case of zero disturbances the responses of $\mathcal{S}_{NL,CL}(\overline{\chi})$ and $\mathcal{S}_{L,CL}(\overline{\chi})$ are denoted by $y(t)\big|_{\xi=0}$ and $\delta y(t)\big|_{\xi=0}$, respectively.

According to [30] and [31] the difference between the step responses of the linear approximant and the nonlinear model is an adequate variable to demonstrate the performance of a linear controller. According to Subsections 6.3.1 and 6.3.2, the performance of $\mathcal{S}_{L,CL}(\overline{\chi})$ for $\delta\omega(t)$ and zero external disturbances, i.e., $\xi_1(t) = 0$ and $\xi_2(t) = 0$ is inherently satisfactory. So, this performance can be considered to be the "ideal" one.

To evaluate quantitatively the performance of the proposed control scheme with respect to a desired maneuver, a set of metrics is introduced. These metrics depend upon the difference $y(t)-\delta y(t)\big|_{\xi=0}-\overline{y}$ and the initial time instant, let t_0. The infinity norm and the H_2 norm of the deviations between the nonlinear closed loop system and the closed loop system of the linear approximant, will be considered to be the metrics of the performance. For each performance variable, i.e., for $i\in\{1,2\}$, the following two metrics are first introduced:

• *Cost of the infinity norm of the variations*

$$J_\infty=\frac{\max\limits_{i=1,2}\left\{\left\|y_i(t)-\delta y_i(t)\big|_{\xi=0}-\overline{y}_i\right\|_\infty\right\}}{\max\limits_{i=1,2}\left\{\left\|\delta y_i(t)\big|_{\xi=0}-\delta y_i(t_0-)\big|_{\xi=0}\right\|_\infty\right\}}\times 100\% \tag{6.17a}$$

• *Cost of the H_2 norm of the variations*

$$J_2=\left(\frac{\sum\limits_{i=1}^{2}\left\|y_i(t)-\delta y_i(t)\big|_{\xi=0}-\overline{y}\right\|_2^2}{\sum\limits_{i=1}^{2}\left\|\delta y_i(t)\big|_{\xi=0}-\delta y_i(t_0-)\big|_{\xi=0}\right\|_2^2}\right)^{\frac{1}{2}}\times 100\% \tag{6.17b}$$

where

$$\|f\|_\infty=\sup_{t\in\left[t_0,T_{\max}\right]}\left|f(t)\right|,\ \|f(t)\|_2^2=\int_{t_0-}^{T_{\max}}f(t)^2\,dt$$

The costs J_∞ and J_2 are defined for $t\in\left[t_0,T_{\max}\right]$. The parameter $T_{\max}$ is selected to be equal to the time required for all state and input variables of $\mathcal{S}_{L,CL}(\overline{\chi})$ to settle around their steady state values in a zone smaller than a margin denoted by ϵ_T, for stepwise external command and zero disturbances. The margin ϵ_T is set by the designer.

In order to take advantage of the characteristics of both the infinity norm and H_2 norm, the overall performance of the nonlinear closed loop system is proposed here to be evaluated by the composite cost function

$$\tilde{J} = (1-\mu) J_\infty + \mu J_2 \tag{6.17c}$$

where the weighting factor $\mu \in [0,1]$.

If the external commands are of the step form, i.e., $\delta\omega(t) = \tilde{\omega} u_s(t-t_0)$ where $\tilde{\omega}$ is a constant real vector and $u_s(t)$ is the unit step signal, then as $t \to +\infty$ the responses $y(t)\big|_{\xi=0}$ and $\delta y(t)\big|_{\xi=0}$ tend to respective steady state values. For this case, the following additional costs are defined:

• *Cost of the steady state error*

$$J_1 = \left\{ \frac{\sum_{i=1}^{2} \left[\lim_{t\to+\infty} \left| y_i(t)\big|_{\xi=0} - \delta y_i(t)\big|_{\xi=0} - \overline{y}_i \right| \right]^2}{\sum_{i=1}^{2} \left[\lim_{t\to+\infty} \left(\delta y_i(t)\big|_{\xi=0} - \delta y_i(t_0-)\big|_{\xi=0} \right) \right]^2} \right\}^{\frac{1}{2}} \times 100\% \tag{6.18a}$$

• *Cost of the overshoot*

$$J_o = \left\{ \frac{\sum_{i=1}^{2} \left\| o(y_i, \delta y_i) \right\|_\infty^2}{\sum_{i=1}^{2} \left[\lim_{t\to+\infty} \left(\delta y_i(t)\big|_{\xi=0} - \delta y_i(t_0-)\big|_{\xi=0} \right) \right]^2} \right\}^{\frac{1}{2}} \times 100\% \tag{6.18b}$$

where $o(y_i, \delta y_i) = 0$ if $\left| y_i(t) - y_i(t_0-) \right| \le \lim_{t\to+\infty} \left| \delta y_i(t)\big|_{\xi=0} - \delta y_i(t_0-) \right|$ else

$$o(y_i, \delta y_i) = \left| y_i(t)\big|_{\xi=0} - y_i(t_0-) \right| - \lim_{t\to+\infty} \left| \delta y_i(t)\big|_{\xi=0} - \delta y_i(t_0-) \right|$$

With respect to the latter two costs, the good performance is classified by the hard constraints

$$J_1 \le \varepsilon_1, \quad J_o \le \varepsilon_o \tag{6.19a,b}$$

where $\varepsilon_1, \varepsilon_o \in R^+$ and are selected by the designer to specify the importance of each criterion. The overall good performance is classified by the inequality

$$\tilde{J} \le \tilde{\varepsilon} \tag{6.20}$$

under the constraints in (6.19), where $\tilde{\varepsilon} \in R^+$ and is selected by the designer. The composite cost criterion in (6.17c) together with the constraints (6.19) covers all performance metrics in (6.17a), (6.17b) and (6.18), thus covering a wide range of different but indispensable design requirements.

If $\xi(t) = 0$, for a transition of $\mathcal{S}_{L,CL}(\bar{\chi})$ from $\bar{\chi}$ to an other operating point, let ρ, the external command is $\delta\omega(t) = \tilde{\omega} u_s(t - t_0)$ where $\tilde{\omega} = \begin{bmatrix} 0_{2\times 2} & I_2 \end{bmatrix}(\rho - \bar{\chi})$. Thus, taking into account the diagonal form with unitary steady state gain of the I/O transfer matrix of $\mathcal{S}_{L,CL}(\bar{\chi})$ and its stability, it is observed that $\lim_{t\to\infty} \delta y(t)\Big|_{\xi=0} = \tilde{\omega}$. For the transition of $\mathcal{S}_{NL,CL}(\bar{\chi})$ from $\bar{\chi}$ to ρ the same external command is considered to be applied.

6.4.2 Simulation Results

To illustrate the performance of the closed loop system, extensive simulation results will be provided. To this end, the parameters of the quadrotor model are considered to be those in [13], [29] and [39]:

$$m_q = 0.4[\text{kg}], J_{q,y} = 3.8278 \cdot 10^{-3}[\text{kg}m^2], g = 9.81[\text{m}/s^2], d = 0.205[\text{m}]$$
$$k_{dt,x} = 0.032[\text{kg}/s], k_{dt,z} = 0.048[\text{kg}/s], k_{a,y} = 5.567 \cdot 10^{-4}[\text{kg}/s], \bar{x}_2 = 1[\text{m}/s]$$
$$K_l = 2.9842 \cdot 10^{-5}[\text{N}/rad/s], \alpha_0 = 189.63, \alpha_1 = 6.0612, \alpha_2 = 0.0122, \beta = 280.19$$

The nominal operating point is $\bar{\chi} = \begin{bmatrix} \bar{u}_1 & \bar{u}_2 & \bar{y}_1 & \bar{y}_2 \end{bmatrix}^T$ where $\bar{u}_1 = 6.0304[\text{V}]$, $\bar{u}_2 = 6.0304[\text{V}]$, $\bar{y}_1 = 1[\text{m/s}]$ and $\bar{y}_2 = 0[\text{m/s}]$. To satisfy stability and disturbance attenuation the parameters of the metaheuristic algorithm are set to be

$$e_{d,\max} = 0.2, \left(k_{2,1}\right)_c = 0, \left(k_{2,2}\right)_c = 0, \left(k_{2,3}\right)_c = 0,$$
$$\left(k_{2,4}\right)_c = 0, \left(k_{2,5}\right)_c = 0, \left(k_{2,6}\right)_c = 0$$
$$\left(\rho\right)_c = 1, \left(\delta\rho\right)_c = 1, \left(k_{2,1}\right)_w = 2, \left(k_{2,2}\right)_w = 2, \left(k_{2,3}\right)_w = 2, \left(k_{2,4}\right)_w = 2,$$
$$\left(k_{2,5}\right)_w = 2, \left(k_{2,6}\right)_w = 2, \left(\rho\right)_w = 1, \left(\delta\rho\right)_w = 1, \lambda = 0.01,$$
$$n_{loop} = 30, n_{rep} = 20, n_{total} = 3 \cdot 10^6$$
$$T_{1,1} = 0.3, T_{1,2} = 0.4, T_{1,3} = 0.5, T_{1,4} = 0.6, T_{1,5} = 0.7, T_{2,1} = 0.3, T_{2,2} = 0.4$$
$$T_{2,3} = 0.5, T_{2,4} = 0.6, T_{2,5} = 0.7, \tau_1 = 0.09[\mathrm{s}], \tau_2 = 0.21[\mathrm{s}], \tau_{\max} = 0.3[\mathrm{s}]$$

Using the above parameters, execution of the metaheuristic algorithm yields

$$\rho = 0.770532,\ \delta\rho = 0.00664283,\ k_{2,1} = 0.613156,\ k_{2,2} = 0.000427085,$$
$$k_{2,3} = -0.665786,\ k_{2,4} = 0.266778,\ k_{2,5} = -1.48116 \text{ and } k_{2,6} = 1.49513$$

resulting in

$$k_{1,1} = 0.795026,\ k_{1,2} = 0.00664283,\ k_{1,3} = -0.666126,\ k_{1,4} = 0.418422,$$
$$k_{1,5} = -1.48802 \text{ and } k_{1,6} = 1.50202.$$

Using the above set of values, the cost criterion is computed to be $J_d = 0.192425$. Thus condition (6.9) is satisfied. Furthermore, note that using the above presented model and controller data, $\mathcal{S}_{L,CL}(\bar{\chi})$ remains stable for all delays satisfying the inequalities $0[s] \leqslant \tau_1 + \tau_2 < 0.395371[s]$.

To illustrate the performance of the closed loop system, the external commands are of the step form and $t_0 = 0$. Furthermore, let $\mu = 0.3$, $\varepsilon_o = 0.05$, $\varepsilon_1 = 0.05$, $\tilde{\varepsilon} = 0.05$ and $\varepsilon_T = 0.01$. For a wide range of amplitudes of the step external commands, i.e., for $\tilde{\omega} = \begin{bmatrix} \tilde{\omega}_1 & \tilde{\omega}_1 \end{bmatrix}^T$ and $\left(\tilde{\omega}_1, \tilde{\omega}_2\right) \in [-10,10]$, the composite cost in (6.17c) and the hard constraints in (6.19a) and (6.19b) is presented in Figure 6.2. It can readily be verified that $\mathcal{S}_{NL,CL}(\bar{\chi})$ behaves satisfactorily, for a wide range of external commands. Note that the gray areas in the upper corners of the contour plot correspond to external command pairs for which the constraints (6.19a) and (6.19b) are not satisfied while the contour corresponding to $\tilde{\varepsilon}$ has been highlighted.

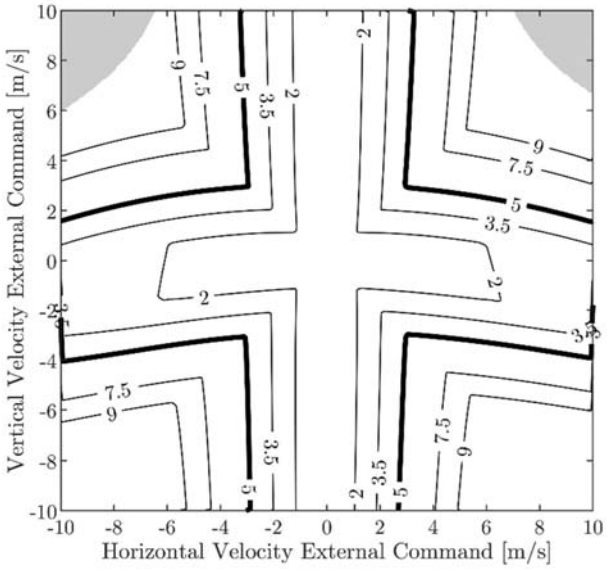

Fig. 6.2 The composite performance metric $\tilde{J}$ at $\bar{\chi}$ for various performance commands

In order to demonstrate the resilience of the proposed control scheme to external disturbances, the responses of the performance variables $y_1(t)$ and $y_2(t)$ of the nonlinear closed loop system will be evaluated under the influence of varying external disturbances and compared to the reference linear model responses, for zero disturbances, using the criterion defined in (6.20) and choosing again $\tilde{\varepsilon} = 0.05$. The disturbances will be considered to be of the form $\xi_i(t) = \tilde{g}_i \tilde{\xi}_i(t - t_0)$ $(i = 1,2)$ with $t_0 = 0$ where $\tilde{g}_i$ are appropriate multipliers and where $\tilde{\xi}_i(t)$ are time varying signals generated using the Dryden continuous turbulence model (indicatively see [40]). The time plot of the disturbances are presented in Figure 6.3. In Figure 6.4, a contour plot of the composite cost in (6.17c) is presented for different values of $\tilde{g}_i$, while the amplitudes of the external commands are chosen to be $\tilde{\omega}_1 = 1.0$[m/s] and $\tilde{\omega}_2 = 0.5$[m/s]. Figure 6.4 implies that the performance of the proposed control scheme is minimally influenced by the disturbances, considering that practically for the whole range of disturbance gains, the composite cost remains lower than 5%.

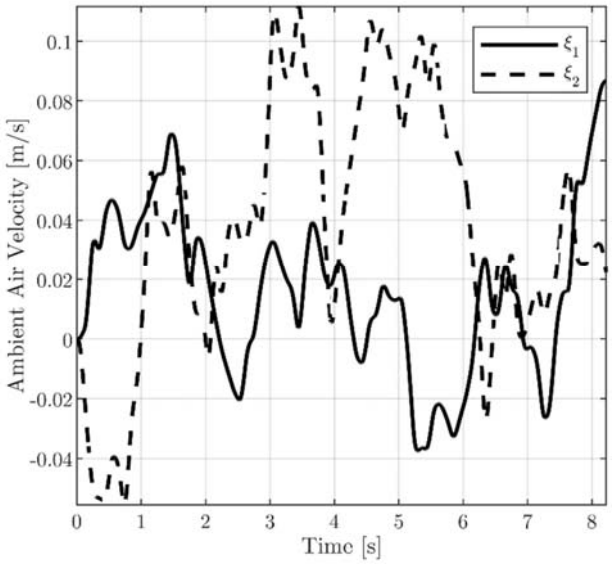

Fig. 6.3 Disturbance signals

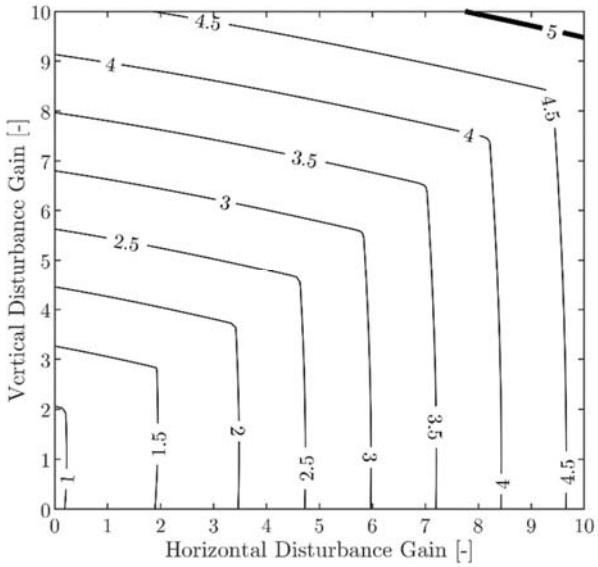

Fig. 6.4 The composite performance metric $\tilde{J}$ at $\overline{\chi}$ for various disturbance multipliers in $[0,10]$

6.5 STEP WISE SAFE SWITCHING

The controller designed in 6.3 is based on the linear approximant of the quadrotor model and so it is efficient around the respective operating points. To achieve maneuvers extending far from the operating point the safe switching approach in [30]

and [31] will be used. To do so, the approach in [31] will be extended here to the continuous time multi delay case. To this end, appropriate definitions will be introduced in the following subsections.

6.5.1 Step Wise Transitions Among Operating Points

The transition among *trim points* or *operating points* is accomplished here using external commands being of the step form. As already mentioned is Subsection 6.3.3, the transition of the system $\mathcal{S}_{L,CL}(\overline{\chi})$ from $\overline{\chi}$ to an other operating point (or trim point) ρ is executed for the case of zero disturbances using the external command $\delta\omega(t) = \tilde{\omega}u_s(t-t_0)$ where $\tilde{\omega} = \begin{bmatrix} 0_{2\times 2} & I_2 \end{bmatrix}(\rho - \overline{\chi})$. This way, the performance output of the linear approximant tends to $\rho - \overline{\chi}$, i.e., $\lim_{t\to+\infty} \delta y(t)\big|_{\xi=0} = \rho - \overline{\chi}$. According to the present approach, for the transition of $\mathcal{S}_{NL,CL}(\overline{\chi})$ from $\overline{\chi}$ to ρ the same external command $\delta\omega(t) = \tilde{\omega}u_s(t-t_0)$ is considered to be applied. For zero disturbances, the system $\mathcal{S}_{NL,CL}(\overline{\chi})$ arrives at a point ρ^*, in general being different than ρ, i.e., $\lim_{t\to+\infty} y(t)\big|_{\xi=0} = \rho^*$.

If $\xi(t) = 0$, then for $\mathcal{S}_{NL,CL}(\overline{\chi})$ to be retained at the operating point ρ^*, the external command $\omega(t)$ must be retained around a stationary value vector denoted by ϕ. The vector ϕ is uniquely determined by (6.16) after taking into account that $\Delta u = \begin{bmatrix} 0_{2\times 2} & I_2 \end{bmatrix}(\rho - \overline{\chi})$ and $\Delta x = {}^{(\rho)}\overline{x} - \overline{x}$ where ${}^{(\rho)}\overline{x}$ is the steady state vector of $x(t)$ for the case where the inputs and the outputs in $\mathcal{S}_{NL,CL}(\overline{\chi})$ are retained at ρ. Recall that for every ${}^{(\rho)}\overline{y} = \begin{bmatrix} 0_{2\times 2} & I_2 \end{bmatrix}\rho$, the vectors ${}^{(\rho)}\overline{u} = \begin{bmatrix} I_2 & 0_{2\times 2} \end{bmatrix}\rho$ and ${}^{(\rho)}\overline{x}$ are uniquely determined by ${}^{(\rho)}\overline{y}$.

To describe the transition from one operating point to another, using the controller $\mathcal{C}(\overline{\chi})$, consider the notations: Let ρ_s denote the initial (starting) trim point and ρ_f be the destination (final) trim point. Similarly to the above procedure, the external command is

$$\delta\omega(t) = \phi + \tilde{\phi} u_s(t - t_0) \tag{6.21}$$

where $\phi = [0_{2\times 2} \quad I_2](\rho_s - \bar{\chi})$ is the stationary external command vector retaining the closed loop system $\mathcal{S}_{NL,CL}(\bar{\chi})$ at ρ_s and $\tilde{\phi} = [0_{2\times 2} \quad I_2](\rho_f - \rho_s) = [0_{2\times 2} \quad I_2]\left[(\rho_f - \bar{\chi}) - (\rho_s - \bar{\chi})\right]$

Clearly, for $\xi(t) = 0$ and using (21), the system $\mathcal{S}_{NL,CL}(\bar{\chi})$ arrives at a trim point ρ_f^*, in general being different than ρ_f, i.e., $\lim_{t\to+\infty} y(t)\big|_{\xi=0} = \rho_f^*$.

To evaluate the performance of the transitions with external commands of the form (6.21), the cost criteria in (6.19) and (6.20) will be used. The external command in (6.21) depends upon ϕ and $\tilde{\phi}$. Clearly, $\delta\omega(t_0 -) = \phi$. In general, the closed loop response depends upon $\delta\omega(t)$ for $t \geq t_0$ and $\delta\omega(t_0 -)$. So the cost functions $\tilde{J}$, $\tilde{J}_1$ and $\tilde{J}_o$, depending upon the operating point $\bar{\chi}$, can be expressed in the following function forms:

$$\tilde{J} = \tilde{J}(\delta\omega(t), \delta\omega(t_0 -), \bar{\chi}) \tag{6.22a}$$

$$J_1 = J_1(\delta\omega(t), \delta\omega(t_0 -), \bar{\chi}) \tag{6.22b}$$

$$J_o = J_o(\delta\omega(t), \delta\omega(t_0 -), \bar{\chi}) \tag{6.22c}$$

6.5.2 Step Wise Safe Transition: The Design Procedure

The set of all operating points constitutes, in general, a hypersurface in $R^{4\times 1}$, which is called *operating surface*. Consider a finite set of *nominal operating points* or *nominal trim points*, let $\mathrm{X} = \{\bar{\chi}_1, ..., \bar{\chi}_\mu\}$. For every nominal operating point $\bar{\chi}_j$ in X, where $j \in \{1, ..., \mu\}$, the respective linear approximant is denoted by $\mathcal{S}(\bar{\chi}_j)$ and the respective controller is denoted by $\mathcal{C}(\bar{\chi}_j)$. The respective nonlinear closed loop

systems are denoted by $\mathcal{S}_{NL,CL}(\overline{\chi}_j)$ while the respective closed loop systems of the linear approximant are denoted by $\mathcal{S}_{L,CL}(\overline{\chi}_j)$.

For the system $\mathcal{S}_{NL,CL}(\overline{\chi}_j)$ to be retained at the trim point ρ_s the external command must be retained at a stationary value $\phi = \begin{bmatrix} 0_{2\times 2} & I_2 \end{bmatrix}\left(\rho_s - \overline{\chi}_j\right)$. For the transitions of $\mathcal{S}_{L,CL}(\overline{\chi}_j)$ from ρ_s to ρ_f the external command is

$$\delta\omega(t) = \begin{bmatrix} 0_{2\times 2} & I_2 \end{bmatrix}\left\{\left(\rho_s - \overline{\chi}_j\right) + \left[\left(\rho_f - \overline{\chi}_j\right) - \left(\rho_s - \overline{\chi}_j\right)\right] u_s\left(t - t_0\right)\right\} =$$

$$= \begin{bmatrix} 0_{2\times 2} & I_2 \end{bmatrix}\left[\rho_s - \overline{\chi}_j + \left(\rho_f - \rho_s\right) u_s\left(t - t_0\right)\right] \tag{6.23}$$

Using (6.23), it holds that $\lim_{t\to+\infty} \delta y(t)\big|_{\xi=0} = \rho_s - \overline{\chi}_j$. Also, using (6.23), the system $\mathcal{S}_{NL,CL}(\overline{\chi}_j)$ arrives at another point ρ_f^* such that $\lim_{t\to+\infty} y(t)\big|_{\xi=0} = \rho_f^*$. To evaluate the performance of $\mathcal{S}_{NL,CL}(\overline{\chi}_j)$ with respect to $\mathcal{S}_{L,CL}(\overline{\chi}_j)$, the cost functions in (6.22) will be used.

Around each nominal operating point $\overline{\chi}_j$ in X, there is an area called *target operating area*. The target operating area is denoted by $T(\overline{\chi}_j)$. In order to determine $T(\overline{\chi}_j)$, the following cost function is defined:

$$J_T\left(\rho, \overline{\chi}_j\right) = (1-\mu)\max\left\{\left\|\begin{bmatrix} 0 & 0 & 1 & 0 \end{bmatrix}\left(\rho - \overline{\chi}_j\right)\right\}\right. +$$

$$\left.\mu\left\{\left[\begin{bmatrix} 0 & 0 & 1 & 0 \end{bmatrix}\left(\rho - \overline{\chi}_j\right)\right]^2 + \left[\begin{bmatrix} 0 & 0 & 1 & 0 \end{bmatrix}\left(\rho - \overline{\chi}_j\right)\right]^2\right\}^{\frac{1}{2}} \tag{6.24}$$

Clearly, the above cost depends upon $\omega = \begin{bmatrix} 0_{2\times 2} & I_2 \end{bmatrix}\rho \in R^{2\times 1}$. Thus, the cost can be expressed as

$$J_T\left(\rho, \overline{\chi}_j\right) = J_T\left(\omega, \overline{\chi}_j\right) \tag{6.25}$$

Also it is observed that similarly to $\tilde{J}$, the cost J_T is a composite infinity / Euclidean norm cost, having the same weighting factors with $\tilde{J}$.

Define the area $R_j(\gamma) = \left\{\rho \in R^{4\times 1} : J_T\left(\rho, \bar{\chi}_j\right) \le \gamma\right\}$ or equivalently

$$R_j(\gamma) = \left\{\rho \in R^{4\times 1} : J_T\left(\omega, \bar{\chi}_j\right) \le \gamma\right\} \tag{6.26}$$

where $\gamma \in R_+$.

Let

$$\gamma_j^* = \max\left\{\gamma \in R_+ : \tilde{J} < \tilde{e} \wedge J_1 < e_1 \wedge J_o < e_o, \forall \omega \in R_j(\gamma)\right\} \tag{6.27}$$

where $\tilde{e}$, e_1 and e_o are the thresholds of precision in the target operating area. The target area is determined to be

$$T\left(\bar{\chi}_j\right) = R_j\left(\gamma_j^*\right) \tag{6.28}$$

In the present version of the definition of the target area it is observed that the composite cost attenuates the need for the definition of the tolerant operations area (see [31]), so this definition will not be included.

For each nominal trim point $\bar{\chi}_j \in \mathrm{X}$, the set of *adjacent nominal trim points*, denoted by Λ_j, is defined here to be

$$\Lambda_j = \left\{\bar{\chi}_k \in \mathrm{X} : T_R(\bar{\chi}_k) \cap T_R(\bar{\chi}_j) \neq \varnothing\right\} \;;\; k \in \{1,...,m\}$$

The above definition is a modification of the respective definition in [30] and [31]. Particularly, here it is not required for the union of two adjacent target areas to be a subset of the tolerance areas of the respective adjacent nominal trim points. In accordance with [30] and [31], for the implementation of the stepwise safe switching procedure the *dense web principle* is required to be fulfilled. The dense web principle is formulated here by the following two conditions

$$\Lambda_j \neq \varnothing, \forall j \in \{1,...,\mu\},\ \bigcup_{j=1}^{\mu}\left(\bigcup_{\bar{\chi}_k \in \Lambda_j} T_R(\bar{\chi}_k) \right) \neq \varnothing$$

The first of the above conditions implies that there are no isolated nominal trim points, while the second implies that there are no isolated subsets of nominal trim points.

The transition between two trim points is called safe if both points belong to the same target area. According to the dense web principle, there is always a sequence of *safe transitions* from any trim point to any trim point in $\bigcup_{j=1}^{\mu} T_R(\bar{\chi}_j)$ with appropriate intermediate stations in $\bigcup_{j=1}^{\mu} T_R(\bar{\chi}_j)$. Any sequence of safe transitions is also called safe. Here, all maneuvers are analyzed to a sequence of safe transitions.

Consider the transition from a starting trim point $\rho_s = \rho_1 \in T\left(\bar{\chi}_j\right)$ on the trim point $\rho_1 \in T(\bar{\chi}_k) \cap T(\bar{\chi}_j)$ using the controller $\mathcal{C}(\bar{\chi}_j)$ where $\bar{\chi}_j$ and $\bar{\chi}_k$, with $j,k \in \{1,\ldots,m\}$ and $j \neq k$, are two adjacent trim point. The system $\mathcal{S}_{NL,CL}(\bar{\chi}_j)$ arrives at the point ρ_1^* being near enough to ρ_1. Clearly, if the criterion $J_1 \leq e_1$ is satisfied for appropriate e_1 then ρ_1^* is near enough ρ_1 and $\rho_1^* \in T(\bar{\chi}_k) \cap T(\bar{\chi}_j)$. After a time period $T_{\max} = t_s$ the controller is switched to $\bar{\chi}_k$ and the transition from ρ_1^* to $\rho_2 \in T\left(\bar{\chi}_k\right)$ starts. The system $\mathcal{S}_{NL,CL}(\bar{\chi}_k)$ arrives at a point ρ_2^* being near enough to ρ_2 and $\rho_2^* \in T(\bar{\chi}_k) \cap T(\bar{\chi}_k)$ under the condition $J_1 \leq e_1$.

The time t_s is set to be $t_s = \max\left\{t_{s,1}, t_{s,2}\right\}$, where $t_{s,v}$ with $v \in \{1,2\}$ is the settling time of the v_{th} output of $\mathcal{S}_{L,CL}(\bar{\chi}_j)$. To compute $t_{s,v}$ consider the case where $T_{v,1} \neq T_{v,2} \neq T_{v,3} \neq T_{v,4} \neq T_{v,5}$ ($v = 1,2$), the settling time, let $t_{s,v}$ for each performance output is evaluated through solving the equation

$$\sum_{q=1}^{5} \frac{\exp\left(-\dfrac{t_{s,v}-\tau_1-\tau_2}{T_{v,q}}\right)}{\prod_{i=1,i\neq q}^{5}\left(1-\dfrac{T_{v,i}}{T_{v,q}}\right)} = \varepsilon_s \quad (v=1,2)$$

where ε_s is a positive percentile number used to define the convergence of the the response to the steady state value.

Now we are in position to present the stepwise safe switching algorithm.

Stepwise Safe Switching Algorithm

Modules

Step 1: Determine the set of nominal trim points $\mathrm{X} = \left\{\overline{\chi}_1,...,\overline{\chi}_\mu\right\}$.

Step 2: Determine the set of linear approximants $\left\{\mathcal{S}(\overline{\chi}_1),...,\mathcal{S}(\overline{\chi}_\mu)\right\}$

Step 3: Determine the set of controllers $\left\{\mathcal{C}(\overline{\chi}_1),...,\mathcal{C}(\overline{\chi}_\mu)\right\}$

Step 4: Using $\mathcal{S}_{NL,CL}(\overline{\chi}_j)$ and $\mathcal{S}_{L,CL}(\overline{\chi}_j)$ for $j \in \{1,...,\mu\}$, determine the set of target operating areas $\left\{T_R(\overline{\chi}_1),...,T_R(\overline{\chi}_\mu)\right\}$

Step 5: Determine Λ_j for $j \in \{1,...,\mu\}$ and check the density of the web.

Step 6: If the web is dense, go to Step 7. Otherwise, go to **Step 1** to choose a new set of more dense nominal trim points.

Transition

Step 7: Read the initial trim point, let ρ_s (using measurements) belonging to a target operating area.

Step 8: Read the final trim point ρ_f (desired trim point of the maneuver) being set by the designer and belonging to a target operating area.

Step 9: Choose a pair of target operating areas $\left(T_R(\overline{\chi}_s), T_R(\overline{\chi}_f)\right)$, such that ρ_s lies within $T_R(\overline{\chi}_s)$ and ρ_f lies within $T_R(\overline{\chi}_f)$.

Step 10: Determine the sequence of nominal operating points $\overline{\chi}_{k_0}, \overline{\chi}_{k_1}, ..., \overline{\chi}_{k_\sigma}$ where every two consecutive points are adjacent and where $\overline{\chi}_s = \overline{\chi}_{k_0}$ and $\overline{\chi}_f = \overline{\chi}_{k_\sigma}$ (according to the dense web principle such a sequence always exist).

Step 11: Determine the sequence of trim points $\rho_0, \rho_1, ..., \rho_{\sigma-1}, \rho_\sigma$ where the trim point $\rho_\lambda \in T_R(\overline{\chi}_{k_{\lambda-1}}) \cap T_R(\overline{\chi}_{k_\lambda})$ for $\lambda \in \{1, ..., \sigma - 1\}$ and $\rho_0 = \rho_s$, $\rho_\sigma = \rho_f$ (according to the dense web principle such a sequence always exist).

Step 12: Set $\lambda = 1$

Step 13: Switch to controller $\mathcal{C}(\overline{\chi}_{k_{\lambda-1}})$ and force the closed loop system from $\rho_{\lambda-1}$ to ρ_λ.

Step 14: Wait for $t_s = \max\left\{t_{s,1}, t_{s,2}\right\}$, till the closed loop dynamic nonlinear time delay system approaches its steady state values, namely a trim point ρ_λ^* being near ρ_λ.

Step 15: If $\rho_\lambda^* \in T_R(\overline{\chi}_{k_{\lambda-1}}) \cap T_R(\overline{\chi}_{k_\lambda})$ go to ***Step 16***, else set $\rho_s = \rho_\lambda^*$ and go to ***Step 8***.

Step 16: Set $\rho_\lambda = \rho_\lambda^*$, increment the iteration number, i.e., $\lambda = \lambda + 1$, and return to ***Step 13***.

6.5.3 Performance of the Stepwise Safe Switching Design Procedure

6.5.3.1 Definitions

In order to demonstrate the performance of the proposed stepwise safe switching scheme, the numerical data for the quadrotor model presented in Subsection 6.3.3 are used. Two adjacent nominal trim points are $\overline{\chi}_1 = \left[\overline{u}_{1,1} \quad \overline{u}_{1,2} \quad \overline{y}_{1,1} \quad \overline{y}_{1,2}\right]^T$ and $\overline{\chi}_2 = \left[\overline{u}_{2,1} \quad \overline{u}_{2,2} \quad \overline{y}_{2,1} \quad \overline{y}_{2,2}\right]^T$. With respect to $\overline{\chi}_1$ it holds that $\overline{u}_{1,1} = 6.0304[\text{V}]$, $\overline{u}_{1,2} = 6.0304[\text{V}]$, $\overline{y}_{1,1} = 1[\text{m/s}]$ and $\overline{y}_{1,2} = 0[\text{m/s}]$. This trim point is the one considered in Subsection 6.3.3. Hence, the controller parameters of this trim point are those derived in Subsection 6.3.3. With respect to the trim point $\overline{\chi}_2$, it holds that $\overline{u}_{2,1} = 6.1559[\text{m/s}]$, $\overline{u}_{2,2} = 6.1559[\text{m/s}]$, $\overline{y}_{2,1} = 4[\text{m/s}]$, $\overline{y}_{2,2} = 3[\text{m/s}]$. Assuming that the desired closed loop transfer matrix for this trim point is identical to that for $\overline{\chi}_1$ and applying the proposed in Subsection 6.3.1 metaheuristic algorithm using the same set of quadrotor parameters, the feedback matrix elements are derived to be $k_{1,1} = 0.0018$, $k_{1,2} = -0.2805$, $k_{1,3} = -0.6201$, $k_{1,4} = -0.3187$, $k_{1,5} = -0.7016$, $k_{1,6} = 0.7163$, $k_{2,1} = -0.2047$, $k_{2,2} = -0.2879$, $k_{2,3} = -0.6205$, $k_{2,4} = -0.4822$, $k_{2,5} = -0.6936$ and $k_{2,6} = 0.7083$. Using the above controller parameters the disturbance attenuation cost is derived to be $J_d = 0.2153$ and the linear approximant closed loop system remains stable for $0 \leqslant \tau_1 + \tau_2 < 0.307299$. Let $\tilde{e} = 0.04$, $e_o = 0.05$ and $e_1 = 0.05$. Applying series of computations it can be observed that appropriate target operating areas, in the space of the nominal points of the performance outputs are those presented in Figure 6.5. The upper right portion of the target area of $\overline{\chi}_1$ overlaps the lower left portion of the target area of $\overline{\chi}_2$.

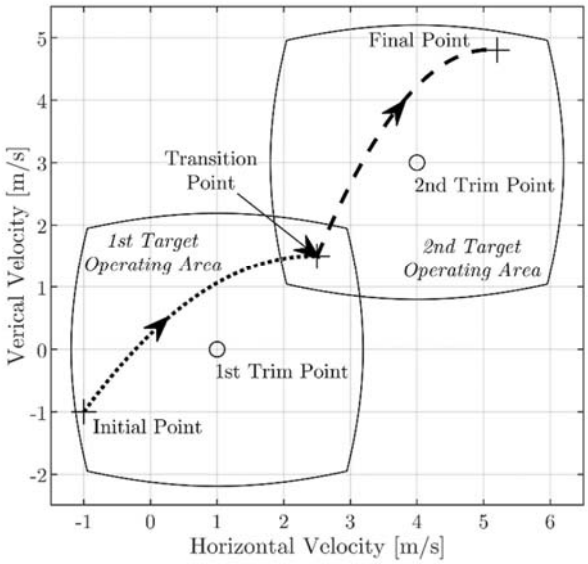

Fig. 6.5 A step wise point transition and the relative target operating areas.

In what follows, it will be assumed that the desired trajectory of the quadrotor passes through the following sequence of trim points

$$\rho_0 = \begin{bmatrix} \rho_{0,1} & \rho_{0,2} & \rho_{0,3} & \rho_{0,4} \end{bmatrix}^T$$
$$\rho_1 = \begin{bmatrix} \rho_{1,1} & \rho_{1,2} & \rho_{1,3} & \rho_{1,4} \end{bmatrix}^T$$
$$\rho_2 = \begin{bmatrix} \rho_{2,1} & \rho_{2,2} & \rho_{2,3} & \rho_{2,4} \end{bmatrix}^T$$

where $\rho_{0,1} = 5.9889[\text{V}]$, $\rho_{0,2} = 5.9889[\text{V}]$, $\rho_{0,3} = -1[\text{m/s}]$, $\rho_{0,4} = -1[\text{m/s}]$, $\rho_{1,1} = 6.0931[\text{V}]$, $\rho_{1,2} = 6.0931[\text{V}]$, $\rho_{1,3} = 2.5[\text{m/s}]$, $\rho_{1,4} = 1.5[\text{m/s}]$, $\rho_{2,1} = 6.2307[\text{V}]$, $\rho_{2,2} = 6.2307[\text{V}]$, $\rho_{2,3} = 5.2[\text{m/s}]$ and $\rho_{2,4} = 4.8[\text{m/s}]$. The first and the second trim points belong to the first target operating areas while the second and the third trim point belongs to the second target operating area. With respect to the waiting time between switching points, let $\varepsilon_s = 0.01$.

6.5.3.2 Performance of the Switching Scheme without Disturbances

In order to demonstrate the performance of the proposed switching control scheme, including the influence of the wireless networks and

transmission/reconstruction protocols, simulation will be performed using Matlab/Simulink software while simulation of the wireless network is carried out using the TrueTime 2.0 addon (see also [41]). Assuming that the disturbances are equal to zero and after computing t_s to be $t_s = 6.0075[s]$ and applying the stepwise safe switching algorithm yields $\rho_1^* = \begin{bmatrix} \rho_{1,1}^* & \rho_{1,2}^* & \rho_{1,3}^* & \rho_{1,4}^* \end{bmatrix}^T$ and $\rho_2^* = \begin{bmatrix} \rho_{2,1}^* & \rho_{2,2}^* & \rho_{2,3}^* & \rho_{2,4}^* \end{bmatrix}^T$, where $\rho_{1,1}^* = 6.09308[\mathrm{V}]$, $\rho_{1,2}^* = 6.09308[\mathrm{V}]$, $\rho_{1,3}^* = 2.25052[\mathrm{m/s}]$, $\rho_{1,4}^* = 1.49970[\mathrm{m/s}]$, $\rho_{2,1}^* = 6.2306[\mathrm{V}]$, $\rho_{2,2}^* = 6.2306[\mathrm{V}]$, $\rho_{2,3}^* = 5.2044[\mathrm{m/s}]$ and $\rho_{2,4}^* = 4.7981[\mathrm{m/s}]$. In Figures 6.6 to 6.13, the closed loop system responses for the actuatable inputs and state variables are presented. In particular, in Figures 6.6 to 6.11 the responses for the state variables are presented while in Figures 6.12 and 6.13 the voltage supplies to the motors of the quadrotor are presented. For comparison reasons, in the above figures, the respective single step closed loop responses are presented for the transition between ρ_0 and ρ_2 without switching the controller in ρ_1. With respect to the actuatable inputs, they do not present significant fluctuations, being easily implementable. With respect to the switching scheme, it can be verified that the performance variables of the system, i.e., the horizontal and vertical velocity of the quadrotor, follow accurately the model responses, generating an overall cost $\tilde{J}$ being equal to 1.8208%, being lower than the bound set for the definition of the target operating areas. With respect to the remaining state variables, it is important to mention that they remain in appropriate bounds. For comparison reasons, it is mention that the respective cost for a single step maneuvering approach becomes 9.0204%. This is more than 4.5 larger than the respective criterion for the switching approach.

With respect to the settling time of the nonlinear closed loop response, although one would expect the settling time of the switching control scheme to be double as compared to the resulting settling time of the single step approach, considering that in the switching case two consecutive step responses are evaluated, for the first performance variable the settling time is only 40.53% larger. For the second performance variable the settling time of the switching control scheme is 96.55% larger. Note that choosing $\varepsilon_s = 0.05$, which corresponds to a faster change between

operating areas, the settling time of the first performance variable is 22.02% larger than the single step approach and the settling time of the second performance variable is 76.22% larger than the single step approach. The cost criterion does not significantly change.

An interesting issue is the comparison of the present switching and time delay design scheme to one not taking into account the time delays of the network. This is a widely used consideration in the field. To this end, the controller derived in section 6.3 is computed for the case where the controller delays tend to zero. The derived controller is applied to the nonlinear time delay networked system. The performance cost for this case is computed to be at least ten times larger than the performance cost of the controller involving time delays.

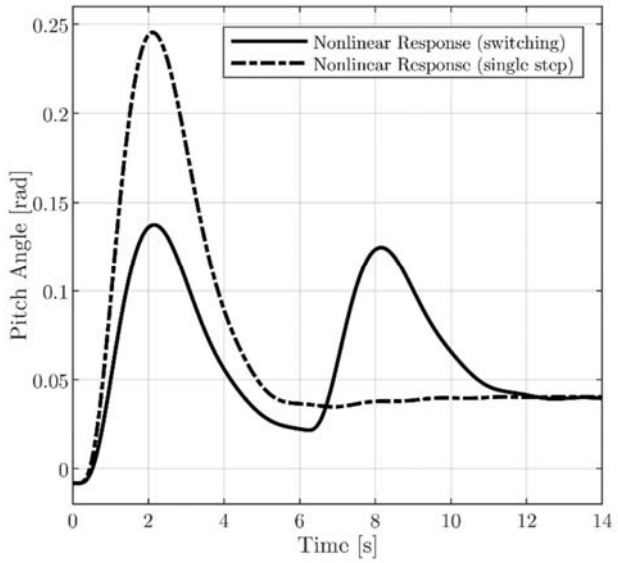

Fig. 6.6 Pitch angle

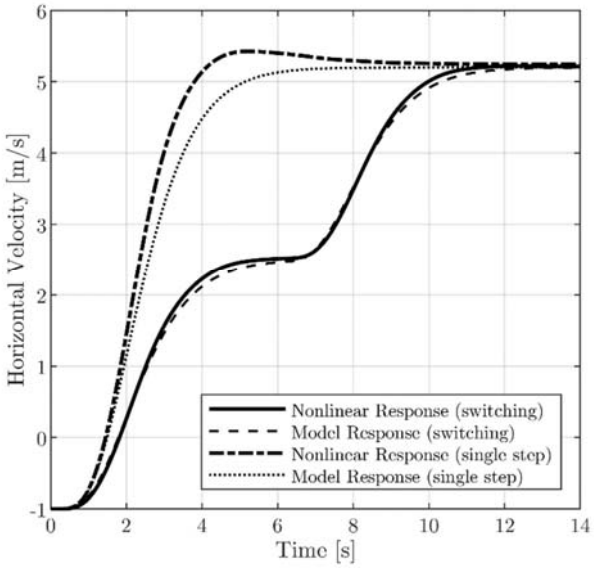

Fig. 6.7 Horizontal velocity

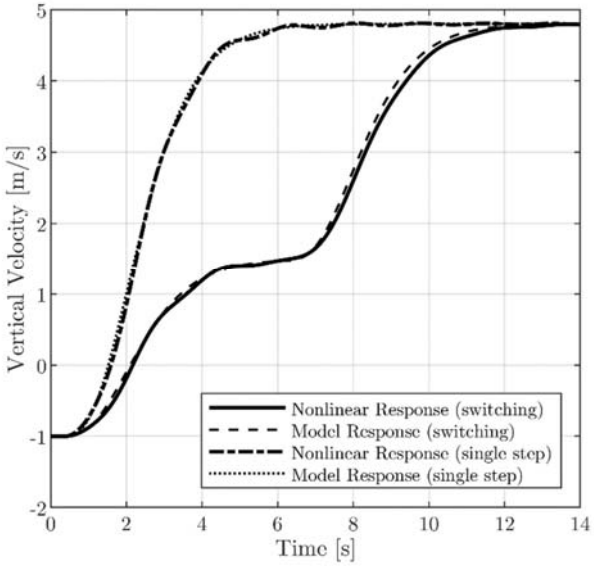

Fig. 6.8 Vertical velocity

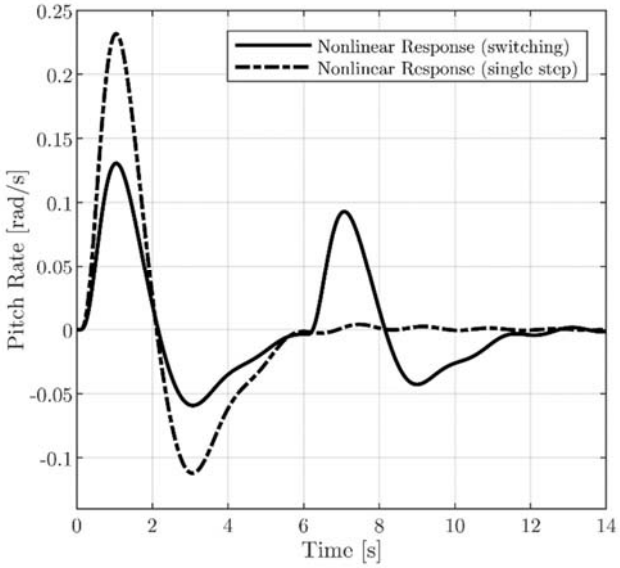

Fig. 6.9 Pitch rate

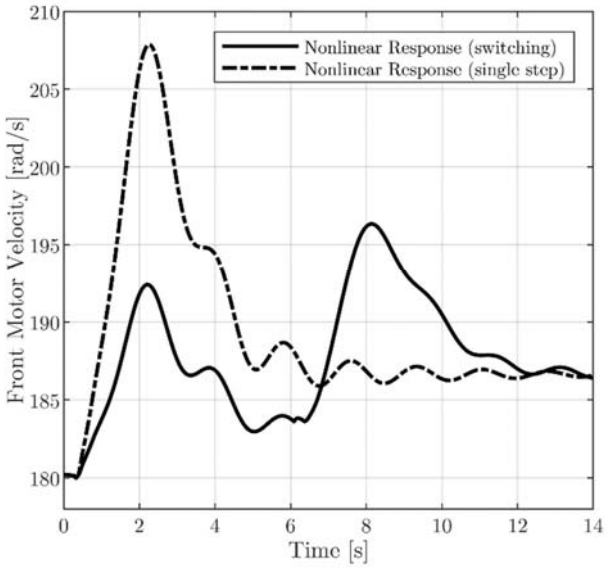

Fig. 6.10 Front motor velocity

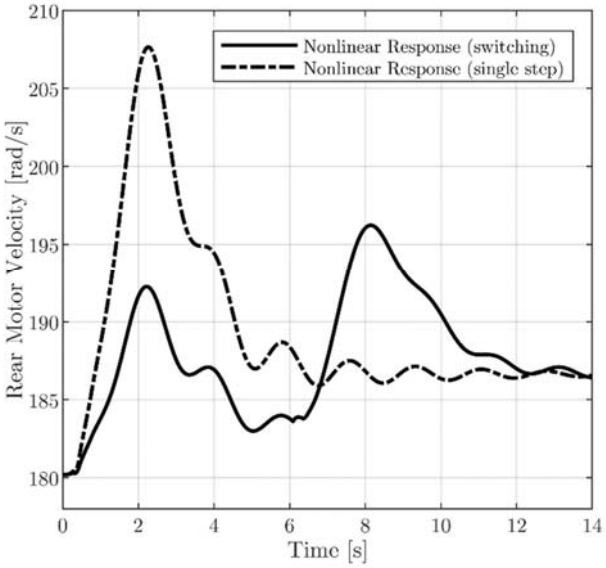

Fig. 6.11 Rear motor velocity

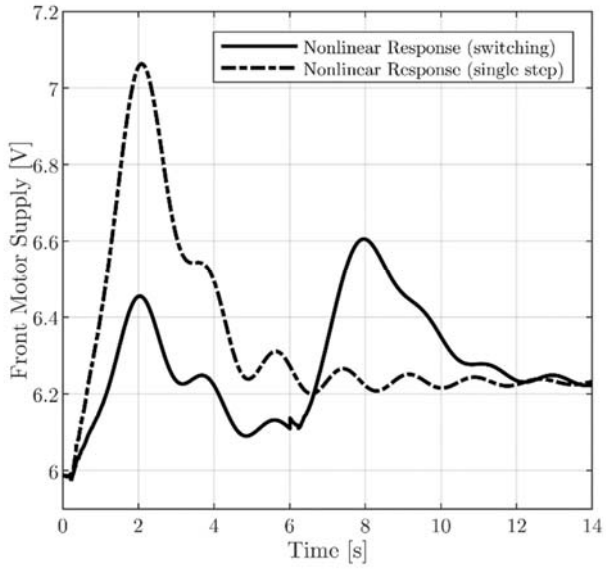

Fig. 6.12 Front motor voltage supply

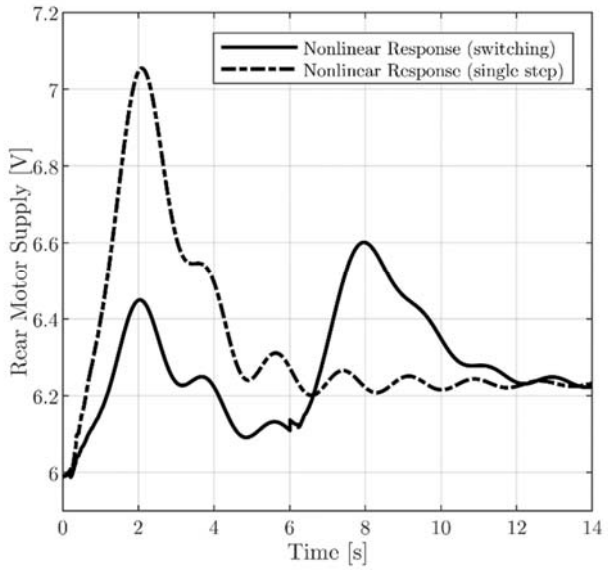

Fig. 6.13 Rear motor voltage supply

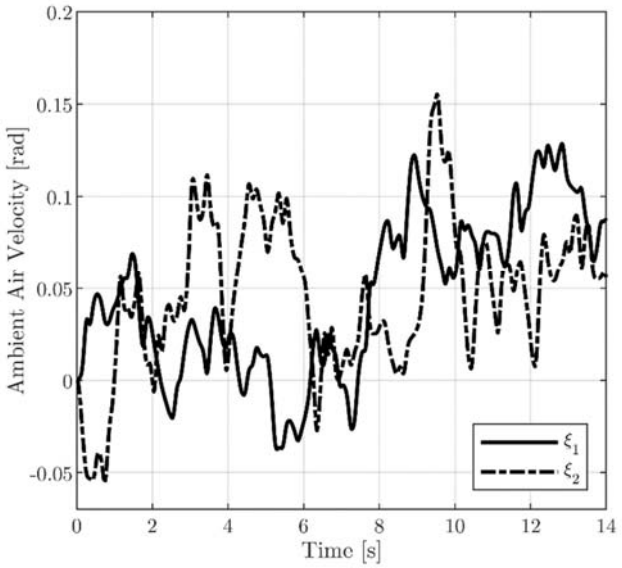

Fig. 6.14 Disturbance signals

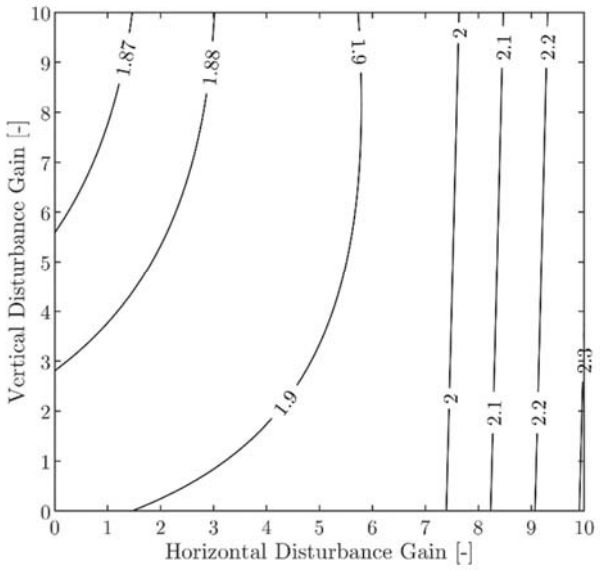

Fig. 6.15 Cost criterion contour plot

6.5.3.3 Performance of the Switching Scheme under the influence of Disturbances

In order to demonstrate the resilience of the proposed control scheme to external disturbances, a similar approach to the one presented in section 6.3. In what follows, $\tilde{\xi}_i(t)$ will be considered to be as presented in Figure 6.14. In Figure 6.15, a contour plot of the criterion in (6.14a) is presented for different values of $\tilde{g}_i$, assuming the same switching scheme defined in Figure 6.5. Figure 6.15 implies that the performance of the proposed control scheme is minimally influenced by the disturbances, considering that practically for the whole range of disturbance gains, the cost criterion remains close to the disturbance free case, well under the 4% limits set for the cost criterion.

6.6 SUMMARY

For a wide range of maneuvers and wireless control configuration, the goal of independent horizontal and vertical velocity for quadrotors has been achieved by proposing a stepwise safe switching algorithm for non-linear time delay systems, using dynamic multi delay controllers and approximately minimizing a composite cost

criterion including the infinity norm and the H_2 norm of the variations around trim points, under hard constraints for the overshoot and the steady state values of the performance variables. The controllers have been determined using a mixed analytic/metaheuristic scheme satisfying the design requirements of I/O decoupling, stability, and disturbance attenuation. The proposed scheme is tolerant to atmospheric disturbances, communication delays and variations of the delays, as well as large maneuver commands and model nonlinearities. The extension of the present results to combined lateral and longitudinal maneuvers is currently under investigation, following the block decoupling design requirements (see [42]).

REFERENCES

[1] Zhang, D., Qi, H., Wu, X., Xie, Y., Xu, J.: The Quadrotor Dynamic Modeling and Indoor Target Tracking Control Method, *Mathematical Problems in Engineering* (2014)

[2] Magalhaes, G. M., Santos, E. G., Borges, L. M., Cunha, A. E. C., Comparison and Implementation of Control Strategies for a Quadrotor. In: *XIII Simpósio Brasileiro de Automação Inteligente*, 133-138 (2017)

[3] Garcia, R. A., Rubio, F. R., Ortega, M. G.: Robust PID Control of the Quadrotor Helicopter. *IFAC Proceedings Volumes*, **45**(3), 229-234 (2012)

[4] Moreno-Valenzuela, J., Perez-Alcocer, R., Guerrero-Medina, M., Dzul, A.: Nonlinear PID-Type Controller for Quadrotor Trajectory Tracking. *IEEE/ASME Transactions on Mechatronics*, **23**(5), 2436-2447 (2018)

[5] Chehadeh, M. S., Boiko, I.: Design of rules for in-flight non-parametric tuning of PID controllers for unmanned aerial vehicles. *Journal of the Franklin Institute*, **356**, (474-491) (2019)

[6] Outeiro, P., Cardeira, C., Oliveira,P.: Lqr/mmae height control system of a quadrotor for constant unknown load transportation. In: *Proceedings of the 13th APCA International Conference on Control and Soft Computing (CONTROLO)*, 389-394 (2018)

[7] Safaei, A., Mahyuddin, M. N.: Optimal model-free control for a generic MIMO nonlinear system with application to autonomous mobile robots. *International Journal of Adaptive Control and Signal Processing*, **3**, 792-815 (2018)

[8] Ozturk, O., Ozkan, H. M.: Optimal Control of Quadrotor Unmanned Aerial Vehicles on Time Scales. *International Journal of Difference Equations*, **13**, 41-54 (2018)

[9] Sabatino, F. *Quadrotor control: modeling, nonlinear control design, and simulation*, Master's Degree Project, KTH Electrical Engineering (2015)

[10] Arrosida, H., Effendi, R., Agustinah, T., Pramudijanto, J.: Design of Decoupling and Nonlinear PD Controller for Cruise Control of a Quadrotor. In: , *International Seminar on Intelligent Technology and its Applications (ISITIA)*, (57-61) (2015)

[11] Leonardo, S., Zaira, P., Duque, M.: Nonlinear Control of the Airship Cruise Flight Phase with Dynamical Decoupling. In: *Electronics, Robotics and Autonomous Mechanics Conference*, 473-477 (2008)

[12] Neto, G. G., dos Santos Barbosa, F., de Oliveira Jr, J. G., Angelico, B. A.: State feedback decoupling control of a 2DoF Helicopter. In: *XIII Simpósio Brasileiro de Automação Inteligente*, 398-403 (2017)

[13] Kouvakas, N. D., Koumboulis, F. N., Independent Velocity Control of the Longitudinal Motion of Quadrotors. In: *Proceedings of the 7th International Conference on Systems and Control*, 194-200 (2018)

[14] Cai, W., She, J., Wu, M., Ohyama, Y.: Disturbance suppression for quadrotor UAV using sliding-mode-observer-based equivalent-input-disturbance approach. *ISA Transactions* (2019)

[15] Wang, X., Sun, S., van Kampen, E.-J., Chu, Q.: Quadrotor Fault Tolerant Incremental Sliding Mode Control driven by Sliding Mode Disturbance Observers. *Aerospace Science and Technology*, **87**, 417-430 (2019)

[16] Wang, B., Yu, X., Mu, L., Zhang, Y.: Disturbance observer-based adaptive fault-tolerant control for a quadrotor helicopter subject to parametric uncertainties and external disturbances. *Mechanical Systems and Signal Processing*, **120**, 727-743 (2019)

[17] Rios, H., Falcon, R., Gonzalez, O. A., Dzul, A.: Continuous Sliding-Mode Control Strategies for Quadrotor Robust Tracking: Real-Time Application. *IEEE Transactions on Industrial Electronics*, **66**(2), 1264-1272 (2019)

[18] Chen, M., Xiong, S., Wu, Q., Tracking Flight Control of Quadrotor Based on Disturbance Observer. *IEEE Transactions on Systems, Man, and Cybernetics: Systems* (2019)

[19] Qian, L., Liu, H. H. T.: Path Following Control of A Quadrotor UAV with A Cable Suspended Payload Under Wind Disturbances. *IEEE Transactions on Industrial Electronics*, **67**(3), 2021-2029 (2020)

[20] Yuan, Y., Cheng, L., Wang, Z., Sun, C.: Position tracking and attitude control for quadrotors via active disturbance rejection control method. *Science China: Information Sciences*, **62** (2018)

[21] Baldini, A., Felicetti, R., Freddi, A., Longhi, S., Monteriu, A.: Direct position control of an octarotor unmanned vehicle under wind gust disturbance. In: *Proceedings of the 2019 International Conference on Unmanned Aircraft Systems (ICUAS)*, 684-691 (2019)

[22] Goslinski, J., Kasinski, A., Giernacki, W., Owczarek, P., Gardecki , S.: A Study on Coaxial Quadrotor Model Parameter Estimation: an Application of the Improved Square Root Unscented Kalman Filter. *Journal of Intelligent and Robotic Systems*, **95**, 491-510 (2019)

[23] Shraim, H., Awada, A., Youness, R.: Survey on Quadrotors: Configurations, Modeling and Identification, Control, Collision Avoidance, Fault Diagnosis and Tolerant Control. *IEEE Aerospace and Electronics Systems Magazine*, **33**(7), 14-33 (2018)

[24] Xiong, S., Chen, M., Wu, Q.: Predictive control for networked switch flight system with packet dropout. *Applied Mathematics and Computation*, **354**, 444-459 (2019)

[25] Gonzaleza, A., Cuencab, A., Balaguerb, V., Garcia, P.: Event-triggered predictor-based control with gain-Scheduling and extended state observer for networked control systems. *Information Sciences*, **491**, 90-108 (2019)

[26] He, L., Zhang, J., Hou, Y., Liang, X., Bai, P.: Time-Varying Formation Control for Second-Order Discrete-Time Multi-Agent Systems With Directed Topology and Communication Delay. *IEEE Access*, **7**, 33517-3352 (2019)

[27] Guerrero, J. A., Garcia, P. C., Challal, Y.: Quadrotors Formation Control: A Wireless Medium Access Aware Approach, *Journal of Intelligent and Robotic Systems*, **70**, 221-231 (2013)

[28] Koumboulis, F. N., Tzierakis, K. G.: Meeting Transfer Function Requirements via static measurement output feedback. In: *Journal of the Franklin Institute*, **335B**(4), 661-667 (1998)

[29] Kouvakas, N. D., Koumboulis, F. N., Giannaris, G. L., Vouyioukas, D.: Wireless Longitudinal Motion Controller Design for Quadrotors. In: *Proceedings of the 2020 International Conference on Unmanned Aircraft Systems (ICUAS)*, 1350-1358 (2020)

[30] Koumboulis, F. N., King, R. E., Stathaki, A.: Logic-Based Switching Controllers â€“ A Stepwise Safe Switching Approach, *Information Sciences*, **177**(13) 2736-2755 (2007)

[31] Koumboulis, F. N., Tzamtzi, M. P.: Multivariable Step-Wise Safe Switching Controllers. In: *Proceedings of the International Conference on Computational Intelligence for Modelling, Control and Automation and International Conference on Intelligent Agents, Web Technologies and Internet Commerce (CIMCA-IAWTIC'05)* (2005)

[32] Koumboulis, F. N., Kouvakas, N. D., Giannaris, G. L., Vouyioukas, D.: Independent motion control of a tower crane through wireless sensor and actuator networks. *ISA Transactions*, **60**, 312-320 (2016)

[33] Rosario-Gabriel, I., Cortes, H. R.: Aircraft Longitudinal Control based on the Lanchester's Phugoid Dynamics Model. In: *Proceedings of the 2018 International Conference on Unmanned Aircraft Systems (ICUAS)*, 924-929 (2018)

[34] Dhadekar, D. D., Talole, S. E.: Robust Fault Tolerant Longitudinal Aircraft Control. *IFAC-PapersOnLine*, **51**(1), 604-609 (2018)

[35] Gossmann, F., Svaricek, F., Gabrys, A.: Control of Longitudinal Aircraft Motion with Loadcase Robustness using LPV-Control with Partly-Measurable Parameters. In: *Proceedings of the 2018 AIAA Guidance, Navigation, and Control Conference*, 1-13 (2018)

[36] Koumboulis, F. N., Kouvakas, N. D.: I/O Decoupling with Simultaneous Disturbance Rejection of General Neutral Time Delay Systems via a Measurement Output Feedback Dynamic Controller. In: *Proceedings of the 21st Mediterranean Conference on Control and Automation (MED)*, 890-895 (2013)

[37] Giannaris, G. L., Kouvakas, N. D., Koumboulis, F. N., Vouyioukas, D.: Towards Remote Control of Planar Redundant Robotic Manipulators. In: *Proceedings of the IEEE 21st International Conference on Intelligent Engineering Systems (INES 2017)*, 231-236 (2017)

[38] Koumboulis, F. N., Kouvakas, N. D.: A three term controller for ride comfort improvement. In: *Proceedings of the 19th Mediterranean Conference on Control & Automation (MED)*, 114-119 (2011)

[39] Derafa, L., Madani, T., Benallegue, A.: Dynamic Modelling and Experimental Identification of Four Rotors Helicopter Parameters. In: *Proceedings of the IEEE International Conference on Industrial Technology (ICIT)* 2006.

[40] Hakim, T. M. I., Arifianto O.: Implementation of Dryden Continuous Turbulence Model into Simulink for LSA-02 Flight Test Simulation. *Proceedings of the 5th International Seminar of Aerospace Science and Technology* 2017

[41] Cervin, A., Henriksson, D., Lincoln, B., Eker, J., Årzén, K.-E. :How Does Control Timing Affect Performance? Analysis and Simulation of Timing Using Jitterbug and TrueTime. *IEEE Control Systems Magazine*, **23**(3), 16-30, (2003)

[42] Koumboulis, F. N., Kouvakas, N. D.: Block decoupling of general neutral multi delay systems *Proceedings of the International Conference on Emerging Technologies and Factory Automation (ETFA)* 2011

Chapter 7: Conclusions and Future Work

7.1 CONCLUSIONS

In the present dissertation wireless remote control for different systems such as electric motors, tower cranes, robotic manipulators and quadrotors that present huge interest in industrial applications was investigated.

The problem of wireless remote control is the presence of varying time delays imposed from wireless network infrastructure communication between sensors and controller and between controller and actuators. The undeterministic (time varying), asychronous with packet loss imperfect channels comes in contrast with the traditional control method designs. These imperfections dramatically deteriorates the performance of the closed loop and may lead the system in fatal unstability. The current trend of facing to this issue is to develop new communication infrastructure decreising the delays but still remain time varying, unknown and uncertains. In the present dissertation we moved forward to the opposite direction. The controller's design was effectuated using larger but constant delays.

The amount of the constant delays depends on the order and the number of controlled variables of such multivariables systems. From the control point of view the transfer matrix design requirements such as input output decoupling, command following and disturbance attenuation in presense of large but known delays was investigated for the first time in this dissertation. We demonstrated that these control schemes are independed from the communication protocol used which greately facilitates the applications.

Towards the above aims, the following particular results have been derived:

- In order to achieve speed control of a Permanent Magnet Synchronous Motor, in the presence of time delays due to wireless signal transmission between the controller and the motor, a two-stage decoupling controller has been used and the controller parameters selection algorithm has been appropriately extended to cope with the influence of the delays and to derive a closed loop system that remained stable even in the presence of them.
- An appropriate realizable multi-delay dynamic controller has been designed based on the linear approximant of a tower crane and applied on the realistic nonlinear

model. The variability of the time delays in the communication between sensors to controller and controller to actuators, which is generally induced by wireless network has a significant impact on the stability and robustness of the controller, was successfully handled with the development of a synchronization algorithm. At the same time, a signal reconstruction algorithm ensures the accurate signal transmission between the plant and the controller.

- The problem of remote control of a planar redundant manipulator has been studied, using a static feedback with dynamic precompensator including time delays.
- The problem of I/O decoupling with simultaneous disturbance attenuation via a wireless remote controller has been studied for a quadrotor in longitudinal motion under the influence of atmospheric disturbances. An appropriate realizable dynamic controller depending upon constant communication delays has been designed. Constant communication delays have been achieved using the proposed synchronization/signal reconstruction algorithm. Using a metaheuristic algorithm, the stability of the closed loop system has been satisfying. The proposed controller provides tolerance to communication noise and package receipt delays.
- For a wide range of maneuvers and wireless control configuration, the goal of independent horizontal and vertical velocity for quadrotors has been achieved by proposing a stepwise safe switching algorithm for non-linear time delay systems, using dynamic multi delay controllers and approximately minimizing a composite cost criterion including the infinity norm and the H_2 norm of the variations around trim points, under hard constraints for the overshoot and the steady state values of the performance variables. The proposed scheme is tolerant to atmospheric disturbances, communication delays and variations of the delays, as well as large maneuver commands and model nonlinearities.

In the context of this dissertation the results presented here are based on the following publications presented at international conferences and journals.

[P1] N. D. Kouvakas, F. N. Koumboulis, G. L. Giannaris and D. Vouyioukas, "Towards Wireless Control for a Permanent Magnet Synchronous Motor," in

Proceedings of the IEEE International Conference on Emerging Technologies and Factory Automation (ETFA 2014), Barcelona, Spain, 16-19 September, 2014.

[P2] Fotis N. Koumboulis, N. D. Kouvakas, G. L. Giannaris and D. Vouyioukas, "Independent motion control of a tower crane through wireless sensor and actuator networks," in *ISA Transactions*, vol. 60, pp. 312-320, 2016.

[P3] G. L. Giannaris, N. D. Kouvakas, F. N. Koumboulis and D. Vouyioukas, "Towards Remote Control of Planar Redundant Robotic Manipulators", Proceedings of the IEEE 21st International Conference on Intelligent Engineering Systems (INES 2017), pp. 231-236, Larnaca, Cyprus, October 20-23, 2017.

[P4] Kouvakas, N. D., Koumboulis, F. N., Giannaris, G. L., Vouyioukas, D.: Wireless Longitudinal Motion Controller Design for Quadrotors. In: *Proceedings of the 2020 International Conference on Unmanned Aircraft Systems (ICUAS)*, 1350-1358 (2020).

[P5] G. L. Giannaris, N. D. Kouvakas, F. N. Koumboulis and D. Vouyioukas, "Switching wireless control for longitudinal quadrotor manouvres", accepted for publication in *Journal of Intelligent Robotic Systems (JINT)*.

7.2 FUTURE WORK

Future research will proceed to the following directions:

a. Embedment of the proposed communication protocol to low level control platforms like Arduino Robot and PIC32MK.
b. Extend the results to other applications such as aquatic vehicles, mobile robots and microrobots.
c. Extend the results to other transfer matrix design requirements such as exact model matching, exact disturbance rejection and asymptotic tracking.

Appendices

Appendix A

Analytic expressions of the nonzero elements of $\tilde{A}$ and $\tilde{B}$ matrices

$$\tilde{a}_{1,1} = a_{4,5}b_{5,1}\left(a_{2,2}\left\{a_{3,3}\left[a_{5,5}+b_{5,1}\left(k_{2,5}+k_{2,6}\right)\right]-2a_{3,5}b_{5,1}k_{2,3}\right\}-2a_{2,5}a_{3,3}b_{5,1}k_{2,2}\right)$$

$$\tilde{a}_{1,2} = -a_{4,5}b_{5,1}\Big[2a_{2,5}b_{5,1}\left(a_{3,1}k_{2,3}-a_{3,3}k_{2,1}\right)+a_{2,1}\left\{a_{3,3}\left[a_{5,5}+b_{5,1}\left(k_{2,5}+k_{2,6}\right)\right]- -2a_{3,5}b_{5,1}k_{2,3}\right\}\Big]$$

$$\tilde{a}_{1,3} = -a_{4,5}b_{5,1}\Big[2\left(a_{2,1}a_{3,5}-a_{2,5}a_{3,1}\right)b_{5,1}k_{2,2}+a_{2,2}\left\{a_{3,1}\left[a_{5,5}+b_{5,1}\left(k_{2,5}+k_{2,6}\right)\right]- -2a_{3,5}b_{5,1}k_{2,1}\right\}\Big],$$

$$\tilde{a}_{1,5} = a_{4,5}b_{5,1}^2\left[a_{2,1}a_{3,3}k_{2,2}+a_{2,2}\left(a_{3,1}k_{2,3}-a_{3,3}k_{2,1}\right)\right]$$

$$\tilde{a}_{1,6} = a_{4,5}b_{5,1}^2\left[a_{2,1}a_{3,3}k_{2,2}+a_{2,2}\left(a_{3,1}k_{2,3}-a_{3,3}k_{2,1}\right)\right]$$

$$\tilde{a}_{2,1} = -a_{4,5}b_{5,1}\left\{-2b_{5,1}\left(a_{2,5}k_{2,2}+a_{3,5}k_{2,3}\right)+a_{3,3}\left[a_{5,5}+b_{5,1}\left(k_{2,5}+k_{2,6}\right)\right]+ +a_{2,2}\left[a_{3,3}+a_{5,5}+b_{5,1}\left(k_{2,5}+k_{2,6}\right)\right]\right\}$$

$$\tilde{a}_{2,2} = b_{5,1}\Big[a_{2,1}a_{4,5}\left[a_{3,3}+a_{5,5}+b_{5,1}\left(k_{2,5}+k_{2,6}\right)\right]+a_{2,5}\Big(a_{3,3}\left\{2a_{4,5}b_{5,1}k_{2,4}+ +a_{4,4}\left[a_{5,5}+b_{5,1}\left(k_{2,6}-k_{2,5}\right)\right]\right\}-2a_{4,5}b_{5,1}k_{2,1}\Big)\Big]$$

$$\tilde{a}_{2,3} = b_{5,1}\Big[a_{4,5}\left\{a_{3,1}\left[a_{5,5}+b_{5,1}\left(k_{2,5}+k_{2,6}\right)\right]-2a_{3,5}b_{5,1}k_{2,1}\right\}+ +a_{2,2}\Big(a_{3,5}\left\{2a_{4,5}b_{5,1}k_{2,4}+a_{4,4}\left[a_{5,5}+b_{5,1}\left(k_{2,6}-k_{2,5}\right)\right]\right\}+a_{3,1}a_{4,5}\Big)\Big]$$

$$\tilde{a}_{2,4} = a_{4,5}b_{5,1}\left(a_{2,2}\left\{a_{3,3}\left[a_{5,5}+b_{5,1}\left(k_{2,5}+k_{2,6}\right)\right]-2a_{3,5}b_{5,1}k_{2,3}\right\}-2a_{2,5}a_{3,3}b_{5,1}k_{2,2}\right)$$

$$\tilde{a}_{2,5} = -b_{5,1}\Big(b_{5,1}\Big[a_{4,5}\left(a_{2,1}k_{2,2}+a_{3,1}k_{2,3}\right)-a_{3,3}\left(a_{4,5}k_{2,1}+a_{2,5}a_{4,4}k_{2,2}\right)\Big]+ +a_{2,2}\left\{a_{3,3}\left[a_{4,5}b_{5,1}k_{2,4}+a_{4,4}\left(a_{5,5}+b_{5,1}k_{2,6}\right)\right]-b_{5,1}\left(a_{4,5}k_{2,1}+a_{3,5}a_{4,4}k_{2,3}\right)\right\}\Big)$$

$$\tilde{a}_{2,6} = b_{5,1}^2\left\{a_{3,3}\left(a_{4,5}k_{2,1}-a_{2,5}a_{4,4}k_{2,2}\right)-a_{4,5}\left(a_{2,1}k_{2,2}+a_{3,1}k_{2,3}\right)+ +a_{2,2}\left[a_{4,5}\left(k_{2,1}-a_{3,3}k_{2,4}\right)+a_{4,4}\left(a_{3,3}k_{2,5}-a_{3,5}k_{2,3}\right)\right]\right\}$$

$$\tilde{a}_{3,1} = a_{4,5}b_{5,1}\left[a_{2,2}+a_{3,3}+a_{5,5}+b_{5,1}\left(k_{2,5}+k_{2,6}\right)\right]$$

$$\tilde{a}_{3,2} = b_{5,1}\Big(-a_{2,5}\left\{2a_{4,5}b_{5,1}k_{2,4}+a_{4,4}\left[a_{5,5}+b_{5,1}\left(k_{2,6}-k_{2,5}\right)\right]+ +a_{3,3}\left[a_{4,4}+a_{5,5}+b_{5,1}\left(k_{2,6}-k_{2,5}\right)\right]\right\}-a_{2,1}a_{4,5}\Big)$$

$$\tilde{a}_{3,3} = b_{5,1}\Big(-a_{3,5}\left\{2a_{4,5}b_{5,1}k_{2,4}+a_{4,4}\left[a_{5,5}+b_{5,1}\left(k_{2,6}-k_{2,5}\right)\right]+$$

$$+a_{2,2}\left[a_{4,4}+a_{5,5}+b_{5,1}\left(k_{2,6}-k_{2,5}\right)\right]\Big\}-a_{3,1}a_{4,5}\Big)$$

$$\tilde{a}_{3,4}=-a_{4,5}b_{5,1}\Big\{-2b_{5,1}\left(a_{2,5}k_{2,2}+a_{3,5}k_{2,3}\right)+a_{3,3}\left[a_{5,5}+b_{5,1}\left(k_{2,5}+k_{2,6}\right)\right]+$$

$$+a_{2,2}\left[a_{3,3}+a_{5,5}+b_{5,1}\left(k_{2,5}+k_{2,6}\right)\right]$$

$$\tilde{a}_{3,5}=b_{5,1}\Big\{-b_{5,1}\left[a_{4,5}k_{2,1}+a_{4,4}\left(a_{2,5}k_{2,2}+a_{3,5}k_{2,3}\right)\right]+a_{3,3}\left[b_{5,1}\left(a_{4,5}k_{2,4}-\right.\right.$$

$$\left.-a_{2,5}k_{2,2}\right)+a_{4,4}\left(a_{5,5}+b_{5,1}k_{2,6}\right)\Big]+a_{2,2}\Big[b_{5,1}\left(a_{4,5}k_{2,4}-a_{3,5}k_{2,3}\right)+$$

$$+a_{4,4}\left(a_{5,5}+b_{5,1}k_{2,6}\right)+a_{3,3}\left(a_{4,4}+a_{5,5}+b_{5,1}k_{2,6}\right)\Big]\Big\}$$

$$\tilde{a}_{3,6}=b_{5,1}^{2}\Big\{a_{2,5}\left(a_{3,3}+a_{4,4}\right)k_{2,2}+a_{3,5}\left(a_{2,2}+a_{4,4}\right)k_{2,3}+$$

$$+a_{4,5}\Big[\left(a_{2,2}+a_{3,3}\right)k_{2,4}-k_{2,1}\Big]-\Big[a_{2,2}a_{3,3}+\left(a_{2,2}+a_{3,3}\right)a_{4,4}\Big]k_{2,5}\Big\}$$

$$\tilde{a}_{4,1}=-a_{4,5}b_{5,1},\tilde{a}_{4,2}=a_{2,5}b_{5,1}\Big[a_{3,3}+a_{4,4}+a_{5,5}+b_{5,1}\left(k_{2,6}-k_{2,5}\right)\Big]$$

$$\tilde{a}_{4,3}=a_{3,5}b_{5,1}\Big[a_{2,2}+a_{4,4}+a_{5,5}+b_{5,1}\left(k_{2,6}-k_{2,5}\right)\Big]$$

$$\tilde{a}_{4,4}=a_{4,5}b_{5,1}\Big[a_{2,2}+a_{3,3}+a_{5,5}+b_{5,1}\left(k_{2,5}+k_{2,6}\right)\Big]$$

$$\tilde{a}_{4,5}=-b_{5,1}\Big[-b_{5,1}\left(a_{2,5}k_{2,2}+a_{3,5}k_{2,3}-a_{4,5}k_{2,4}\right)+a_{4,4}\left(a_{5,5}+b_{5,1}k_{2,6}\right)+$$

$$+a_{3,3}\left(a_{4,4}+a_{5,5}+b_{5,1}k_{2,6}\right)+a_{2,2}\left(a_{3,3}+a_{4,4}+a_{5,5}+b_{5,1}k_{2,6}\right)\Big]$$

$$\tilde{a}_{4,6}=b_{5,1}^{2}\Big[\left(a_{2,2}+a_{3,3}+a_{4,4}\right)k_{2,5}-a_{2,5}k_{2,2}-a_{3,5}k_{2,3}-a_{4,5}k_{2,4}\Big]$$

$$\tilde{a}_{5,2}=-a_{2,5}b_{5,1},\tilde{a}_{5,3}=-a_{3,5}b_{5,1},\tilde{a}_{5,4}=-a_{4,5}b_{5,1}$$

$$\tilde{a}_{5,5}=b_{5,1}\left(a_{2,2}+a_{3,3}+a_{4,4}+a_{5,5}+b_{5,1}k_{2,6}\right),\tilde{a}_{5,6}=-b_{5,1}^{2}k_{2,5},\tilde{a}_{6,5}=-b_{5,1}$$

$$\tilde{b}_{1,1}=a_{4,5}a_{5,5}b_{5,1}\Big[a_{2,2}\left(a_{3,3}k_{2,1}-a_{3,1}k_{2,3}\right)-a_{2,1}a_{3,3}k_{2,2}\Big]$$

$$\tilde{b}_{2,1}=b_{5,1}\Big\{a_{4,5}a_{5,5}\left(a_{2,1}k_{2,2}+a_{3,1}k_{2,3}\right)-a_{3,3}\Big[a_{2,5}a_{4,4}a_{5,5}k_{2,2}+a_{4,5}\left(a_{5,5}k_{2,1}-\right.$$

$$\left.\left.-a_{2,1}k_{2,2}\right)\Big]\Big\}+a_{2,2}\Big\{a_{3,3}\Big[a_{4,5}b_{5,1}\left(a_{5,5}k_{2,4}-k_{2,1}\right)+a_{4,4}a_{5,5}\left(a_{5,5}+b_{5,1}k_{2,6}\right)\Big]-$$

$$-b_{5,1}\Big[a_{3,5}a_{4,4}a_{5,5}k_{2,3}+a_{4,5}\left(a_{5,5}k_{2,1}-a_{3,1}k_{2,3}\right)\Big]\Big\}$$

$$\tilde{b}_{3,1}=b_{5,1}\Big[a_{4,4}a_{5,5}\left(a_{2,5}k_{2,2}+a_{3,5}k_{2,3}\right)+a_{4,5}\left(a_{5,5}k_{2,1}-a_{2,1}k_{2,2}-a_{3,1}k_{2,3}\right)\Big]-$$

$$-a_{3,3}\Big\{a_{4,4}\left(a_{5,5}b_{5,1}k_{2,6}-a_{2,5}b_{5,1}k_{2,2}+a_{5,5}^{2}\right)-b_{5,1}\Big[a_{2,5}a_{5,5}k_{2,2}+$$

$$+a_{4,5}\left(k_{2,1}-a_{5,5}k_{2,4}\right)\Big]\Big\}+a_{2,2}\Big\{-b_{5,1}\Big[a_{3,5}a_{5,5}k_{2,3}+a_{4,5}\left(k_{2,1}-a_{5,5}k_{2,4}\right)\Big]+$$

$$+a_{4,4}\left(a_{5,5}b_{5,1}k_{2,6}-a_{3,5}b_{5,1}k_{2,3}+a_{5,5}^{2}\right)+$$

$$+a_{3,3}\Big[a_{4,5}b_{5,1}k_{2,4}+\left(a_{4,4}+a_{5,5}\right)b_{5,1}k_{2,6}+a_{5,5}^{2}+2a_{4,4}a_{5,5}\Big]\Big\}$$

$$\tilde{b}_{4,1}=a_{4,4}a_{5,5}^{2}-a_{4,5}b_{5,1}k_{2,1}-a_{2,5}a_{4,4}b_{5,1}k_{2,2}-a_{2,5}a_{5,5}b_{5,1}k_{2,2}-$$

$$-a_{3,5}a_{4,4}b_{5,1}k_{2,3}-a_{3,5}a_{5,5}b_{5,1}k_{2,3}+a_{4,5}a_{5,5}b_{5,1}k_{2,4}+a_{4,4}a_{5,5}b_{5,1}k_{2,6}+$$

$$+a_{3,3}\Big[a_{5,5}\left(2a_{4,4}+a_{5,5}\right)+b_{5,1}\left(a_{4,5}k_{2,4}-a_{2,5}k_{2,2}\right)+\left(a_{4,4}+a_{5,5}\right)b_{5,1}k_{2,6}\Big]+$$

$$a_{2,2}\Big[a_{3,3}a_{4,4}+2a_{3,3}a_{5,5}+2a_{4,4}a_{5,5}+a_{5,5}^{2}+$$

$$+b_{5,1}\left(a_{4,5}k_{2,4}-a_{3,5}k_{2,3}\right)+\left(a_{3,3}+a_{4,4}+a_{5,5}\right)b_{5,1}k_{2,6}\Big]$$

$$\tilde{b}_{5,1}=b_{5,1}\left(a_{2,5}k_{2,2}+a_{3,5}k_{2,3}-a_{4,5}k_{2,4}\right)-a_{5,5}\left(2a_{4,4}+a_{5,5}\right)-\left(a_{4,4}+a_{5,5}\right)b_{5,1}k_{2,6}$$
$$-a_{3,3}\left(a_{4,4}+2a_{5,5}+b_{5,1}k_{2,6}\right)-a_{2,2}\left(a_{3,3}+a_{4,4}+2a_{5,5}+b_{5,1}k_{2,6}\right)$$

$$\tilde{b}_{6,1}=a_{2,2}+a_{3,3}+a_{4,4}+2a_{5,5}+b_{5,1}k_{2,6}$$